

AD-A031 078

ROCKWELL INTERNATIONAL THOUSAND OAKS CALIF SCIENCE --ETC F/G 7/4
ANALYTICAL APPLICATIONS OF ELECTRON SPIN RESONANCE.(U)

SEP 76 I B GOLDBERG

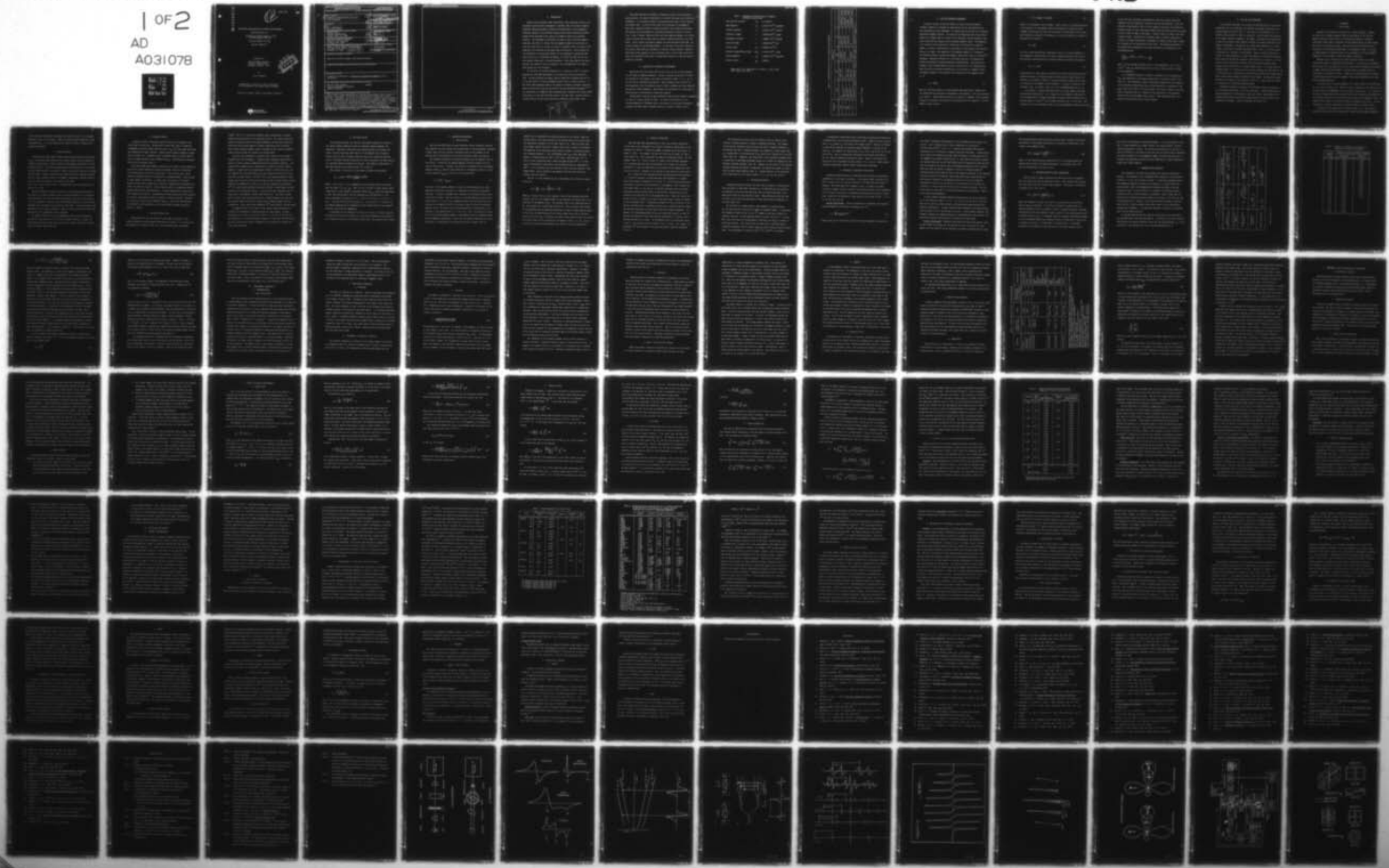
N00014-73-C-0325

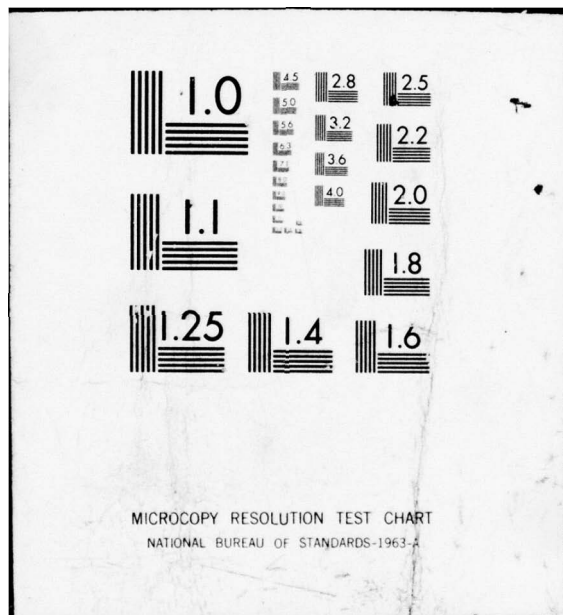
UNCLASSIFIED

SC549.19TR

• NL

1 OF 2
AD
A031078





AD A031078

SC549.19TR

24

11
P

ANALYTICAL APPLICATIONS OF ELECTRON SPIN RESONANCE

Technical Report No. 7

Covering the Period January 1, 1976
through September 30, 1976

Contract N00014-73-C-0325

Task No. NR051-553

Prepared for

Office of Naval Research
800 North Quincy Street
Arlington, Virginia 22217

by

Ira B. Goldberg

D D C
DRAFTED
OCT 22 1976
C
RECORDED

Reproduction in whole or in part is permitted
for any purpose of the United States Government

Approved for public release; distribution unlimited



Science Center
Rockwell International

Unclassified

SECURITY CLASSIFICATION OF THIS PAGE (When Data Entered)

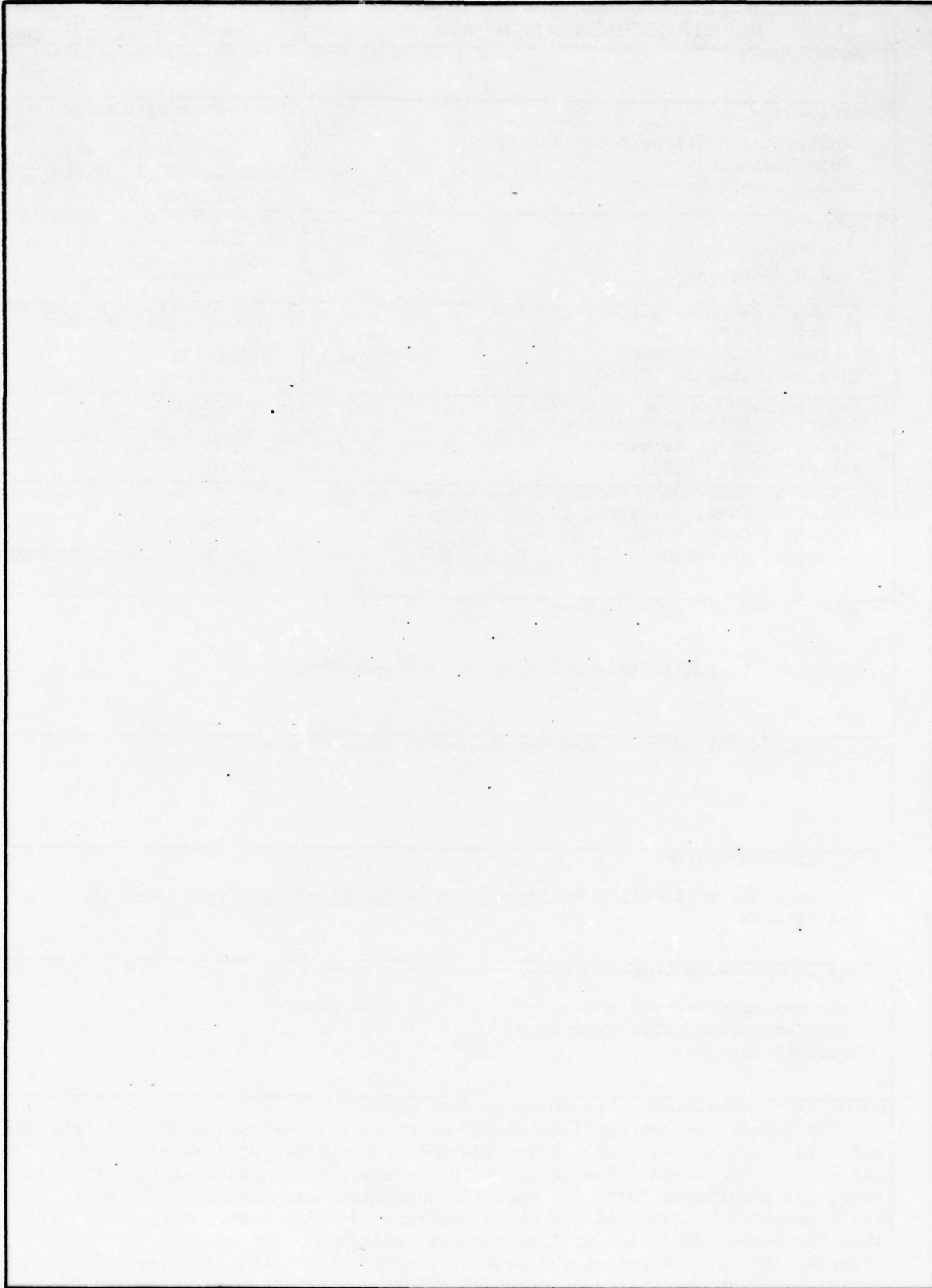
DD FORM 1473 EDITION OF 1 NOV 65 IS OBSOLETE
1 JAN 73

Unclassified

SECURITY CLASSIFICATION OF THIS PAGE (When Data Entered)

Unclassified

SECURITY CLASSIFICATION OF THIS PAGE(When Data Entered)



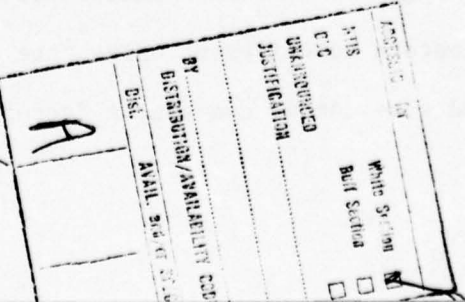
Unclassified

SECURITY CLASSIFICATION OF THIS PAGE(When Data Entered)

I. INTRODUCTION

Electron spin resonance (ESR) spectroscopy (also sometimes called by the synonymous terms electron paramagnetic resonance, EPR, and electron magnetic resonance, EMR, spectroscopy) is based on the absorption of electromagnetic radiation (usually in the microwave region) which causes transitions between energy levels produced by the action of a magnetic field on an unpaired electron. The phenomenon is basically the same as that in nuclear magnetic resonance (see Chap. 3), except that the magnetic moment of an electron is about 658 times that of a proton, so that in a magnetic field the energy level separation for electrons is 658 times that of the proton. This accounts for the difference in the spectral regions of the techniques at equivalent magnetic fields (e.g., 60-100 MHz for NMR vs. 9.5-35 GHz for ESR) and for the much greater sensitivity of the ESR technique. Thus, while many of the basic concepts are common to the two techniques, the instrumentation and range of applications are very different.

The discovery of the ESR phenomenon by E. Zavoisky in 1944^{1,2,1} actually predated the first NMR experiments by the physicists Purcell and Bloch in 1946. The ESR technique was mainly used by physicists in England and the U.S. in the late 1940's to study paramagnetic metal ions in crystal lattices. In the 1950's ESR techniques began to be applied to chemical problems, especially those involving free radicals and radical ions and relaxation processes.^{57,109} The availability of commercial ESR instrumentation, especially the Varian V4500 spectrometer in 1957 and the V4502 system a few years later, spurred vigorous research efforts in this field which have continued to the present time.



Since ESR requires the presence of unpaired electrons in the substance being analyzed, its range of application is narrower than many other analytical techniques. It is uniquely suited to the detection and study of free radicals and radical ions. It has also been used for the analysis of paramagnetic metal ions, especially those of transition metals, rare earths and actinides. ESR signals are also exhibited by carbonaceous materials, defects in solids (e.g., F and V centers, impurity sites, and from radiation damage), for triplet states in solids and for many atoms and several diatomic molecules in the gas phase. Solid, liquid, and gaseous samples, and even biological materials, can be used directly in the ESR spectrometer. At the time of the first edition of this series (1963) ESR was considered a relatively young technique. Numerous applications have appeared in the intervening years, and its high sensitivity, speed, and specificity have made it an important method for a special class of analytical problems.

II. PRINCIPLES OF ELECTRON SPIN RESONANCE

Many books and reviews have been written about the use of ESR techniques for the study of chemical phenomena. Because a detailed description of ESR is not possible in this chapter, the reader is directed to Refs. 3, 5, 7, 10, 23, 58, and 110 for additional information. These references were selected for their generality, the introductory nature of their treatment and their detailed description of ESR techniques. This chapter will be devoted to a discussion of those features of ESR needed for analytical purposes.

Because ESR is utilized in many different research areas, magnetic parameters are cited in a great variety of units. To reduce the difficulty of converting parameters to different units, the values of the relevant fundamental constants and some useful conversion factors are given in Tables 1 and 2.

Table 1. Fundamental Constants Used in Magnetic Resonance Spectroscopy*

Free Electron g-factor	g_e	2.002319313
Bohr Magneton	β_e	9.274078×10^{-21} erg/Gauss
Planck's Constant	h	6.626176×10^{-27} erg/sec
Velocity of Light	c	2.9979246×10^{10} cm/sec
Boltzmann's Constant	k	1.380662×10^{-16} erg/deg
Electron Change	e	$4.8032424 \times 10^{-10}$ esu
Electron Mass	m_e	9.109534×10^{-28} g
Electron Charge/Electron Mass	e/m_e	5.272764×10^{17} esu/g
Nuclear Magneton	β_N	5.050824×10^{-23} erg/Gauss
Proton g-factor	g_H	5.585564

*Taken from E. R. Cohen and B. N. Taylor, J. Phys. Chem. Ref. Data 2, 663 (1973).

Table 2. Conversion Factors for Use in Electron Spin Resonance

To Convert To	Multiply to		
	erg	cm^{-1}	MHz
erg	5.0340×10^{15}	1.5092×10^{20}	6.2414×10^{11}
cm^{-1}	1.9865×10^{-16}	1.0	2.9979×10^4
MHz	6.6262×10^{-21}	3.3356×10^{-5}	1.0
eV	1.6022×10^{-12}	8.0655×10^3	2.4180×10^8
G	1.85697×10^{-20}	(g/g_e)	0.93481×10^{-4} (g/g_e)
			2.80247 (g/g_e)
			1.15902×10^{-14} (g/g_e)
			1.0

1 Gauss = 10^4 Tesla

A. THE SPIN RESONANCE PHENOMENON

The basic concepts of ESR are similar to those of nuclear magnetic resonance (Chapter 3) although the applications and the instrumentation of the techniques are quite different. An electron may be pictured as a spinning, negatively-charged, particle. By virtue of its charge and spin, the electron behaves as a magnet (just as a loop of wire carrying a current produces a magnetic field) and can interact with an external magnetic field. The magnetism of an electron can be expressed by saying that an electron has a magnetic moment, μ , which is proportional to e/m_e where e is the charge on the electron and m_e is its mass. The magnitude of the magnetic moment of a "classical" free electron would be β_e , the Bohr magneton, which has a value of 9.2732×10^{-21} erg/gauss. Because an electron is a sub-atomic particle, its momentum and energy are governed by quantum mechanical considerations. Each electron is assigned a spin quantum number M_s which is either $+1/2$ or $-1/2$ denoting that there are only two possible orientations of an electron in a magnetic field. The magnetic moment of the electron in the direction of the magnetic field, μ_z , is

$$\mu_z = -g\beta_e M_s \quad (1)$$

where g , called the g -factor or spectroscopic splitting factor, depends upon the orbital and the electronic environment of the electron. For a free electron g_e is about 2. When unpaired electrons are placed in a magnetic field, measured in gauss (or oersted), the energy of the electrons will be changed by a certain number of ergs, given by

$$E = -\mu H = g\beta M_s H = \pm 1/2(g\beta H) \quad (2)$$

where H is the magnetic field strength. Those of spin $-1/2$ (pointing opposite to the direction of the magnetic field) will decrease in energy by about $1/2(g\beta H)$, while those with spin $+1/2$ (pointing in the direction of the field) will increase in energy by a like amount, so that the difference in energy in between the two levels is

$$\Delta E = g\beta H \quad (3)$$

Just as in other spectroscopic experiments, there is a certain frequency of electromagnetic radiation that will induce transitions between these states. The frequency associated with this energy difference satisfies the equation

$$\Delta E = h\nu = g\beta H \quad (4)$$

In distinction to other types of spectroscopy, in which the energy levels are essentially fixed, in ESR spectroscopy the splitting of energy levels, and, therefore, the frequency capable of causing transitions between these levels, is a function of the magnetic field strength, H . Putting in values for the constants in Eq. (4) yields a value for ν/H of 2.8026 MHz/gauss for $g = g_e$.

It is helpful to compare ESR spectroscopy to nuclear magnetic resonance and absorption spectroscopy. For a magnetic field strength of 3400 gauss (a field strength which is commonly employed) the energy level difference due to electron spins is 6.31×10^{-17} ergs (0.00091 Kcal/mole) and ν is 9.53 GHz. This frequency lies in the microwave region of the electromagnetic radiation spectrum,

so that the most convenient instrumentation used will involve radar-type components such as waveguides, microwave cavities, and klystrons. Note that identical considerations hold for proton magnetic resonance, but because the hydrogen nucleus is about 1800 times heavier than the electron, and its g-value is about 5.585, for NMR at 3400 gauss, ν would be about 14.5 MHz in the radio frequency region. Because ΔE is relatively small for ESR in comparison to visible or infrared spectroscopy, differences in behavior other than a different frequency of the transition are also noted. The relative population of two energy levels separated by an energy difference ΔE is governed by the Boltzmann equation

$$\frac{n_{+1/2}}{n_{-1/2}} = e^{-\Delta E/kT} = e^{-hv/kT} \sim 1 - \frac{hv}{kT} \quad (5)$$

where k is the Boltzmann constant, and T is the temperature. For a ΔE of 6.3×10^{-17} ergs, the relative population of the two energy levels is 0.9984 at room temperature.

It is sometimes possible to produce a sufficient rate of transitions to cause the population of the higher energy state to be equal to that of the lower one. This phenomenon, known as saturation, depends upon the intensity of the microwave radiation and upon the time required for a molecule in the upper level to fall back to the lower level. This time, related to the spin-lattice relaxation time, is a measure of the interaction of the unpaired electron with its environment (the lattice). When saturation begins, the signal level decreases and the signal broadens.

B. THE BASIC ESR EXPERIMENT

A very simple instrument for carrying out ESR spectroscopy at microwave frequencies and, for comparison, the familiar spectrometer operating in the visible region are shown in Fig. 1. The source of the microwave (or r.f.) radiation (often about 9.5 GHz) is a klystron. The microwaves are conducted to the sample through a waveguide. The sample, contained in the sample tube, is held in a microwave cavity between the poles of a magnet operating in the region of 3400 gauss. The detector is a diode which produces a d.c. output related to the level of incident microwave power. The d.c. from the crystal is displayed on a recorder or oscilloscope. While it would be possible to operate in a mode analogous to visible spectrometers, by holding the magnetic field fixed and varying the frequency of the klystron, in practice it is much easier to hold the klystron frequency fixed and vary the magnetic field because then the cavity acts as a high-Q tuned circuit. At a given klystron frequency there is a certain value of the field strength that satisfies Eq. (4). At this value of H , transitions are induced from the lower to the upper energy level, and microwave energy is absorbed by the sample. The microwave energy falling on the crystal is then smaller, and the d.c. output from the crystal as a function of H , shows the absorption band.

Although this method of operation of an ESR spectrometer is possible, it is not usually used because of its poor sensitivity. Various modifications involving modulation of the magnetic field and lock-in (phase-sensitive) or superheterodyne detection give much higher sensitivity and are used in most commercial instruments. These are described in Section III.

C. g-FACTORS

1. The g-Tensor

Equation (1) introduces the g-factor as a single parameter. However, the value of g is highly dependent upon the environment of the electron. Unpaired electrons which are not in s orbitals will generate a magnetic field which either adds or subtracts from the applied field, and thus changes the value of the g-factor from g_e . The actual value will depend upon the orientation of the molecule with respect to the magnetic field. In the gas or liquid phases the observed g-factor is the average of the three diagonal components of the g-tensor so that the system is isotropic.

Analysis can be carried out for liquid systems as well as for single crystals and powders or randomly-oriented solids. A crystal with low symmetry will have $g_x \neq g_y \neq g_z$ where the x , y and z axes relate to molecular coordinates. A single crystal will then exhibit a g-factor which is dependent upon its orientation in the magnetic field. A powder of the same material will exhibit a broad spectrum which covers the magnetic field range determined by the maximum and minimum g-factors.

A molecule which is axially symmetric in a single crystal is characterized by a $g_{\perp} = g_x = g_y$ and $g_{\parallel} = g_z$. When the z axis is parallel to the field, the observed g-factor is independent of the rotation of the molecule. In a powder the spectra are characterized by an unusual shape which is basically the envelope of all possible orientations of the molecule with respect to the magnetic field. The magnetic field range of the spectrum would be determined by g_{\parallel} and g_{\perp} . Various representative spectra resulting from powdered samples are shown in Fig. 2.

An electron will always have its g-factor equal to g_e . The reason for deviations from g_e result from coupling of residual orbital angular momentum

in the molecule (contributed for example from excited states) to the angular momentum or spin of the electron. When the orbital angular momentum is small, g approaches g_e . It is this property that makes the g -factor diagnostic of particular materials.

2. Organic Radicals

Virtually all π -type organic radicals have g -factors within a few percent of g_e . For the most part g -factors are slightly greater than g_e ranging from 2.0025 for hydrocarbons to about 2.0100 for some highly substituted or sulfur-centered radicals. The g -factor depends upon the distribution of the unpaired electron among atoms in the radical or radical ion, and the spin-orbit coupling of those atoms. Heavier atoms have much larger spin-orbit coupling constants, and for a given aromatic nucleus, for example a semiquinone, halogen substitution will cause the g -factors to increase in the order $g(H) < g(F) < g(Cl) < g(Br) < g(I)$. The same holds true for substitution of heterocyclic atoms.

One would think that g -factors would be a good qualitative indication of the nature of a radical; however, there are other parameters (e.g., hyperfine splittings) which are often more easily measured and also serve this purpose. It is also important to mention that the ESR signal amplitude is quantitatively dependent upon the square of the g -factor (vide infra). For most purposes, ESR spectrometers can be used to measure g with an accuracy better than ± 0.001 unit, making this error unimportant in most analyses.

At present, there is no set of comprehensive tables of ESR parameters. Some may be found in Refs. 11, 16 and 70 for organic radicals. Solvent and medium effects may also affect the g -factor, but in most cases these contributions are smaller than ± 0.001 unit.

3. Inorganic Radicals

Inorganic radicals, excluding transition metal ions, encompass a very broad range of structures. Systems which contain many atoms in asymmetric arrangements typically exhibit g-factors near to g_e , but with larger deviations than exhibited by organic radicals. Radicals which contain symmetric arrangements of atoms; e.g., octahedral (AB_6), tetrahedral (AB_4), or linear (ABC or AB), can exhibit g-factors very different than g_e . The g-factors of inorganic radicals are discussed in Ref. 6.

Since most atoms and inorganic radicals are not stable at room temperature and are not usually detected in solution using ESR, they are of relatively little importance in analytical applications. Only certain atoms, namely those with S-ground states can be detected in condensed phases. These include H, alkali metal, and N-atoms. In these cases, the g-factor is isotropic. Diatomic species cannot generally be detected at temperatures much higher than 100°K, and rarely in solution. This is because there is considerable angular momentum which allows rapid relaxation. At lower temperatures, spectra with axial symmetry are observed. Representative systems include O_2^{\cdot} and NO adsorbed on surfaces, and halogen molecule ion defects in halide crystals. Generally, g_{\perp} is near g_e , but g_{\parallel} is very different than g_e . O_2^{\cdot} has also been observed in solutions at room temperature, but is most likely strongly solvated or bound to a cation.

4. Transition Metal Ions

Transition metal ions also exhibit a wide range of g-factors. Most transition metal ions have unpaired electrons in d-levels. If it were not for the presence of a crystal field, all of the transition metal ions except

d^5 (Mn^{2+} , Fe^{3+} , etc.) states would exhibit large contributions of angular momentum from the orbital of the unpaired electron. The crystal field will quench or partially quench this angular momentum, and thus many transition metal ions yield strong signals at ambient temperatures and in solution. Small residual angular momenta usually increase the spin lattice relaxation time and thus increase the intensity of the ESR signal.

g-factors and linewidths of transition metal ions are very strongly dependent upon the environment. Strongly bonded complexing agents tend to quench the orbital angular momentum and shift the g-factors toward g_e . The ligand field strength alone is insufficient to quench the orbital angular momentum. Ligands which are symmetrically bonded to a metal ion (e.g., six CN^- ligands) will cause splitting of the five d-electron levels into three lower and two upper states. Thus Cr^{3+} (d^3), which usually exhibits a broad signal and $g \neq g_e$ will now have one electron in each of three orbitals and is therefore non-degenerate so that $g \sim g_e$, and the linewidth also decreases. Ti^{3+} (d^1) under these conditions would still exhibit a broad signal; and the g-factor will be different from g_e . If now one CN^- were replaced by an OH^- group, than a "tetragonal" crystal field would occur. This would further split the three lower energy orbitals into a single energy level lower than the original energy level and two energy levels slightly higher than the original one. Thus, under these conditions Ti^{3+} would exhibit a strong signal.

A complete review of the effect of the crystal field environment on g-factors and linewidths is beyond the scope of this chapter. For more information, the reader is directed to Refs. 1, 5, 48, 68, 69, 85, and 110. The possibility of utilizing different ligands to cause shifts in ESR spectra and detect selectively specific components in the analysis of mixtures has hardly been exploited.

5. Gas Phase Species

For gas phase species, the electron spin angular momentum is coupled to the orbital angular momentum as well as rotational angular momentum (for molecules). Typically, atoms yield very intense spectra, but diatomic and linear triatomic molecules yield spectra of considerably lower intensity because there are many occupied rotational states each exhibiting different lines. Nonlinear triatomic molecules can often be detected, but their spectra are relatively weak and difficult to analyze. The details of ESR spectra of gas phase species can be found in Refs. 20, 24 and 25.

The *g*-factor of an atom in the gas phase is given by the equation

$$g_J = 1.0023 + \frac{J(J+1) + S(S+1) - L(L+1)}{2J(J+1)} \quad (6)$$

where $J = L+S, L+L-1, \dots, L-S$, depending on the particular state of the atom. Note that when $L = 0$, $g_J = g_e$. This is true of H and N in their ground states. Oxygen exists in the thermally accessible states $^3P_{2,1,0}$, where the superscript is $2S+1$ (spin multiplicity) and the subscripts are the values of J . The letter represents the value of L (i.e., S for $L = 0$; P for $L = 1$; D for $L = 2$, etc.). For both the 3P_2 and 3P_1 states, $g_J = 1.5$, but for $J = 0$, there is no net angular momentum (g_J is undefined) and even though there are two unpaired electrons, this state is diamagnetic.

A discussion of the coupling of rotation to the spin of diatomic molecules is beyond the scope of this chapter, but sufficient information is available in the literature so that, if the analytical need arise, the spectrum can be found.

D. HYPERFINE INTERACTIONS

1. Line Positions

Well resolved ESR spectra of many substances contain hyperfine structure. This hyperfine structure allows the identification of the paramagnetic substance in many cases, and also provides information about the environment of the molecule and the distribution of the electron density within the molecule.

The resonance frequency of an electron depends upon the magnetic field at the electron. Previously the applied magnetic field was assumed to be the field at the electron. Actually, the electron is affected by both the applied magnetic field, H_0 , and any local fields due to the magnetic fields of nuclei, or other effects, H_{local} , so that Eq. (7) may be written

$$h\nu = g\beta(H_0 + H_{\text{local}}) \quad (7)$$

The effect of the magnetic moments of nuclei on the ESR spectrum is called hyperfine interaction, and leads to a splitting of the ESR line (hyperfine structure). Consider a hydrogen atom, composed of an unpaired electron associated with a proton. Since the proton is a charged spinning particle with a nuclear spin, I , of $1/2$, it has a magnetic moment, and the electron will be affected by the magnetic field of the proton as well as that of the applied magnetic field. The proton can be oriented parallel or antiparallel to the direction of the applied field, $M_I = +1/2$ or $M_I = -1/2$. The relative orientation of the nuclear magnetic moment in the magnetic field is unchanged during electron magnetic transitions, so that only two allowed transitions can occur. The result is a splitting of the original line into a doublet (Fig. 3).

Another way of visualizing the resulting spectrum is as follows: When the proton points in the same direction as the applied field, the electron finds the appropriate resonance H at the lower value of H_0 . When the proton magnetic moment opposes the field, a higher value of H_0 is needed for resonance. The magnitude of the splitting, usually given in gauss, is called the hyperfine coupling constant, a . For the hydrogen atom, a_H is about 506 gauss. In general, a single nucleus of spin I , will cause a splitting into $(2I + 1)$ lines, so that interaction with a single nitrogen nucleus (N^{14} , $I = 1$) will cause a splitting into three lines, and unpaired electrons in manganese(II) (Mn^{55} , $I = 5/2$) interacts with the nucleus to form a six-line spectrum. Many common nuclei, such as carbon-12 and oxygen-16 have zero spin and do not interact with the electron.

The $(2I + 1)$ line positions H_k for an equivalent set of nuclei are given by Eq. (8),

$$H_k = \frac{h\nu}{g\beta_e} - a_i M_i - \frac{a_i^2}{H} \left[I(I+1) - M_i^2 \right] \quad (8)$$

where $a_i = hA_i/g\beta$, and A_i is the isotropic value of the hyperfine splitting constant, and M_i is the quantum number of the component of nuclear spin in the direction of the magnetic field. The bracketed term on the right-hand side of Eq. (8) accounts for a second-order correction. This is usually small enough to be neglected when the hyperfine splittings are small at large applied fields. In that case, the ESR spectrum of $2I+1$ evenly spaced lines will be centered around the field $h\nu/g\beta_e$. Deviations from first order result because the electron and nuclear spins are not decoupled by the magnetic field; i.e., the values of M_i and M_S are not good quantum numbers and cannot be treated independently.

2. Relative Intensities

When the high field approximation is valid, the relative intensities of the lines of an equivalent set of nuclei are given by coefficients of the expansion of $(a+b+c+\dots)^n$ where the number of symbols within the bracket is equal to $(2I+1)$. For example, for spin $1/2$ there are two terms, for spin 1, three terms, etc., and n represents the number of equivalent nuclei. For the simplest case; i.e., nuclei of spin $1/2$, $(a+b)^n$ is the binomial expansion. For a spectrum with more than one equivalent set of nuclei, the relative intensity of a line is proportional to the product of the degeneracies from each set of nuclei. Examples of the analyses of ESR spectra are given below.

For a system with the unpaired electron interacting with two equivalent $I = 1/2$ nuclei (protons), the analysis shows that formation of a triplet occurs with relative intensities 1:2:1 (Fig. 4). The two protons may either both oppose or both act in the direction of the magnetic field, causing the two extreme lines, or they may act in opposite directions from one another, essentially canceling their effect on the electron, resulting in the line located at the same position as the unperturbed line. Since this latter condition can occur in either of two ways, this center line is twice as intense as the two extreme lines. Continuing an analysis in this way results in the general conclusion that n equivalent protons cause a splitting into $n+1$ lines; the relative intensities of these lines follow the binomial expansion. For example, the p-benzosemiquinone ion has four equivalent protons, so that its ESR spectrum shows five lines with relative intensities of 1:4:6:4:1, and a coupling constant of 2.4 gauss. For the general case of n equivalent nuclei of spin I , the resulting spectrum exhibits $(2nI + 1)$ lines. For example, two equivalent N^{14} nuclei produce a five-line spectrum of relative intensities 1:3:5:3:1.

For nonequivalent nuclei, each will interact with the electron with a different coupling constant to produce a hyperfine splitting. For example, if the electron interacts with one proton (H_1) with a coupling constant a_1 , and another (H_2) with a coupling constant a_2 , assuming a_1 is much larger than a_2 , a doublet due to the interaction of H_1 , split into a doublet due to H_2 will result (Fig. 5a). Similarly, the interaction of two equivalent hydrogens with a second pair of equivalent hydrogens results in a triplet of triplets for very different coupling constants (Fig. 5b). However, as the values of the coupling constants approach one another in magnitude, the spectra may appear to differ from the above simple behavior (Fig. 5c). Further details on the interpretation of ESR spectra can be found in Refs. 3, 5, 7, 10, 23, 58, and 110.

3. Second-Order Effects

Although second-order effects are small and can usually be neglected, and they contribute no additional information to the ESR spectrum that would not be obtained in the first-order spectrum, they can cause distortions in the spectrum of which the user should be aware. These distortions take the form of shifts in the lines and splittings of lines which would be degenerate in the first-order case.

For the case of a single nucleus, which exhibits a large splitting, Eq. (8) shows that the lines will no longer be uniformly spaced. A representative example is shown in Fig. 6 for a V^{4+} complex in CS_2 which exhibits an isotropic spectrum. In this spectrum there is no line, for $M_I = 0$. If there were, this line would not be equivalent to the field at $h\nu/g\beta_e$ in contrast to first-order spectra. Also notice that the lines are not uniformly spaced. Incomplete averaging of the g- and/or hyperfine tensor causes non-uniform amplitudes. This phenomenon is typical for Mn^{2+} , V^{4+} , and VO^{2+} in solutions.

An additional second-order effect occurs when the spectra are produced by a molecule with a set of several equivalent nuclei. Usually the total nuclear spin $I = n \cdot I_x$ where I_x is the spin of the single nucleus. However, according to the rules of addition of quantized angular momentum, I can also be less than nI_x . For example, for three nuclei of $I_x = 1/2$, I can be $3/2$, but it can also be $1/2$. Thus, a second-order splitting can be observed according to Eq. (8), when the hyperfine splitting is large. Figure 7 illustrates this process for four "equivalent" protons, where $I = 2, 1$, and 0 . Alkyl radicals and many F-substituted radicals exhibit second-order splittings.

4. Mechanism of Hyperfine Interactions

Hyperfine interactions can be classified into isotropic and anisotropic components as in the case of g-factors. In solutions, where the molecule is free to rotate, only the isotropic portions of the hyperfine splittings are observed. The anisotropic part averages to zero. In spectra of single crystals or powders, both the isotropic and anisotropic parts can be separated. As in the case of g-factors, the hyperfine splitting can be written in tensor form. Details of the analyses of these spectra can be found in Refs. 1, 5, 6, 23, 48, 85, 100, and 110.

Contact Interactions: Contact interactions are dependent upon unpaired electron density at the nucleus, according to Eq. (9)

$$A_1 = \frac{8\pi}{3h} g\beta_e g_N \beta_N |\psi(0)|^2 \quad (9)$$

where g_N and β_N are the nuclear g-factor and nuclear magneton, respectively,

and $|\psi(0)|^2$ represents the probability of the unpaired electron being at the nucleus. Only s-orbitals have a finite probability at the nucleus, for all others $|\psi(0)|^2 = 0$ at $r = 0$. However, many systems with unpaired electrons in p- or d-orbitals do exhibit isotropic splittings. In these cases, the p-orbital will polarize the inner shell electrons, as illustrated for the CH fragment of an aromatic system in Fig. 8. Note that the p-orbital contains the unpaired electron, but the C(sp²)-H(s) bond is polarized such that the spin near the C-atom is the same as that of the unpaired electron in the p-orbital while that near the H-atom is opposite to that of the unpaired electron. Splittings which result when the spin at the nucleus is parallel to the unpaired electron are said to be positive, while those which result when the spin at the nucleus is opposite to the unpaired electron are said to be negative. Alternatively, spin can be transferred to another atom such as between the p-orbital of a carbon atom and the proton of an adjacent CH₃ group. The spin on the proton in this case is of the same direction as the p-orbital. This is often called hyperconjugation.

In most systems containing unpaired electrons there are local variations of the spin direction (Refs. 1, 5, 6, 7, 10, 14, 23, 38, 48, 58, 95, and 110). Thus the net spin at a given nucleus is the difference between positive and negative contributions. In many transition metal complexes, the dominant hyperfine splitting is due to the nucleus of the ion. In most organic radicals, and inorganic radicals, the unpaired electron is delocalized over the molecule, and significant hyperfine splittings will be observed for many atoms.

Dipolar Interactions: Hyperfine splittings which arise from dipolar interactions between the nucleus and the electron can only be resolved for rigid samples, and are therefore not as important in analytical applications as hyper-

fine splittings which arise from contact interactions. Equation (10) governs the behavior of the dipolar interaction as a function of orientation of the radical in the magnetic field,

$$E(\theta) = g\beta_e g_N \beta_N \frac{1 - 3\cos^2\theta}{\langle r^3 \rangle} \cdot S \cdot I \quad (10)$$

where r is the electron-nuclear separation and θ is the angle between the applied field and the line joining the dipoles. The average of Eq. (10) over all orientations θ is equal to zero.

E. ELECTRON-ELECTRON DIPOLAR INTERACTIONS

Triplet states of organic molecules and high spin states of transition metal ions have more than one unpaired electron. These electrons may interact with each other by virtue of their dipole moments. The energy of interaction is similar to Eq. (10), and is

$$E(\theta) = \left[g^2 \beta^2 \frac{1 - 3\cos^2\theta}{\langle r^3 \rangle} \right] \cdot S_1 \cdot S_2 \quad (11)$$

When this coupling is strong, the system is very anisotropic, and solution spectra cannot be observed. If the term in brackets is smaller than the resonant frequency, then for powdered, frozen or crystalline samples "forbidden transitions" can also be observed at about one-half of the normal applied field. In single crystals, the $g = 2$ resonance lines are strongly orientation-dependent, so that in powdered samples the resonance profile is spread over a large field. In addition to the $\Delta M_s = 1$ transitions, a forbidden " $\Delta M_s = 2$ " forbidden resonance can be observed at about one-half of the normal resonance field.

This line is only slightly orientation-dependent. It is weak relative to the $\Delta M_s = 1$ lines exhibited by a single crystal, but strong relative to typical spectra exhibited by a powder. The transition probabilities of the $\Delta M_s = 2$ line are difficult to calculate so that this line can only be used to determine the relative amounts of the paramagnetic sample, and has often been used to determine the population of states in which there may be a small separation of singlet and triplet energies.

F. LINESHAPES AND RELAXATION

The lineshapes in electron spin resonance are typically Lorentzian or Gaussian. The equations of the normalized lines (integral of the absorption between $H = 0$ to $H = \infty$) are given in Table 3. Lorentzian lineshapes reflect the fundamental magnetic resonance and relaxation of a single transition, while Gaussian lines are inhomogeneously broadened envelopes of narrower unresolved lines. As will be seen, it is important to determine whether a derivative curve is either Gaussian or Lorentzian. Table 4 shows that the Gaussian curve decreases much more rapidly in the wings of the line than does the Lorentzian curve. However, in the field between the magnetic resonance center and ± 0.7 times the peak-to-peak width, there is little distinction between both lineshapes. It is therefore important to analyze the lineshape away from the central portion.

It was mentioned earlier that many ESR transitions can be saturated by the available power in an ESR spectrometer. A solution of the Bloch equations which govern the relaxation behavior shows that the power absorbed, P_a , is proportional to the imaginary part of the complex susceptibility χ'' ,

Table 3. Comparison of Normalized Lorentzian and Gaussian Lines*

	Lorentzian Lineshape	Gaussian Lineshape
Equation for Normalized Absorption	$Y = \frac{1}{\pi\Gamma} \cdot \frac{\Gamma^2}{\Gamma^2 + (H-H_O)^2}$	$Y = \left(\frac{\ln 2}{\pi}\right)^{1/2} \cdot \frac{1}{\Gamma} \exp\left[-\frac{\ln 2(H-H_O)^2}{\Gamma^2}\right]$
Half Width at Half Height	Γ	Γ
Equation for First Derivative	$Y' = -\frac{1}{\pi\Gamma} \cdot \frac{2\Gamma^2(H-H_O)}{[\Gamma^2 + (H-H_O)^2]^2}$	$Y' = -\frac{2(\ln 2)^{3/2}}{\pi^{1/2}\Gamma^3} \cdot (H-H_O) \exp\left[-\frac{\ln 2(H-H_O)^2}{\Gamma^2}\right]$
Peak-to-Peak Amplitude	$2Y'_{\max} = \frac{3\sqrt{3}}{4\pi} \cdot \frac{1}{\Gamma^2}$	$2Y'_{\max} = 2\left(\frac{8}{\pi e}\right)^{1/2} \frac{\ln 2}{\Gamma^2}$
Peak-to-Peak Width	$\Delta H_{pp} = \frac{2}{\sqrt{3}} \Gamma$	$\Delta H_{pp} = \left(\frac{2}{\ln 2}\right)^{1/2} \Gamma$

*Taken from Ref. 2.1

Table 4. Diagnostic Criteria for Derivatives of Gaussian and Lorentzian Lineshapes

$\frac{(H - H_0)}{1/2\Delta H_{pp}}$	Height Above Baseline/Maximum Height	
	Lorentzian	Gaussian
1.00	1.000	1.000
1.40	0.911	0.849
1.50	0.870	0.808
1.60	0.828	0.733
1.70	0.784	0.661
1.80	0.739	0.587
1.90	0.696	0.515
2.00	0.653	0.446
2.20	0.572	0.331
2.40	0.500	0.222
2.60	0.436	0.146
2.80	0.379	0.092
3.00	0.333	0.055
3.50	0.240	0.012
4.00	0.177	.002
4.50	0.133	
5.00	0.102	
6.00	0.063	
7.00	0.041	
8.00	0.029	
10.00	0.015	

$$P_a \propto \chi'' H_1^2 = \frac{\omega_o \omega \gamma \chi_o T_2 H_1^2}{1 + (\omega_o - \omega)^2 T_2^2 + \gamma H_1^2 T_1 T_2} \quad (12)$$

where the equation is given in terms of frequency ($2\pi\omega$) units rather than magnetic field. The parameter χ_o is the static magnetic susceptibility, H_1^2 is the r.f. magnetic field and is proportional to the incident microwave power, γ is the magneto-gyric ratio $g\beta/\hbar$, and T_1 and T_2 are the spin-lattice and spin-spin relaxation times. The means by which energy is dissipated is strictly through spin lattice relaxation at the rate governed by T_1 . Thus, as long as $\gamma H_1^2 T_1 T_2 \ll 1$ the population of the spins will be undisturbed from that given in Eq. (5), and the power pumped into the system is effectively dissipated. However, when $\gamma H_1^2 T_1 T_2 \sim 1$, then the spins are being pumped to a higher level at a rate faster than they can relax to the level established by thermal equilibrium. The ratio of the numerator and denominator determine the net power absorbed. An increase in the denominator reflects a decrease of the population difference between spins in the upper and lower states, while the absorption of power by the remaining spins is still linear with H_1^2 . At this point, P_a will increase more slowly than linearly with incident power. At the limit where $\gamma H_1^2 T_1 T_2 \gg 1$, the power absorbed will approach a constant value because sufficient energy will be put into the system to maintain an equal spin population. This is known as saturation. In the absence of saturation, the linewidth is governed only by T_2 .

A "rule of thumb" can be given to predict the effect of incident power which is typically valid above 77°K. If W is the microwave energy in the cavity, and P is the incident power

$$W = P \frac{2Q_L}{\omega} \quad (13)$$

where Q_L is Q of the cavity containing the sample. Usually the sample is placed in the region where H_1 is a maximum. In this case, one can neglect the electric field component of the r.f. field, and it can be shown that

$$2P \frac{Q_L}{\omega} \sim \frac{1}{4\pi} H_{1(\max)}^2 (V_c/4) \quad (14)$$

where V_c is the cavity volume. The component of the field which causes resonance is actually 1/2 of H_1^2 calculated in Eq. (14). Combining all of the appropriate constants,

$$H_1(G) = 6.3 \left[\frac{P(\text{watts}) Q_L}{v(\text{MHz}) V_c(\text{cm}^3)} \right]^2 \quad (15)$$

Typical values of Q_L for a rectangular cavity are often between 1000 and 5000, depending upon the sample. If the value calculated for H_1^2 is in the order of, or greater than the peak-to-peak linewidth, then the spectrometer is invariably set in a region which can saturate the sample. In that case, the investigator should determine carefully whether the sample is being saturated. Typical values can be used to illustrate this process. Assume $Q_L \sim 4000$, $v = 10^4$ MHz, $P = 1$ mW, and $V_c = 10 \text{ cm}^3$. Equation (15) gives $H_1 \sim 0.04$ G. This is probably large enough to begin to saturate many organic radicals which exhibit linewidths in the order of 0.06 G or less, but will not saturate transition metal ions in which the linewidths are usually greater than about 2 G.

It is important therefore to determine that in an analytical experiment, the incident power does not cause saturation of the spin system. Before this can be ascertained, the behavior of detectors used in ESR must be understood. There are two regions in detector response. These are the square-law region

where the output voltage is linear with power, and the linear region where the output voltage is proportional to the square root of the incident power. This is confusing unless it is realized that $E_{in}^2 \propto P_{in}$, so that in the linear region $E_{out} \propto E_{in}$ while in the square-law region $E_{out} = E_{in}^{1/2}$. For reasons of sensitivity, the ESR spectrometer is usually set so that the detector is in the linear region. Thus, in the absence of saturation, the ESR signal amplitude will be proportional to the square root of the incident power.

III. EXPERIMENTAL TECHNIQUES

A. INSTRUMENTATION

1. Basic Spectrometer

Since the radiation used in ESR spectroscopy is in the microwave region, an understanding of ESR instrumentation requires some knowledge of the operation of microwave components. A brief description of these and other spectrometer components and the design of a typical commercial ESR spectrometer will be given. Detailed discussions of the design and operating techniques of ESR spectrometers can be found in the general references, particularly in the books by Alger,³ Poole,⁸⁷ Wilmhurst,¹¹⁵ and Ingram.⁵⁸ A typical spectrometer (Fig. 9) consists of the radiation source, the klystron, and the wave guide, attenuators, isolators and couplers for conveying the radiation to the sample contained in a resonant cavity. The microwave radiation is maintained monochromatic at the resonant frequency by an AFC feedback circuit. The sample cavity is usually contained on one arm of a balanced hybrid T or circulator bridge. Absorption of energy by the sample causes a change in the microwave energy reflected to the diode detector. The magnetic field at the sample is produced by a large electromagnet which is slowly (several minutes to several hours) scanned and by modulation coils which cause a sinusoidal variation of the field at the

modulation frequency (typically 35 Hz to 100 KHz). This field modulation causes the signal reaching the crystal detector to be modulated. The detected signal is amplified, demodulated with a phase-sensitive detector, and the resulting dc voltage displayed on a recorder. As a result of the use of field modulation, the demodulated signal is approximately equal to the derivative of the absorbed power as a function of magnetic field.

2. Spectrometer Components

a. Klystrons

The source of radiation is a klystron. These are available for frequencies of 2.5 to 220 GHz, although most analytical work is performed in the X-band (3 cm) region at about 9 GHz. A klystron can be tuned over about $\pm 3\%$ of its central frequency by varying the dimensions of the resonant cavity inside the tube. The output frequency is also a function of the resonator and reflector voltages applied to the klystron by the power supply. It is usually stabilized against temperature variations by immersion in an oil bath or by forced air or water cooling. A feedback automatic frequency control (AFC) circuit, utilizing a portion of the signal fed back from the sample cavity, stabilizes the klystron frequency to about 1 to 10 ppm. The output power of typical klystrons used in ESR spectrometers is about 150 to 700 mW. Recently solid state Gunn diodes have also been used for ESR.

b. Waveguides, Attenuators, Isolators

The microwave radiation is conducted to the bridge, sample, and detector by a waveguide, which is a hollow, rectangular tube of copper or brass plated with silver or iridium. The dimensions of the wave guide depend upon the

wavelength of the microwave radiation employed. For X-band the cross-sectional dimensions are 0.9 by 0.4 in. The microwave power propagated down the waveguide can be decreased by inserting a variable attenuator, consisting of a piece of resistive material, into the waveguide. The power at the sample may thus be attenuated by a factor of 10^2 to 10^6 (20 to 60 dB). Reflection of microwave power back to the klystron is prevented by an isolator, which is a strip of ferrite material that passes microwaves in only one direction. This helps to stabilize the klystron frequency.

c. Cavities

The sample is contained in a resonant cavity (Fig. 10). This is essentially a piece of wave guide one or more half-wave lengths long in which a standing wave is set up. The cavity is analogous to a tuned circuit (e.g., a parallel R-L-C combination) used at lower frequencies. A measure of the quality of the cavity, which directly affects spectrometer sensitivity, is its Q-value or Q-factor, defined as

$$Q = \frac{\text{energy stored in cavity}}{\text{energy lost per cycle}} \quad (16)$$

The standing wave in the cavity is composed of both magnetic and electric fields at right angles to each other. Two cavities which are frequently employed are the rectangular TE_{102} cavity and the cylindrical TE_{011} cavity. The rectangular cavity used on Varian spectrometers is shown in Fig. 11. Typically the Q of a cavity without a sample (the "unloaded Q") is about 7000 for such a cavity. Since the component of the microwave radiation which interacts with the sample is the rf magnetic field, the sample is located in the cavity where this field

is at its highest. The rf electric field also interacts with the sample, however, and if the sample has a high dielectric constant (i.e., is "lossy") the Q of the cavity may be decreased significantly. Therefore, the sample is usually located in the cavity in a position of maximum rf magnetic field and the minimum rf electric field. Rectangular flat cells with a thickness of about 0.25 mm and sample volume of 0.05 ml are often used for aqueous samples (which are particularly lossy) in rectangular cavities. With such a cell the loaded Q of the cavity is about 2250. Tubing of 3- to 5-mm i.d. with sample volumes of about 0.15 to 0.5 ml can be used with samples that are not lossy.

Other variations of the basic cavity design include rotatable cavities for studying anisotropic effects in single-crystal and solid-sample studies. Dual cavities, consisting of two TE_{102} cavities joined to form a TE_{104} cavity, can be employed for simultaneous spectroscopic observation of a sample and a standard. These are particularly useful for precise g-value determinations and quantitative measurements. Slots can be machined into the walls of the cavity (parallel to the current direction in the walls) without degrading appreciably the cavity Q factor. Observation of species generated by irradiation of the sample with ultraviolet or visible light can thus be carried out. Cells are also available for electrogeneration of paramagnetic species directly in the cavity and for chemically producing them by flow mixing reagent streams near the sensitive portion of the cavity.

The components of the microwave assembly can be coupled together by a variety of methods. Frequently irises or slots of various sizes are used. For example, the resonant cavity can be attached to the waveguide with a standard sized flange and coupled by an iris. Matching of waveguide elements (which is

analogous to impedance matching in conventional circuits) is accomplished by screws or stubs, which can be positioned in the wave guide or across the coupling iris (see Fig. 11).

d. Detectors

Detectors used for microwave radiation for frequencies of 3 GHz and above are diodes that convert the rf radiation to dc. These diodes are biased so that they do not rectify the modulation frequencies (100 kHz or smaller). Thus a detected 100 kHz modulated rf wave consists of a 100 kHz signal. Initially, silicon-crystal detectors, usually selected for low noise characteristics, were used. To minimize 1/f noise, which is fairly high for this type of detector, 100 kHz magnetic-field modulation is used. A problem with 100 kHz modulation is that sidebands at about 36 milligauss on either side of the absorption line may arise; these are troublesome if the signal linewidth is less than about 60 milligauss, which is typical of organic radicals in solution. Superheterodyne methods can be employed in such cases, but such spectrometers, which require two klystrons, usually do not permit high incident powers and are sometimes difficult to tune and lock so that they have not found wide general application. More recently Schottky-barrier diodes and backward diodes have been used as detectors. They do not require as much incident rf power to bias them in their most sensitive regions and they have lower 1/f noise characteristics. Microwave transistors recently developed also show promise as detectors for some ESR applications.

e. Magic T and Circulator Bridges

Rather than employ a detection technique that requires the observation of a small decrease in a large zero signal, which prevents very high

amplification, a bridge arrangement is generally used. This permits the observation of a small microwave signal and is analogous to the resistance-bridge arrangement used in gas chromatography. Microwave bridges (which are analogous to impedance bridges in conventional circuits) can be of the "magic T" or "hybrid T," or circulator variety. A magic T bridge is shown in Fig.

12. Power from the klystron and attenuator entering arm A will divide between arms B and C if the impedance of B and C is the same; no power will enter arm D, to the detector. Under these conditions the bridge is said to be balanced. If the impedance of arm B changes, say because the Q of a resonant cavity coupled to the end of arm B changes when ESR absorption by the sample occurs, the bridge becomes unbalanced and the difference between the power reflected from arms B and C enters into arm D, and is detected.

Circulators behave in a similar way to hybrid T bridges. As before, microwave power enters, but is divided between the clockwise and counter-clockwise paths. Since the reflected power from each arm must complete a loop, twice as much power is incident on the cavity. As before, the difference between the power reflected from arms analogous to C and B of the hybrid T enters arm D, which houses the detector. This bridge geometry (whether wave guide, ferrite or strip line) has an advantage over the hybrid T arrangement because it allows twice as much power at the detector and twice as much power into the cavity; thus a better signal-to-noise ratio is obtained with a circulator element as the microwave bridge. A magic T bridge is used in the Varian V-4502 spectrometer while a circulator is employed in the E-line series. In practice the bridge is usually slightly unbalanced initially (i.e., with no ESR signal) to bias the detector into its most sensitive region. Alternatively, power is passed around the bridge element to the detector. This permits the cavity to be coupled to the waveguide for optimum sensitivity.

f. Magnets

An electromagnet capable of producing fields of at least 5000 gauss is required for X-band ESR. The homogeneity of the field for solution studies should be about 50 milligauss for studies of organic radicals and 1 to 2 gauss for most transition metals over the ESR sample region. This homogeneity and stability is much less than that required for high-resolution NMR studies, so that the stabilizing systems, "shimming" coils, and sample spinning techniques used in NMR are not necessary. Thus magnets with four- or six-inch pole piece diameters are often employed in ESR spectrometers, although nine-inch or larger magnets offer wider gaps, which are convenient in many types of ESR work, and allow easier attainment of the required homogeneity over a larger volume. The ESR spectrum is recorded by slowly varying the magnetic field through the resonance condition by sweeping the current supplied to the magnet by the power supply; this sweep is generally accomplished with a variable-speed motor drive. Both the magnet and the power supply may require water cooling. In most cases the magnetic field is regulated by using a feedback circuit to sense changes in the magnetic field and correct for these changes. This approach involves the use of a field-strength sensor (e.g., a Hall probe or rotating coil), which generates a signal that is proportional to the field.

g. Modulation Coils

The modulation of the signal at a frequency consistent with good signal-to-noise ratios in the crystal detector is accomplished by a small alternating variation of the magnetic field. Modulation amplitudes from 0.05 to 40 gauss peak-to-peak are frequently used. This variation is produced by supplying an ac signal to modulation coils oriented with respect to the sample in the same

direction as the magnetic field. For low-frequency modulation (400 Hz or lower) the coils can be mounted outside the cavity and even on the magnet pole pieces. Higher modulation frequencies (1 KHz or higher) cannot penetrate metal effectively, and either the modulation coils must be mounted inside the resonant cavity or cavities constructed of a nonmetallic material (e.g., quartz or ceramic) with a thin silver plating must be employed.

At high modulation amplitudes, (e.g., larger than 10 gauss) heating of the cavity can occur. This causes dimensional changes in the cavity and may result in baseline drift.

3. Commercial Spectrometers

A typical commercial ESR spectrometer is shown in Fig. 13 and several types which are currently in use and their characteristics are shown in Table 5. Although the systems involving low frequencies (200-800 MHz) can employ a small permanent magnet or Helmholtz coils and are relatively inexpensive, their sensitivity is low and they are mainly employed for educational and demonstration purposes. The bulk of the analytical methods and research studies have employed X-band spectrometers. In recent years dedicated minicomputers have been incorporated into the spectrometer and signal-averaging devices (e.g., computers-of-average transients, CAT's) have been used to improve the signal-to-noise in very weak spectra.

B. SENSITIVITY

The sensitivity of a spectrometer, in terms of the smallest detectable concentration of a given species, depends upon spectrometer parameters (e.g., microwave power, cavity Q, bandwidth and detector, klystron and amplifier

Table 5. Typical Characteristics of ESR Spectrometers

Frequency	Sensitivity ¹ (Unpaired Spins)	Cavity	Magnetic Field at Frequency for $g = 2$ (gauss)	Manufacturer ²
335 MHz	10^{14} ΔH	Helix	120	Alpha, Ealing
200-800 MHz		Helix	70-290	Bruker
3 GHz (S-band)	2×10^{13} ΔH		1100	Bruker, Micro-now
9.5 GHz (X-band)	2×10^{11} to 5×10^{10} ΔH	TE_{102} , TE_{104} , TE_{011} , TE_{101}	3400	Bruker JEOL Micro-now Varian Decca Thompson-CSF Ventron Hilger and Watts
24 GHz (K-band)	10^{10} ΔH	TE_{012} , TE_{011}	8600	Bruker JEOL Ventron
35 GHz (Q-band)	$5-6 \times 10^9$ ΔH	TE_{011} , TE_{012}	12500	JEOL Varian Ventron
70 GHz (V-band)	10^9 ΔH	TE_{012} , TE_{011}	25000	Ventron

¹Approximate; represents the minimum number of detectable spins, where ΔH is the signal line-width in gauss at half-maximum absorption with a 1-second time constant

²Alpha Scientific Laboratories, Inc., no longer manufactured
Bruker Instruments, Inc., Billerica, Massachusetts
Decca, no longer manufactured
The Ealing Corp., South Natic, Massachusetts
Hilger and Watts, London, England
JEOL Analytical Instruments, Inc., Cranford, New Jersey
Micro-now Instrument Co., Inc., Chicago, Illinois
Thompson-CSF, no longer manufactured
Varian Instrument Division, Palo Alto, California
Ventron Instruments, Corp., no longer manufactured

noise), signal parameters (e.g., linewidth, relaxation times), and sample characteristics (e.g., solvent). The absorption signal depends on the magnetic susceptibility of the sample, which, in turn, is a function of the number of unpaired electrons or spins contained in the cavity. In general, the minimum number of detectable spins N_{\min} , is proportional to several variables^{39, 87}

$$N_{\min} \propto \frac{\Delta v}{Q_0 \eta v_0} \left(\frac{\Delta f k T}{2 P_0} \right)^{1/2} \quad (17)$$

where Δv is the linewidth of the absorption, Q_0 is the Q of the unloaded cavity, η is the filling factor described in Eq. (18), v_0 and Δv are the frequency and linewidth of the absorption, Δf is the bandwidth of the response of the spectrometer, P_0 is the incident power, k is Boltzmann's constant, and T is the detector temperature in degrees Kelvin. The filling factor measures the effectiveness of coupling of the sample to the microwave magnetic field and is essentially the integral of the power density over the sample divided by the integral of the power density over the volume of the cavity,

$$\eta = \frac{\int_{V_s} H_1^2 dV_s}{\int_{V_c} H_1^2 dV_c} \quad (18)$$

where H_1 is the rf magnetic field, V_s is the sample volume, and V_c is the cavity volume.

To maximize the sensitivity of the spectrometer, several parameters in Eq. (17) can be optimized. For example, the incident power can be increased, assuming that the absorption is not saturated, and the extent of filtering can be increased (i.e., the Δf decreased). Often it is possible to use a higher

microwave frequency (and thus a higher H) to increase the population difference between the two energy levels. For a given quantity of sample, where the geometry is kept the same (except that the dimensions of the cavity are made proportional to the frequency), it can be shown that the sensitivity is proportional to $\nu_0^{7/2}$. In practice, however, the cavity Q decreases at higher frequencies, and klystrons and detectors are more noisy. Theoretically, a hundredfold increase in sensitivity would be expected on increasing the frequency from 9 to 35 GHz, but in fact only a tenfold gain is usually realized. On the other hand, if the sample size is unlimited, the sensitivity per unit volume of sample actually decreases at higher frequencies. It can be shown that if the same geometry is maintained, the minimum detectable concentration is theoretically proportional to $\nu_0^{-1/2}$.

Finally, one must consider the filling factor and the cavity Q . For a given sample the best signal-to-noise ratio is obtained when the cavity Q is reduced to two-thirds of that of the unloaded cavity by introducing the sample. This puts some constraint on the filling factor for a given sample with a minimum reduction of Q . As a general rule, at X-band frequencies, rectangular cavities provide better performance for lossy samples, while cylindrical cavities show better sensitivity for small-volume or solid samples. For X-band spectrometers concentrations of about 10^{-9} M can probably be determined in samples with very low dielectric losses. For aqueous solutions, 10^{-7} M probably represents a realistic estimate of the lower limit of detection. Of course, signal averaging techniques can improve the signal-to-noise and increase the effective sensitivity, assuming that the magnetic field and spectrometer parameters can be maintained constant over the times necessary to accumulate the signals. Signal averaging will probably be more useful in the detection and identification of species than in their quantitative determination.

C. TREATMENT OF DATA FOR ANALYTICAL APPLICATIONS

1. Spectroscopic Analysis

The ESR spectrum is usually recorded directly from a phase-sensitive detector as the first derivative of the absorbed power as a linear function of the applied magnetic field. Spectroscopic analysis; i.e., determination of g-factors, hyperfine splittings, and zero-field splittings, useful for qualitative analysis can be derived directly from this data. This is discussed in all of the general texts.

2. Quantitative Analysis

There are two general types of quantitative analysis that can be carried out using ESR. The first of these is general to analytical spectroscopy and involves the preparation of standards of a similar nature to the unknown, and a comparison of the amplitude of response of the unknown to those of the standard. The second method is essentially an absolute calibration which relies on the fact that the transition probability of the unpaired electron can be calculated accurately from the spectroscopic data. This allows any well-characterized material to be used as a standard.

3. Method of Direct Comparison

When a direct calibration of the signal response is carried out utilizing known samples, generally the peak-to-peak amplitudes of the ESR signal are used as a measure of concentration. For most species, the amplitude of response for a given molecule will be linear with concentration over several orders of magnitude. As the concentration increases, however, the lines will begin to broaden

so that the amplitude will become less than linear with concentration. This broadening is due to exchange of unpaired electrons between molecules which tends to average the hyperfine fields to yield one line at very fast exchange rates. Nevertheless, this broadening will not affect the analysis provided the concentration of the unknown is within the limits of the standards.

There are also several instrumental conditions which must be maintained during the analysis. The ESR spectrometer output is the derivative of the power absorbed, as opposed to optical spectrometers in which the output signal is a function of the relative power absorbed by the sample. Since the ESR signal is usually proportional to the square root of the incident power (Sec. II.F), it is important the incident power be accurately set. It is also important that the iris on the ESR cavity be reset to the same point. This is easily done by keeping the current through the detector (crystal current or leakage current) the same. Finally, even under conditions of partial power saturation of the ESR signal, analyses can be carried out because the response of the unknown will be identical to the standard. The linearity of the ESR signal is dependent upon a small change in the Q-factor of the cavity during resonance. For very intense signals, the Q-factor will change significantly and again the ESR signal will increase less than linearly with concentration.

4. Sample Handling

For accurate analyses, several precautions must be taken to insure that reproducible results are obtained. These are listed below.

1. For liquid and gaseous samples the same cells must be used, and these must be positioned reproducibly in the cavity. Unlike UV spectroscopy, ESR samples are much smaller than the wavelength so that they must be placed at the same region of oscillating magnetic field.

2. For a liquid sample, the same solvent should be used for the standards and samples. Different solvents have different losses, and thus changes in the cavity Q may result if different solvents are used.
3. Solution concentrations of electrolytes greater than ca 0.5 M will alter the cavity Q factor, and thus change the calibration factor.
4. If powdered samples are used, they must also be of the same geometry as the calibration sample, and preferably of the same matrix.

Typically, powdered samples do not affect the Q of the cavity as much as liquids unless they are good conductors.

Several useful techniques to assist analyses have been reported in the literature. Often "flat cells" are used for liquid samples, however, it was found that a cylindrical 3mm tube held in place by Teflon plugs which fit firmly into the collet rings of the ESR cavity (Fig. 11) insure reproducible repositioning of liquid samples.²⁸

Often a dual cavity is used to assure reproducible ESR settings. In this application, an arbitrary reference sample is used, so that if the ESR settings are changed between experiments, the amplitude of the reference will also be altered, and a correction can therefore be made. It has also been pointed out that a double internal standard, i.e., two equal secondary standards placed on opposite sides of the unknown sample in the ESR cavity permit an internal calibration for a single-sample cavity. Dilute Mn²⁺ in a host lattice gives no signal within ± 40 G of $g = 2$ since it exhibits no center line.⁷³ This technique was also found to reduce the error caused by varying amounts of water in biological samples which change the cavity Q.

5. Theory of Absolute Measurements

a. General Case

Part of the versatility of the ESR technique is due to the ability to calibrate the instrument with any standard for the determination of an unknown within the constraints of geometry. Most of the theory which relates the ESR signal amplitude to concentration has been developed for use in gas phase work.^{17,112-114} This approach provides the most general treatment, so that the same approach will be followed here. The general case can be simplified for many specific applications, some of which will be considered. Finally, techniques of determining the double integral of the ESR derivative spectrum and errors involved with it will be discussed.

The imaginary part of the susceptibility which gives rise to power absorption for the transition between states *i* and *j* is given by

$$\chi''_{ij} = \frac{n_{ij}}{h} \mu_{ij}^2 f(v-v_0) \quad (19)$$

where n_{ij} is the difference in the number of molecules in the upper and lower spin states (e.g., $N_{-1/2} - N_{1/2}$), $f(v-v_0)$ is a normalized lineshape such that its integral between $v = 0$ and $v = +\infty$ is unity, and μ_{ij}^2 is the square of the transition probability matrix element for the transition between states *i* and *j*. First $f(v-v_0)$ must be converted to a field-dependent function to be consistent with ESR instrumentation. An effective g-factor, g_{eff} is defined as

$$g_{\text{eff}} = \left(\frac{h}{\beta} \right) \frac{dv}{dH} \quad (20)$$

which is analogous to Eq. (4). Usually $g_{\text{eff}} = g$, except in systems in which the hyperfine splitting or dipolar interaction is of the order of the applied field, so that the high field approximation is no longer valid.

The population n_{ij} is given by

$$n_{ij} = \frac{h\nu_0}{kT} \cdot \frac{\exp(-E_i/kT)}{Z} \cdot N \quad (21)$$

where E_i is the energy of the lower state of the transition excluding the contribution from the electron-magnetic field interaction, N is the total number of molecules in the sample, and Z is the partition function. The term $h\nu_0/kT$ arises from the electron-magnetic field interaction, Eq. (5), for an unsaturated sample. The second term arises from thermally-accessible energy levels. For most species, $\exp(-E_i/kT)$ is equal to unity; however, it is important for gas phase systems and for systems such as those which have low energy excited states such as a singlet-triplet state equilibrium or systems which exhibit very large electron-electron dipolar interactions.

Combining Eqs. (19), (20) and (21), the total number of molecules is given by

$$N = \left(\frac{kT}{h\nu_0} \right) \left[\frac{g_{\text{eff}}}{\mu_{ij}^2 \exp(-E_i/kT)} \right] \int_0^\infty \chi_{ij} dH \quad (22)$$

for a system which exhibits a single transition. In most cases, a system will exhibit many transitions. Often some of these transitions are degenerate or unresolved so that it is easier to determine the integral of χ_{ij} over several transitions. Equation (22) then becomes

$$N = \left(\frac{kT\beta}{h\nu_0} \right) \sum_i \left[\frac{(g_{eff})_i^Z}{\mu_{ij} \exp(-E_i/nT)} \right] \int_0^\infty \chi_{ij} dH \quad (23)$$

At this point the partition function and the transition probabilities should be determined. The partition function Z is given by Eq. (24)

$$Z = \sum_i (2J + 1) \prod_k (2I_k + 1)^{n_k} \exp(-E_i/kT) \quad (24)$$

where n_k is the number of nuclei of spin I_k . J can have the values $|L+S|, |L+S-1|, \dots, |L-S|$ as described in Section II.C.5. (For condensed phase species $L = 0$ so that $J = S$.) The product of $(2I_k + 1)^{n_k}$ is the degeneracy due to hyperfine splitting while $(2J + 1)$ is the degeneracy of the spin state.

The transition probability, μ_{ij}^2 is only dependent upon the g-factor and spin, and is given by Eq. (25).^{5, 23, 58, 110}

$$\mu_{ij}^2 = \frac{1}{2} g^2 \beta^2 (J - M_J) (J + M_S + 1) \quad (25)$$

so that Eq. (24) becomes

$$N = \left(\frac{2kT}{h\nu_0 \beta} \right) \left[\sum \frac{g_{eff}^Z}{g_J^2 (J - M_J) (J + M_J + 1) \exp(-E_{J,MJ}/kT)} \right] \int_0^\infty \chi''_{JM_J} dH \quad (26)$$

Equation (26) can be used for all analyses; however, simpler forms can be determined for specific applications.

b. Condensed Phases

Consider, for example, a radical in a solution or a solid with $S = 1/2$, which exhibits only one line. Most radicals have no near lying electronic energy levels so that $\exp(-E_{S,M_s}/kT) = 1$. The value of Z is therefore $2S+1 = 2$, and $(S-M_s)(S+M_s+1) = 1$. In this case, Eq. (26) becomes

$$N = \left(\frac{2kT}{h\nu_0\beta} \right) \cdot \frac{2}{g} \int_0^{\infty} \chi'' dH . \quad (27)$$

If the spectrum of the radical anion was split by four equivalent protons, the degeneracies of each of the five lines are 1:4:6:4:1. The term $(2I + 1)^{n_k} = 16$. If the center line of degeneracy 6 is used, Eq. (26) then becomes

$$N = \left(\frac{2kT}{h\nu_0\beta} \right) \cdot \frac{32}{6g} \int_0^{\infty} \chi'' dH . \quad (28)$$

It can be shown that by substitution of $g\beta H_0$ for $h\nu_0$, and by summing all of the transitions used for the analysis

$$N = \frac{3kT}{g^2 \beta^2 H_0 [S(S+1)]} \cdot \frac{\prod_{k=1}^5 (2I_k + 1)^{n_k}}{\sum_{\ell} D_{\ell}} \int_0^{\infty} \chi'' dH \quad (29)$$

where $\sum_{\ell} D_{\ell}$ is the sum of the degeneracies of all lines ℓ which are used in the analysis. This form of the equation has been used for most analytical work.

In solids when $S > 1$, the crystal fields may cause splittings of the lines with different values of M_s . A typical example would be Fe^{3+} in a cubic host (MgO, for example), where $S = 5/2$, so that five transitions are observed:

$M_s = -5/2 \rightarrow M_s = -3/2, M_s = -3/2 \rightarrow M_s = -1/2$, etc. The hyperfine splitting due to Fe^{3+} is not resolved so that $Z = 6$. In this case if all of the lines are utilized in the analysis, Eq. (29) may be used to determine N , but if only one of the transitions is utilized, Eq. (26) must be used because $(S-M_s)(S+M_s+1)$ will depend upon which transition is selected. In solution, only one line will be observed, so that Eq. (29) will again be valid.

In solution and under most conditions in solids, and for S-state atoms in the gas phase, Eq. (29) can be used to determine analytical concentrations. Upon the condition that there are large fine splittings due to dipolar interactions, in a solid, the more elaborate form, Eq. (26), must be used.

c. Gas Phase

A typical case in which the exponential in Eq. (21) is not unity is in the analyses of gas phase species. This subject is beyond the scope of this chapter, but has been treated in detail.¹¹² For atoms, there are many cases in which there are thermally-accessible states. For example, the oxygen atom (Section II.C.5) has three states, 3P_2 , 3P_1 , and 3P_0 , with energies of 0, 453, and 647 cal/mole, respectively. The 3P_2 state exhibits four closely-spaced lines on either side of the 3P_2 spectrum. The 3P_0 state is diamagnetic. Depending on which lines are used for the determination of 0, Eq. (26) will have different parameters.

Diatomeric species also have rotational components, thus Z must include the rotational partition function as well. In addition, some of the transitions of diatomics such as NO are not only magnetic, but also electric by virtue of the dipole moment.¹⁷ It is therefore convenient in the case of gas phase atoms and molecules to define a term Q given in Eq. (30)

$$Q = \frac{\beta^2 z}{2} \sum_i \frac{g_{(\text{eff})}}{\mu_{ij}^2 \exp(-E_i/kT)} \quad (30)$$

such that

$$N = \left(\frac{kT}{h\nu_0} \right) Q \int_0^\infty \chi''_{1j} dH \quad . \quad (31)$$

Westenberg¹¹² has calculated an extensive list of values of Q for atoms and diatomics at 300°K which can be used for analysis. Most applications of gas phase analysis have been applied to kinetic studies.

d. Double Integration

The value of $\int \chi'' dH$ must be determined from the derivative spectrum. This requires double integration of the ESR signal or similar handling of the data. For any absorption lineshape $f(H-H_0)$,

$$\int_0^\infty \chi'' dH = \frac{K}{A \cdot H_m \cdot p^{1/2}} \int_{-\infty}^\infty \int_{-\infty}^H \left[\frac{df(H-H_0)}{dH} dH \right] dH \quad (32)$$

where the ESR data are presented as $df(H-H_0)/dH$ and K is an instrumental constant which must be determined by calibration for a constant sample geometry. A is the amplification, and p is the incident power. Equation (32) requires that the signal must be doubly integrated. However, it can also be shown that

$$\int_{-\infty}^\infty \int_{-\infty}^H \left[\frac{df(H-H_0)}{dH} dH \right] dH = \int_{-\infty}^\infty (H-H_0) \frac{df(H-H_0)}{dH} dH \quad . \quad (33)$$

That is, the double integral in the limit of integration from $+\infty$ to $-\infty$ can be written as the integral of the product $(H-H_0)[df(H-H_0)/dH]$, Eq. (33). The advantage of this form is that it converges more rapidly than does the double integral.^{29,30}

Although it is important to double integrate a line over the field range from $+\infty$ to $-\infty$ it is never possible to approach this condition because of interferences due to other spectral lines or instrumental drift. Nevertheless, it is a relatively simple matter to correct the integrated portion of the line to approach the limit.

Figure 14 shows the discrepancy between the line integrated between the limits of $+\infty$ and $-\infty$, and the truncated scan. Notice that the first moment (M) converges more rapidly than does the double integral (I) of the derivative curve. In either case, if the lineshape is known (e.g., Gaussian, Lorentzian or an analytical equation) it is a simple matter to correct the integral. For example, for a truly Lorentzian line, the double integral of the derivative of a Lorentzian absorption is given by Eq. (34) for a spectrum recorded between $H_0 - H_a$ and $H_0 + H_a$.

$$I_L = -\frac{2}{\pi\Gamma} \int_{H_0 - H_a}^{H_0 + H_a} \int_{H_0 - H_a}^H \frac{(H-H_0)dH'}{[\Gamma^2 + (H-H_0)^2]^2} dH =$$

$$\frac{2}{\pi} \left\{ \tan^{-1} \left[\frac{(H-H_a)}{\Gamma} \right] - \frac{(H-H_a)/\Gamma}{1 + \left(\frac{H-H_a}{\Gamma} \right)^2} \right\} \quad (34)$$

On the other hand, the first moment is given by Eq. (35)

$$M_L = -\frac{2}{\pi\Gamma} \int_{H_0 - H_a}^{H_0 + H_a} \frac{(H-H_0)^2 dH}{[\Gamma^2 + (H-H_0)^2]^2} = \frac{2}{\pi} \tan^{-1} \left[\frac{(H-H_a)}{\Gamma} \right] \quad (35)$$

Notice that the I_L is smaller than M_L by an amount approximately proportional to $1/(H-H_0)$ for large scans. Since the scan divided by Γ can be determined from ΔH_{pp} (Table 3), a correction can be made. This procedure is illustrated for the double integral of a line due to ground state O_2 at 298°K in Table 6.^{44a} The oxygen line selected, Line C of Ref. 114, was shown to be Lorentzian. All spectra were recorded over the same magnetic field range but due to pressure broadening, the ratio of scan to linewidth decreases with pressure. Even though the ratio of the scan to the linewidth changes by nearly a factor of 2, the correction term does not change by more than a few percent because the spectrum was recorded well into the wings. Yet this correction would allow for O_2 to be used as a calibration for any other gases in the same container. Correction factors of up to about 35% have been used in a number of samples with good results.⁴⁴ Similar methods have been used for powdered isotropic as well as liquid samples.

e. Sources of Error in Data Handling and Recording

Various sources of error in data handling have been discussed in the literature, and quantitative estimates of some of these errors have been provided.^{63, 67, 90} Some authors include in their errors the assumption that the first derivative data starts at an amplitude of zero. We have made the assumption in the correction factors that the true zero point can be determined.

Baseline: Exact determination of the zero point of the derivative signal amplitude is important. Either an offset, α , or a drift $\beta \cdot H$ (assumed linear with field) will cause significant errors. The error due to a fixed offset will cause an error proportional to the square of the scan range for the first moment calculation, while in the double integral calculation a linear term

Table 5. Double Integral and Corrected Double Integral of a Line of Ground State O_2

Pressure	scan $\frac{\Delta H}{pp}$	I_L^* gain·pressure	Correction Factor	I_L (corrected) gain·pressure
0.096	21.3	4.518	1.115	5.038
"	"	4.453	"	4.965
"	"	4.414	"	4.922
0.175	18.3	4.317	1.136	4.904
"	"	4.400	"	4.998
"	"	4.309	"	4.895
0.312	17.1	4.403	1.147	5.050
"	"	4.391	"	5.036
"	"	4.372	"	5.015
0.414	16.7	4.323	1.151	4.976
"	"	4.312	"	4.963
"	"	4.281	"	4.927
0.518	15.7	4.409	1.162	5.123
"	"	4.290	"	4.985
"	"	4.420	"	5.136
0.697	15.0	4.395	1.170	5.142
"	"	4.322	"	5.056
"	"	4.402	"	5.150
0.857	14.5	4.348	1.177	5.118
"	"	4.233	"	4.982
"	"	4.217	"	4.963
0.999	13.6	4.230	1.191	5.038
"	"	4.130	"	4.919
"	"	4.202	"	5.004
Mean		4.337		5.013
σ		0.091		0.078
Relative Error		2.1%		1.55%

* Experiments were carried out at the same incident power, modulation amplitude, and scan rate.

must also be added. For a baseline drift, the error in the first moment will be proportional to the cube of the scan range while for the double integral, a quadratic term must also be added. Thus the first moment offers another advantage in that baseline errors are minimized. Equations have been derived for double integration in the presence of baseline drift.⁷²

We have found that if a spectrum is symmetrical, or if it is recorded into the wings and there is no drift problem, the average value of all of the data points, equally spaced in field, gives an accurate value of the baseline. When there is a drift problem, the spectrum must be recorded far out into the wings, and a line drawn. A good check to find whether the spectrum does approach the baseline for a Lorentzian curve is to plot the derivative signal amplitude against $1/(H-H_0)^3$. This line should extrapolate to the baseline as $H \rightarrow \infty$, and drifts will become evident. This technique has been utilized in ferromagnetic resonance but it has not been applied to paramagnetic resonance.

Power Saturation: The effect of power saturation has been discussed in Section II.E. Since values of T_1 and T_2 of Eq. (12) are not well-known, it is difficult to correct for errors caused by saturation. Even in this case, if standards of the same material can be obtained and the double integral recorded as a function of power, then one can correct for saturation. However, if these standards are available, the peak-to-peak amplitudes can then be used for analysis.

Modulation Broadening: Up to this point we have assumed that the lineshape is the derivative of the absorption. However, a finite modulation amplitude will cause line broadening. Modulation-broadened lineshapes have been calculated for Gaussian and Lorentzian lines,^{22,99,108} and the relative peak-to-peak linewidth $[(\Delta H_{pp}/\Delta H_{pp}^0) \times 100]$ of a Lorentzian line is shown as a function of

modulation amplitude in Fig. 15. H_m is defined by the equation

$H_m(t) = H_m \cos(2\pi f_m t)$ where f_m is the modulation frequency. (In some papers H_m is defined as half of this value in order to be consistent with spectrometers in which the modulation amplitude is given as twice the peak-to-peak value.) Notice that the maximum signal amplitude occurs when the peak-to-peak linewidth is three times that of the width in the absence of modulation. Even at about half of the maximum sensitivity, ΔH_{pp} is 12% larger than the natural value. Randolph⁹¹ has shown experimentally, and Buckmaster has shown mathematically²² that the total double integral of an ESR curve is linear with modulation amplitude even though the lines are broadened. Thus Eq. (32) is valid. Since the wings of the experimental derivative line are not greatly affected by modulation amplitude even for a broadened line, if ΔH_{pp} at a very low modulation amplitude is known, a correction can still be applied to the lines if the scan is outside of $\pm 5 \cdot \Delta H_{pp}$ (experimental).

Cavity Q, Coupling and Spin Quantity: The effect of coupling of the cavity is critical in obtaining reproducibly quantitative ESR determinations. Cavities can be undercoupled, critically coupled or overcoupled to the waveguide. This coupling is adjusted by the iris (Fig. 11). In a critically coupled cavity, the cavity is matched to the waveguide so that there is a minimum signal at the detector for the spectrometer shown in Fig. 9. To bias the detector, rf power can be brought in from a path around the circulator or magic T. Alternatively, the cavity coupling can be changed to provide reflected power. Critical coupling provides maximum sensitivity, but because of bias requirements this is not always possible.

The sensitivity also depends on the Q-factor of the cavity (Eq. (17)). For small samples the Q at resonance Q_R is approximately equal to Q_0 . For

large spin concentrations, $Q_R < Q_0$, and the signal amplitude becomes non-linear with concentration.¹⁰⁷

For large samples overcoupling and undercoupling yield different results, as shown for a large sample in Fig. 16. Overcoupling (Fig. 16b), because of changes when $Q_R < Q_0$, causes the reflected power to decrease while undercoupling causes the reflected power to increase. A very strong sample can cause a large change in the bias power on the detector causing a weaker signal. Clearly the uncoupled or critically coupled case, which are similar (Fig. 16a), are advantageous.

Bias Power: The bias power at a detector must be set reproducibly using the ammeter or voltmeter provided in the spectrometer. Since the signal does not depend strongly on this power level, it does not contribute a significant error, except at very low levels (< 100 μ A using conventional detectors).

D. TRICKS TO IMPROVE ANALYSIS

1. It is a fairly straightforward matter to utilize a desk calculator for double integral or first moment computations.²⁹ However, it is advantageous to utilize a laboratory computer or a device which permits paper tape output. In this way, more data points can be used and thus errors are reduced by the averaging process and a better value of the baseline can be determined.
2. The effective signal-to-noise ratio of an ESR signal is improved by integration⁸⁸ (Fig. 17) so that even if a signal is scarcely detected on the first derivative presentation it can yield a significant double integral if at least 20 data points per linewidth are used.

3. Often an inhomogeneous magnetic field will produce an asymmetric line. If the ESR spectra can be recorded sufficiently far out into the wings, either the average of all data points or an extrapolation is still valid to determine the baseline. Westenberg¹¹² has pointed out that each half of the double integral will yield different values. This is true only if a truncated scan is used. Since the correction factors do not change rapidly with linewidth, the experimental linewidth in the absence of additional modulation broadening can be used for ΔH_{pp} . Auxiliary coils have also been designed to improve field homogeneity.⁴⁶
4. In the case of baseline drift and interference due to adjacent lines, truncating the double integral and applying a large correction factor minimizes errors resulting from the baseline determination. Up to a 35% correction has been used in our laboratories with reproducibility of $\pm 2\%$ or better.
5. The treatment above has been applied to lines in which $H_o \gg \Delta H_{pp}$. When the line is very broad, Eq. (22) must also be multiplied by a factor H/H_o .³⁴ If the entire analysis is carried out, it is found that for $\Delta H_{pp} < 0.2 H_o$, the lineshape is still sufficiently symmetric for most analyses except that the absorption maximum (derivative zero) shifts slightly upfield from the predicted value.
6. The 100 KHz modulation-detection unit of Varian V4502 ESR spectrometers is constructed using 5% resistors for gain and modulation amplitude settings. For accurate analyses these may be calibrated or rebuilt using precision resistors.^{44a}
7. Dual cavities have been used for a sample and quantitative reference.^{55,66} However, changing the sample geometry will alter the microwave field

at the reference material. Thus, using a dual cavity, comparisons are only valid for nearly constant samples and geometries.^{27,90}

8. In addition to utilizing analog computers, digital computers, and desk calculators for double integral and first moment determinations, first moment balances have been constructed in which the spectrum is cut out and placed along an arm of the balance.⁶⁷

IV. ANALYTICAL APPLICATIONS

A. GENERAL CONSIDERATIONS

Direct analysis by ESR is limited to species containing unpaired electrons. Transition metal ions and their complexes, e.g., Mn(II), Cu(II), and V(IV), have been investigated and a number of analytical methods have been proposed. Paramagnetic organic species, i.e., radical ions ($R\cdot$ and R^+) and free radicals ($R\cdot$) have been investigated extensively. While most of this work has been concerned with theoretical treatments or the elucidation of structure or electron distributions, ESR is also very valuable in the identification and determination of such species. When the species of interest is itself not paramagnetic, it frequently can be converted to a paramagnetic species by an appropriate treatment; such techniques are discussed in IV.B.2. Transient radicals can sometimes be stabilized using a "spin trapping" technique. In addition to these direct methods, indirect determinations, where the effect of the component of interest on the ESR signal of another species is observed, are possible. These may involve changes in the amount of the paramagnetic species, e.g., when the compound of interest "titrates" the detected species to form one which does not produce a signal, or changes in line shape or intensity when the added species affects the relaxation processes of the

paramagnetic one (IV.B.3). Qualitative analysis, such as the identification of radical species, is usually based on an analysis of the hyperfine structure of the spectrum (II.C). The fine detail and wealth of information in the patterns of organic radical species in solution makes this technique particularly useful, especially where only a single paramagnetic species is present. Mixtures of radicals present greater problems because their g-values are often quite close, and complicated overlapping spectra result. However, the resolution is often sufficient to allow separate lines to be detected for each component. Computer simulation methods can also be employed for resolution of such spectra. Although the g-values for most organic species are within about 0.5% of the free electron value (II.B), precise measurement of the g-value can sometimes be used to distinguish between different classes of species (e.g., between hydrocarbon and peroxy radicals) or between different forms of a given metal ion (e.g., V-containing species in petroleum). We will subdivide our discussion of applications according to the nature of the medium, since experimental considerations and the results are somewhat different in liquid, solid and gaseous media. Typical examples of analyses by ESR will be given, but an exhaustive coverage of the literature will not be attempted. The analytical uses of ESR before 1965 have been reviewed^{8,43} and reviews of more recent work are also available.^{35,60,61}

B. LIQUIDS

1. Metal Ions in Solution

a. Analysis of Vanadium in Petroleum

Vanadium exists in the paramagnetic +4 state as the VO^{2+} ion in the p.p.m. range in petroleum oils, predominantly as prophyrin complexes. The interaction

of the unpaired 3d electron with the nucleus ($I = 7/2$) produces an eight-line ESR spectrum which shows a more complex pattern in solution (Fig. 6) because of the anisotropy of the g- and hyperfine tensors. Thus ESR can be used for the direct and rapid determination of V without preliminary separations.^{32,33,92,96,106} The peak height of the first derivative of a given hyperfine line was used for the analysis with vanadyl etioporphyrin I dissolved in a heavy oil distillate as a standard.⁹⁶ Special quartz tubes of 3 mm i.d. were used for the samples. The signal intensity was shown to vary with the square root of r.f. power. The modulation amplitude (ca. 5 gauss) was maintained constant for all samples. Amounts of V in the range of 0.1 to several hundred p.p.m. were determined. ESR has also been employed to demonstrate the existence of V(IV) in several different forms¹⁵ in petroleum.^{32,33} This was accomplished by showing that different fractions of the petroleum showed different isotropic g-values with shifts of 22.3 to 25.8 parts per thousand from the free electron value.

b. Determination of Other Metal Ions in Solutions

A number of studies have been concerned with the effect of instrumental (e.g., receiver gain, G, modulation amplitude, M, and r.f. power, P) and procedural variables on quantitative analysis of transition metal ions by ESR.^{21,50-53,60,76,79,80} A typical analysis is that of Mn(II), which shows a strong, six-line spectrum from interaction of the unpaired electron with the nucleus with $I = 5/2$ and $g = 2$ (Fig. 18). By reproducible tuning of the spectrometer and use of an aqueous quartz flat cell good precision (standard deviation of 0.4%) could be obtained.⁵⁰ At constant r.f. power a plot of $S/G \cdot M$ (where S is the peak-to-peak signal amplitude of the fourth downfield line) was linear with concentration (on a log-log plot) between

10^{-3} and 10^{-6} M Mn^{2+} . An accuracy of 2% was obtained for a useful analysis range of 0.1 to 10^{-6} M. The variation of S with power (P) was also investigated.^{21,80} In general the signal varies nonlinearly with P (Fig. 19). It was suggested that the power dependence could be removed by using as the parameter on the analytical curves $S/G \cdot M \cdot \log P^{80}$ or $S/G \cdot M \cdot P^k$ (where k is a constant near 1/2 which differs slightly for each metal ion; for Mn(II), $k = 0.55$).²¹ Similar techniques have been reported for other transition metal ions; typical results are given in Table 7.

The effect of addition of possible interferences on the ESR results was also investigated.^{51,76} Additives can affect the ESR signal by causing a broadening, by shifting the effective g-factor, or by causing the lines in the signal to split or coalesce, e.g., through changes in complexation of the metal ion. Typical results compiled by Janzen⁶⁰ are shown in Table 8. Consider the case of Cu(II). In non-complexing media Cu(II) shows a broad structureless signal (linewidth 800-900 gauss). Upon the addition of ethylenediamine the broad signal decreases and a 4-line spectrum resulting from hyperfine coupling with the ^{63}Cu and ^{65}Cu nuclei ($I = 3/2$) appears.⁵¹ This quartet spectrum, with interline spacings of 170 G, is more convenient for determining Cu(II) in the presence of species which would show overlapping absorptions. Similarly the $Cu(DDC)_2$ complex (DDC = diethyldithiocarbamate) extracted into benzene showed a quartet useful for Cu(II) analysis.¹¹⁷ The signal intensity depended upon the solvent used for extraction. The intensity in toluene, for example, was only 0.6 that in benzene. While a number of metal ions (Mg^{2+} , Fe^{2+} , Ba^{2+} , Mn^{2+} , Zn^{2+} , Co^{2+} , Po^{2+} , Ni^{2+}) and anions (I^- , Be^- , NO_3^-) did not interfere with the determination, $Mg(II)$ and Cn^- did, probably by destruction of the $Cu(DDC)_2$ complex, e.g.,

Table 7. ESR Determination of Various Ions

Ions		Upper Limit (M)	Lower Limit (M)	Mean k^5	Precision (%)	Error (%)
Mn(II)	(1)	0.1	1×10^{-6}	0.55	± 0.4	2
	(2)	0.005	5×10^{-8}			
	(3)	0.1	1×10^{-6}			
	(5)	0.1	9×10^{-8}			
Cu(II)	(1)	0.1	1×10^{-5}	0.48	0.4	1.5
	(2)	0.1	3×10^{-6}			
	(3)	0.02	5×10^{-6}			
	(5)	1	2×10^{-7}			
Cr(III)	(1)	0.1	8×10^{-5}		± 0.4	2.2
	(2)	0.01	1×10^{-5}			
	(3)	0.2	2×10^{-4}			
VO(II)	(1)	0.05	1×10^{-5}	0.52	± 0.6	1.8
	(5)	0.02	2×10^{-7}			
Fe(III)	(4)	0.1	8×10^{-6}		± 0.4	2.5
	(3)	0.02	7×10^{-5}			
Co(II)	(1)	0.5	1×10^{-6}			
Gd(III)	(2)	0.04	4×10^{-5}			
	(3)	0.1	1×10^{-4}			

¹In aqueous solution taken from Refs. 50, 51, and 76²In aqueous solution taken from Ref. 80³In ethanol solution taken from Ref. 80⁴In acetone solution taken from Ref. 76⁵In aqueous solution taken from Ref. 21

Table 8. Maximum Tolerable Concentrations (M) of Diverse Substances on ESR Spectra of Ions Indicated in Aqueous Solution (From Ref. 60) (Courtesy of Analytical Chemistry)

	Mn(II) ²	Cu(II) ³	Cu-En ⁴	Cr(III) ⁵	VO(II) ⁶
HCl	0.10	0.02	0.20	0.05	0.05 (or 0.04)
HNO ₃	0.02	0.1	0.1	0.1	0.06
HCLO ₄	0.05	0.2	0.05	0.1	0.1
H ₂ SO ₄	0.005	0.01	0.02	0.002	0.02
H ₃ PO ₄	0.005	1.0	0.04	0.02	0.02
KH ₂ PO ₄	0.005	0.02	0.04	0.001	
Formic Acid	0.2	1.8			
Acetic Acid	0.2	0.10	0.2	0.1	0.1
K ₂ HPO ₄				0.0008	0.1
KCl	0.10				
NaCl	0.10				
CaCl ₂	0.10	0.20	0.02	0.05	0.2
MgCl ₂	0.10			0.05	0.1
Zn(NO ₃) ₂	0.02	0.5	0.02	0.2	0.5
KNO ₃	0.02	0.1	0.1	0.1	0.3
Ca(NO ₃) ₂	0.02		0.02	0.2	0.5
NaClO ₄	0.05	0.2	0.05	0.1	0.4
K ₂ SO ₄	0.005				
Na Acetate	0.002	0.10	0.2	0.0005	0.0005
NaF	0.01	0.02			
KBr	0.80	0.20	0.05	0.08	0.3
KI	0.50			0.1	0.5
Na ₂ S ₂ O ₃	0.005				
KCN	5×10 ⁻⁵	0.0001 ⁹		0.0002	0.0002 ¹¹
Na Citrate	5×10 ⁻⁵	0.0001	0.02	0.0001	0.0002 ¹⁰
K Oxalate	0.0001	0.01 ⁸	0.005 ⁷	0.0005	0.0004 ¹⁰
K, Na Tartrate	0.0002	0.0005	0.005	0.0005	0.0001 ¹⁰
EDTA	2×10 ⁻⁵	0.0001 ⁸	0.0001	0.0002	0.0002 ¹¹
KCSN	0.002	0.02 ⁷	0.02 ⁷	0.2	0.05
Na ₂ SO ₃	0.0005				
ZnSO ₄	0.0002	0.002		0.0008	0.02
Na ₂ SO ₄	0.0002	0.02	0.04	0.0005	0.02
MgSO ₄	2×10 ⁻⁵	0.002		0.0008	0.02
C ₂ H ₄ (NH ₂) ₂	2×10 ⁻⁵	0.001 ⁸		0.0001	0.0005
CH ₃ CN	2% (by volume)	2-3%	2-3%	2%	4-5%
CH ₃ OH	1% (by volume)			3%	2%
DMF	1% (by volume)	10%	10%	1%	1%
MnCl ₂		0.20	0.02		
Acetone	1% (by volume)	2-3%	2-3%	2%	2%
Glycerine	1% (by volume)	2-3%	2-3%	.	
NH ₄ OH		0.0001 ⁸	0.20	0.005	0.0005 ¹⁰
Ethanol		2-3%	2-3%		
Dioxane		2-3%	2-3%	1%	2%

¹Maximum concentration that can be added with no effect on the ESR spectra

²1×10⁻³ M Mn(ClO₄)₂ (Ref. 51)

³1×10⁻² M CuSO₄ (Ref. 51)

⁴1×10⁻² M CuSO₄; 1.28 M C₂H₄(NH₂)₂ (Ref. 51)

⁵1×10⁻² M Cr(NO₃)₃ (Ref. 76)

⁶1×10⁻² M VOSO₄ (Ref. 76)

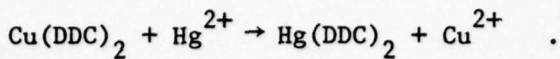
⁷Concentrations greater than this cause precipitation

⁸Quartet observed

⁹Reduction of Cu(II) to Cu(I) occurs and no signal is observed

¹⁰Some new features appeared in spectrum in presence of excess of ligand

¹¹Unusually narrow spectrum with relatively intense peaks



This type of reaction was used as the basis of an indirect method for the determination of Hg^{2+} by noting the decrease in the height of the ESR signal for the Cu(TET)_2 complex (TET = tetraethylthiuram disulfide) upon addition of Hg^{2+} .¹¹⁶

Chelates are able to alter the stability of various ions. For example, the paramagnetic Ag^{2+} ion is stabilized in the complex with tetraethylthiuram disulfide which permits analysis to the 0.1 ppb level.¹¹⁸

When the relaxation time of an ion is very short, the ESR signal may be so broadened that it extends over a very wide magnetic field range and hence is difficult or impossible to observe. For example, Fe^{3+} in aqueous media shows an extremely broad (ca. 1000 G) signal. However, since the relaxation time depends upon the environment of the ion (solvent, ligand), changes in this can sometimes lead to improved signals. Thus Fe(III) in acetone or alcohol in the presence of excess chloride ion gives a sharper signal.^{76,80} Similarly Ni(II) often does not give a useful ESR signal, but the chloroform extract of an aqueous solution containing the toluene-3,4-dithiol complex of Ni(II) can be used for analysis.¹⁹ Numerous possibilities exist for ESR analysis of metal ions in solution¹²⁰ and new applications will undoubtedly appear during the coming years.

Titrations using ESR detection offer the advantages that diamagnetic materials can be detected by indirect methods and that precise repositioning of the sample is not required.

The titrations of As_2O_3 by KMnO_4 was carried out in a recirculating cell, utilizing the detection of the Mn^{2+} ion,² with a precision of better than $\pm 1\%$.

The amplitude of the ESR signal of Mn^{2+} was sufficiently linear with concentration to determine the endpoint of the titration. $K_2Cr_2O_7$ which produces Cr^{3+} may also be a useful titrant.

Determinations of phenanthroline and 2,4,6-tri-pyridyl-s-triazine were carried out using a photochemical titration.⁴⁰ Fe^{2+} was generated photochemically from Fe^{3+} -citrate. The Fe^{2+} then complexes the organic ligand, and the chelate is detected by EPR. The ligand o-bipyridyl was found to complex too slowly with Fe^{2+} to be useful with EPR detection. Similarly, Cu(II) was determined by titration with the photochemically-generated anthraquinone radical anion.⁴¹

2. Organic Species in Solution

Since most organic compounds do not exist as radical species, the analysis of these by ESR requires that they be converted quantitatively or at a constant yield to radicals or radical ions which are stable for a long enough time for an ESR spectrum to be obtained. While a variety of methods exist for producing paramagnetic species and hundreds of radicals and radical ions have been investigated by ESR, there have been very few studies of the quantitative aspects of the radical production or actual quantitative determinations. A number of chemical methods exist for the production of radical ions.^{9,64,102} Radical anions of aromatic compounds are frequently produced by treatment of solutions in aprotic solvents (e.g., dimethoxyethane or tetrahydrofuran) with an alkali metal. Radical cations can be produced by dissolution in concentrated sulfuric acid or by various chemical oxidants. Electrochemical reduction and oxidation is also frequently employed, using external generation in a conventional electrolysis cell and transfer to a sample tube for ESR examination or direct generation in a small electrolytic cell contained in the

resonance cavity (the intra muros technique).^{45,65,75} Radicals can also be produced by photolysis, pyrolysis, and adsorption on various catalytic surfaces.

a. Determination of Polynuclear Aromatic Hydrocarbons

Treatment of low concentrations of certain hydrocarbons with dehydrated silica-alumina catalyst leads to quantitative conversion to the radical cation forms. This reaction was used as the basis of a method for the detection and estimation of anthracene, perylene, 9,10-dimethylanthracene and naphthacene.⁴² Solutions of the hydrocarbon, in amounts of ca. 5 to 200 μ g, in CS_2 or benzene, were treated with activated catalyst (10% Al_2O_3 , 89.8% SiO_2 , 0.05-0.10% Fe_2O_3) and the ESR spectra observed in selected uniform bore 6-mm glass tubes (Fig. 20). Note that the spectra of these adsorbed radical cations are more poorly resolved than those obtained by chemical or electrochemical oxidation. Since the g-values of all of these species are similar, determination of mixtures of these would probably not be possible. The radicals produced by this procedure were stable for at least 20 minutes even when the sample tubes were not protected from oxygen and moisture. Linear plots of signal amplitude (peak-to-peak) vs. amount of hydrocarbon were obtained. The precision and accuracy of the determination was about $\pm 6\%$. Benzene and naphthalene, which do not form radical cations under these conditions, do not interfere.

With care, alkali metals can be used to reduce successively aromatic hydrocarbons.^{44a} A solution of 50 μ g each of perylene and pyrene in dimethoxyethane was reacted in steps using a Pyrex tube with a 3 mm-o.d. side arm (Fig. 21). Initially, the spectrum of the perylene radical anion appears and reaches a steady state. Gradually as the perylene is reduced to the dianion,

the initial spectrum is replaced by the spectrum of the pyrene anion. Thus, independent spectra of both species can be observed. Several experiments gave accuracies of $\pm 5\%$ for the relative amounts of perylene to pyrene.

ESR has also been used to study deuterium exchange in homogeneous and heterogeneous systems.^{30,31} Radical anions were generated from the reaction products. The positions and the relative amounts of deuteration can be determined unambiguously from the hyperfine patterns in ESR spectrum.

b. Determination of Quinones

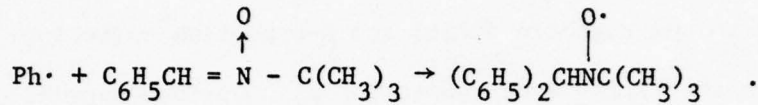
ESR signals obtained from the radical anions of quinones (semiquinones) are easily obtained, for example, by atmospheric oxidation of alkaline aqueous solutions, and are reasonably stable. Although quantitative studies have not been carried out, the effect of pH on the p-benzoquinone radical signal during formation from quinhydrone in deaerated aqueous was investigated.⁸³ The absolute concentration of radical ion was determined by double integration of the ESR signal and comparison to that obtained from peroxyamine disulfonate. At an estimated concentration of p-benzosemiquinone of 6×10^{-6} M the standard deviation was 4%.

Deuteration of hydroquinones was also studied by ESR.¹¹⁹ This paper also provides a good description of the treatment of the data.

c. Spin Trapping Techniques

One difficulty with the ESR analysis of organic species is that the radical-species are often unstable, especially in the presence of oxygen and moisture. This may necessitate rather elaborate measures for their formation and transfer to the spectrometer and may discourage quantitative analytical

applications of many types of compounds. Nitroxide radicals, e.g., $R_2NO\cdot$, are very stable, however, and conversion of an organic species to the nitroxide allows the detection of this species. This technique is called "spin trapping" and involves reaction of the radical with a nitrone or nitroso compound. For example, phenyl radical ($Ph\cdot$) can be trapped by α -phenyl-N-tert-butylnitron. ⁵⁹



While few quantitative studies using spin trapping have been reported, it is a possible analytical method for the determination of unstable radicals.

d. ESR Detector for Liquid Chromatography

Separation of nitroxide radicals by liquid chromatography (LC) on a silica column was monitored by ESR.⁹³ Successive 30-second sweeps were used to record the spectra. Similarly the separation of DPPH from its reaction products by LC was monitored by ESR.

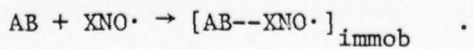
3. Methods Based on Relaxation Times and Reaction Rates

Relaxation methods are based on changes in the shape of the ESR spectrum (e.g., line broadening, signal intensity) because of variations in the environment of the detected radical. A number of methods employ nitroxide radicals as probes. Most nitroxides (Fig. 22) in nonviscous media show a well-defined three-line spectrum with a splitting of ca. 14-17 G attributable to interaction of the unpaired electron with the ^{14}N -nucleus ($I = 1$) (Fig. 23a). The nearest hydrogen atoms are in the γ -position, so hyperfine splitting by these

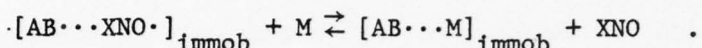
is usually not observed, although they may contribute to the line width (ca. 1 G). When the nitroxide is in a crystal, in a very viscous medium or in any environment where its motion is restricted, a broadened spectrum (known as the rigid glass, powder, polycrystalline or strongly immobilized spectrum) results (Fig. 23b). This broadening is due to the anisotropic g-value (i.e., a g-value which depends upon the orientation of the nitroxide with respect to the magnetic field) and N-hyperfine splitting. These changes in shape from the "free" spectrum to one with various degrees of broadening is the basis of the "spin-labeling" technique for studying the polarity of the environment, the molecular motion and the orientation of a free radical probe introduced into a molecule or membrane.^{49,74} Analytical methods are also based on changes in the nitroxide spectrum.

a. ESR Immunoassay of Drugs-FRAT

The analytical application of spin labeling is based upon generation of the "free" nitroxide spectrum from the "immobilized" one by reaction of a labeled reagent with the compound of interest. Consider, for example, the method for the determination of morphine in urine, saliva, and other biological fluids.⁷¹ A spin-labeled morphine analog (Fig. 24c) (XNO[•]) is prepared. The ESR of this substance shows the typical "free" nitroxide pattern. An antigen form of morphine is also prepared by coupling morphine to bovine serum albumin (BSA) (Fig. 24b). When this antigen is injected into rabbits, antibodies against it are formed; these antibodies (AB) will bind strongly to morphine itself or its spin-labeled form



Thus a reagent prepared by mixing the antibody and labeled drug in such amounts that no free XNO^{\cdot} remains will show an ESR spectrum with the "immobilized" or broadened signal. When the sample presumed to contain morphine (M) is added to the reagent, some of the antibody-bound XNO^{\cdot} will be exchanged by M, thus liberating free XNO^{\cdot} and producing the sharp lined nitroxide spectrum:



Because of the specificity of the antibody, appearance of the "free" ESR spectrum is evidence of morphine or its close analogs (e.g., codeine, ethyl morphine); other drugs of abuse, such as barbiturates, amphetamines, methadone, etc., do not interfere. Calibration curves of free signal height against amount of drug can be used to determine the quantities of drug in the sample. Prepared reagent for morphine and other drugs is commercially available. This technique, call FRAT (an acronym for "free radical assay technique") uses very small samples (e.g., $20\mu\text{l}$ of urine), is very rapid (ca. 1 min) and is specific. The reagent is expensive, however. The use of similar methods applied to enzymes and interferences are discussed in a recent review.⁶¹

b. Determination of Dissolved Oxygen

Oxygen is a paramagnetic triplet. Dissolved oxygen leads to line broadening in the ESR spectrum of a radical, because the oxygen-radical interaction contributes to the relaxation of the free radical. The extent of this broadening depends upon the oxygen concentration, so that the method can be used to measure dissolved oxygen.⁸⁹ The linewidth of the nitroxide radical

2,2,6,6-tetramethylpiperidinox (TMP) (Fig. 22) at a concentration of 0.34 mM varied from its oxygen-free value of 0.55 G to up to 4G; the results showed a fair amount of scatter, so the method is only semiquantitative.

A method based on oxygen's effect on the spin-lattice relaxation time has also been proposed.⁵⁶ The ESR spectrum of a free radical (of an unspecified nature) which originates in a terphenyl coolant of a reactor was studied as a function of incident microwave power. Because the radical has a long spin-lattice relaxation time, the ESR signal saturates fairly easily, and the signal height decreased with increasing r.f. power in the absence of oxygen. Addition of oxygen decreases the relaxation time and changed the nature of the peak height vs. r.f. power relation. This change was used to estimate the oxygen content and was proposed for oxygen concentrations as low as 10^{-5} M.

c. Determination of Hydroperoxides by Reaction with DPPH

The effect of substances which react and decrease the signal of a stable free radical can be employed as an indirect method of analysis. Thus the measurement of the rate of reaction of the stable radical diphenylpicrylhydrazyl (DPPH) with several hydroperoxides was proposed as a method of determination of the hydroperoxide.¹⁰⁴ The ESR signal of DPPH or that of a new species formed on reaction was monitored with time and the hydroperoxide concentration was calculated based on the measured rate of reaction. Although different hydroperoxides could be distinguished based on their different reaction rates, the specificity of the method is probably not very good and interferences and temperature control may be a problem.

A similar technique utilizing diphenylamine which reacts with the hydroperoxide to form diphenylnitroxide has also been reported.^{65a} This technique involves the increase in signal due to the free radical.

C. GASES

Most gaseous systems which contain paramagnetic atoms or molecules are of interest in studies of either kinetics of flames. This subject has been reviewed in detail.¹¹² Rarely are atoms obtained in an environment which needs to be analyzed, and most paramagnetic molecules are not stable. Exceptions to this rule are O_2 , NO and NO_2 , although O_2 itself is typically not of interest. O_2 in the metastable $^1\Delta_g$ state is a unique case for which few techniques are available for analysis.

1. Analysis of NO and NO_2

O_2 usually interferes with EPR determinations in the gas phase. At low pressures, the X-band spectrum of O_2 exhibits several thousand lines which extend from about 2 KG to beyond 20 KG. At high pressures, O_2 exhibits several broad lines. However, electric field modulation (Stark modulation), in addition to magnetic field modulation can eliminate the spectrum of non-polar molecules.²⁶ Using this technique, Uehara and Arimitsu¹⁰⁵ developed an ESR cavity and sampling system which permits air at ambient pressure to be monitored for NO_2 with a sensitivity of 10 ppm. They also utilized a low-temperature trapping technique in which NO and NO_2 are deposited in a trap while the air is pumped out. This technique provided a sensitivity of about 30 ppb for both NO and NO_2 . They suggest the utilization of this technique for exhaust gases.

2. Singlet Molecular Oxygen

O_2 can be formed in the metastable singlet state ($^1\Delta_g$) which is paramagnetic by virtue of its orbital angular momentum.^{37,77} It is of current

interest in air pollution studies as well as in synthetic procedures. Optical and infrared absorption cannot be used with this molecule. However, a red emission which is proportional to the square of the concentration can be easily detected but needs to be calibrated for each system. EPR provides a useful quantitative technique for this material,³⁶ and can be used with accuracies of several percent.^{44b} A calibration of the optical emission vs. the square of the pressure determined by ESR is shown in Fig. 25.

D. SOLIDS

The analysis of solids has not received much attention. This may be due in part to difficulties in sample placement. However, ESR offers a non-destructive tool which, once calibrated, can provide rapid analyses.

1. Mn²⁺ in Calcium Carbonate

Mn²⁺ in calcium carbonate exhibits a spectrum which consists of six intense lines as well as some weaker transitions between those lines. Samples of barnacle shells were analyzed for Mn^{2+¹²} by grinding the material, and positioning a sample of about 10 mg in the center of the cavity. The amplitude of the signal was used as a measure of concentration, and was calibrated against atomic absorption measurements. The limits of detection were about 20 ppb, and agreed to within $\pm 3\%$ of the atomic absorption determination.

2. Active Surface Area

It was mentioned in Section IV.3 that metal oxide catalysts can oxidize many aromatic molecules. In order to determine the surface oxygen content of MnO₂ as an oxidizing agent⁸⁴ two methods were used. In the first, diphenyl-

picrylhydrazine ($DPPH_2$) was reacted with the MnO_2/O_2 system to yield the diphenylpicrylhydrazyl radical (DPPH). The concentration of the DPPH was then determined by ESR. The second technique involved the direct absorption of DPPH from a solution in benzene, in which a reduction of the DPPH concentration is determined.

3. Ferromagnetic Systems

A discussion of ferromagnetic resonance is beyond the scope of this chapter. However, for many systems, the spins of the sample may be considered to be completely aligned in the magnetic field. Thus the magnetization (M_F) of a ferromagnetic material is given by Eq. (36)

$$M_F = n_{eff} g \beta N_F \quad (36)$$

where n_{eff} is the effective number of spins per atom and N_F is the number of ferromagnetic molecules. In contrast, the magnetization of a non-dilute paramagnetic material (M_P) is given by Eq. (37)

$$M_P = \frac{g^2 \beta^2 S(S+1) H_0}{3k(T-\theta)} N_P \quad (37)$$

where θ is the Curie temperature, and N_P is the number of paramagnetic molecules. Thus, to utilize ESR to determine the quantity of ferromagnetic material, Eq. (29) can be used if the first term on the right-hand side is replaced by $1/(n_{eff} \beta)$.

This technique was used to determine the amount of fine-grained metallic iron in lunar return samples.⁵⁴ The ESR spectrometer was calibrated with

$\text{MnSO}_4 \cdot \text{H}_2\text{O}$ as a paramagnetic standard, where $\theta = -26^\circ$, $g = 2.000$ and $S = 5/2$.

Often θ is sufficiently close to 0 for even pure materials, so that it can be neglected, however, $\text{MnSO}_4 \cdot \text{H}_2\text{O}$ is an exception.

D. STANDARDS

The usual criteria for the selection of a primary or secondary standard such as ease of preparation, availability, stability, and reproducibility also apply to ESR. Two types of samples are typically used, those which provide a quantitative standard and those which provide a magnetic field standard.

1. Magnetic Field Standards

Standards to calibrate the magnetic field must exhibit sharp lines, and have spacings between lines that are known exactly. In addition, the spectrum of the standard should extend over the range of magnetic field of the sample. There are many of these standards in use, but several examples will be given below.

Wursters Blue Perchlorate in Ethanol¹¹¹

The perchlorate salt of $\text{N},\text{N},\text{N}',\text{N}'\text{-tetramethyl-p-phenylenediamine}$ is easily prepared. The spectrum of the material dissolved in deoxygenated absolute ethanol exhibits an apparent g-factor of 2.00305 ± 0.00001 and hyperfine splittings due to two equivalent nitrogen atoms of 7.051 ± 0.009 G, 12 equivalent protons of 6.773 ± 0.005 G, and 1.989 ± 0.009 G. An intense spectrum is observed over a range of about 80 G.

Mn^{2+} Standard⁹⁴

Usually SrO powder contains sufficient Mn^{2+} to give a strong ESR signal which exhibits six lines of a width of 1.5 G. The g-factor is 2.0012 ± 0.0002

and the hyperfine splitting is 83.71 G. The line positions should be calculated to at least second order (Eq. (8)) to be used as a standard.

Perylene Radical Cation

The perylene radical cation is prepared by adding a small amount of perylene to 98% sulfuric acid, and degasing the solution. The spectrum is characterized by a g-factor of 2.002569 ± 0.000006 ^{78,97} and three sets of hyperfine splittings 4.053, 3.054, and 0.446 G,¹³ each for four equivalent protons.

2. Quantitative Standards

a. Liquids

A number of dissolved paramagnetic materials provide good quantitative standards. The following have been utilized:

α, α' -diphenylpicrylhydrazyl can be weighed and dissolved readily in many polar and nonpolar solvents. However, this material is not stable for long periods of time.¹⁸

Potassium peroxyamine disulfonate [$K_2NO(SO_3)_2$] is a useful standard for aqueous solutions, although it is not stable in solution for more than about a day. However, the concentration can be determined optically.⁶² The molar extinction coefficient is 1690 at 248 m μ and 2.08 at 545 m μ .⁸¹ 0.05 M carbonate retards decomposition. The spectrum consists of three lines of equal intensity with a hyperfine splitting of 13.05 ± 0.03 G.

Nitroxide Radicals. Several tetramethyl piperidyl nitroxides have been found to form stable radicals which can be used in aqueous or nonaqueous solvents.^{61,111}

$CuSO_4 \cdot 5H_2O$ can be dissolved in aqueous media; however, the signal is quite broad. Similarly, $MnSO_4 \cdot H_2O$ ($S = 5/2$) exhibits a six-line spectrum.

These have been used extensively for quantitative analysis ($\text{CuCl}_2 \cdot 2\text{H}_2\text{O}$, and $\text{MnCl}_2 \cdot 4\text{H}_2\text{O}$ have also been used³⁴).

A brief note describes the use of quinhydrone in buffered media to obtain a constant concentration of the semiquinone radical anion.⁸³

b. Solids

Numerous solid single crystals and powders have been used for analysis. Standards include DPPH, $\text{CuSO}_4 \cdot \text{H}_2\text{O}$, and F-centers in alkali halides⁵⁵ which can be determined by optical absorption. $\text{MnSO}_4 \cdot \text{H}_2\text{O}$ can be weighed directly.^{54, 98} Single crystals of $\text{CuSO}_4 \cdot 5\text{H}_2\text{O}$ which can also be weighed are anisotropic, so that the calibration factor must include the correct value of g. The powder exhibits an irregularly-shaped spectrum. Many pure materials can be used; however, it is important to determine the Curie temperature of the material. Dilute materials, such as F-centers or transition metals in host matrices can be assumed to have a Curie temperature of 0°K. If transition metal ions in foreign matrices are to be used, the concentration must be determined by optical or chemical means.

c. Gases

In studies of kinetics using flow techniques, the ESR spectrometer is often calibrated by titration of one of the atoms of interest, with a titrant that reacts rapidly with the atoms on the time scale of the flow reactor or with O_2 or NO gas. For sampling measurements, either $\text{O}_2^{103, 114}$ or NO^{17} must be used. Typically, total pressures between 0.5 and 4 torr are used to keep exchange and pressure broadening to sufficiently low levels.

Acknowledgements

This work was supported in part by the Office of Naval Research.

References

1. Abragam, A., and B. Bleaney, Electron Paramagnetic Resonance of Transition Ions, Clarendon Press, Oxford, 1970.
2. Agerton, M., and E. G. Janzen, Anal. Lett., 2, 457 (1969).
3. Alger, R. S., Electron Paramagnetic Resonance. Techniques and Applications, John Wiley-Interscience, New York, 1968.
4. Allain, Y., J. P. Krebs, and J. de Gunzbourg, J. Appl. Phys., 39, 1124 (1968).
5. Atherton, N. M., Electron Spin Resonance, Halsted Press, London, 1967.
6. Atkins, P. W., and M. C. R. Symons, The Structure of Inorganic Radicals, Elsevier, Amsterdam, 1967.
7. Ayscough, P. B., Electron Spin Resonance in Chemistry, Methuen, London, 1967.
8. Bard, A. J., "Electron Spin Resonance" in Standard Methods of Chemical Analysis, Vol. 3, F. J. Welcher, ed., D. Van Nostrand, Princeton, New Jersey, 1966, pp. 616-635.
9. Bard, A. J., A. Ledwith, and J. J. Shine, Adv. Phys. Org. Chem., 13, 155 (1976).
10. Bersohn, M., and J. C. Baird, Electron Paramagnetic Resonance, Benjamin, New York, 1966.
11. Bielski, B. H. J., and J. M. Gebecki, Atlas of Electron Spin Resonance Spectra, Academic Press, New York, 1967.
12. Blanchard, S. C., and N. D. Chasteen, Anal. Chim. Acta, 82, 113 (1976).
13. Bolton, J. R., J. Phys. Chem., 71, 3702 (1967).
14. Bolton, J. R., "Electron Spin Densities" in Radical Ions, E. T. Kaiser and L. Kevan, eds., Interscience, New York, 1968. Chapter 1.

15. Boucher, L. J., E. C. Tynan, and T. F. Yen, in T. F. Yen, Electron Spin Resonance of Metal Complexes, Plenum Press, New York, 1969.
16. Bowers, K. W., Adv. Magn. Resonance, 1, 317 (1965).
17. Breckenridge, W. H., and T. A. Miller, J. Chem. Phys., 56, 475 (1972).
18. Bridge, N. K., Nature, 185, 31 (1960).
19. Brinkman, W. J., and H. Freiser, Anal. Lett. 4, 513 (1971).
20. Brown, J. M., "Electron Resonance of Gaseous Free Radicals" in Magnetic Resonance, Vol. 4, M. T. P. International Reviews of Science; Physical Chemistry, C. A. McDowell, ed., Butterworth, London, 1973, Chapter 7.
21. Bryson, W. G., D. P. Hubbard, B. M. Peake, and J. Simpson, Anal. Chim. Acta, 77, 107 (1975).
22. Buckmaster, H. A., and J. C. Dering, J. Appl. Phys., 39, 4486 (1968).
23. Carrington, A., and A. D. McLachlan, Introduction to Magnetic Resonance, Harper and Row, New York, 1967.
24. Carrington, A., Microwave Spectroscopy of Free Radicals, Academic Press, London, 1974.
25. Carrington, A., D. H. Levy, and T. A. Miller, Adv. Chem. Phys., 18, 149 (1970).
26. Carrington, A., D. H. Levy, and T. A. Miller, Rev. Sci. Instrum., 38, 1183 (1967).
27. Casteleijn, G., J. J. ten Bosch, and J. Smidt, J. Appl. Phys., 39, 4375 (1968).
28. Chang, R., Anal. Chem., 46, 1360 (1974).
29. Cope, F. W., "A Method for Digital Calculation of Absolute Free Radical Concentrations," Report NADC-MR-6804 (AD 671 809) May, 1968.
30. Davis, K. P., and J. L. Garnett, J. Phys. Chem., 75, 1175 (1971).
31. Davis, K. P., J. L. Garnett, and J. H. O'Keefe, Chem. Comm., 1672 (1970).
32. Dickson, F. E., C. J. Kunesh, E. L. McGinnis, and L. Petrakis, Anal. Chem., 44, 978 (1972).

33. Dickson, F. E., and L. Petrakis, *Anal. Chem.*, 46, 1129 (1974).
34. Dohrmann, J. K., *Ber. Bunsenges, Phys. Chem.*, 74, 575 (1970).
35. Eargle, D., *Anal. Chem.*, 40, 303R (1968).
36. Falick, A. M., "An EPR Study of the O_2 ($^1\Delta_g$) Molecules" University of California Radiation Laboratory, Berkeley, California, Report UCRL-17453 (1967).
37. Falick, A. M., B. H. Mahan, and R. J. Myers, *J. Chem. Phys.*, 42, 1837 (1975).
38. Farach, H. A., and C. P. Poole, Jr., *Adv. Magn. Resonance*, 5, 229 (1973).
39. Feher, G., *Bell System Tech. J.*, 36, 449 (1957).
40. Fitzgerald, J. M., and J. L. Beck, *Anal. Lett.*, 3, 531 (1970).
41. Fitzgerald, J. M., and D. C. Warren, *Anal. Lett.*, 3, 623 (1970).
42. Flockhart, B. D., and R. C. Pink, *Talanta*, 9, 931 (1962).
43. Flockhart, B. D., and R. C. Pink, *Talanta*, 12, 529 (1965).
44. (a) Goldberg, I. B., unpublished results; (b) Goldberg, I. B., and A. T. Pritt, unpublished results.
45. Goldberg, I. B., and A. J. Bard, "The Application of ESR Spectroscopy to Electrochemistry" in Magnetic Resonance in Chemistry and Biology, J. N. Herak and K. J. Adamic, eds., Dekker, New York, 1975, Chapter 10.
46. Goldberg, I. B., and H. R. Crowe, *J. Magn. Resonance*, 18, 497 (1975).
47. Goldberg, I. B., H. R. Crowe, and D. Pilipovich, *Chem. Phys. Lett.*, 33, 347 (1975).
48. Goodman, B. A., and J. B. Raynor, *Adv. Inorg. Chem. Radiochem.*, 13, 135 (1970).
49. Griffith, O., and A. Waggoner, *Account Chem. Res.*, 2, 17 (1969).
50. Guilbault, G. G., and G. J. Lubrano, *Anal. Letters*, 1, 725 (1968).
51. Guilbault, G. C., and T. Meisel, *Anal. Chem.*, 41, 1100 (1969).

52. Guilbault, G. G., and T. Meisel, *Anal. Chem. Acta*, 50, 157 (1970).
53. Guilbault, G. G., and E. S. Moyer, *Anal. Chem.*, 42, 471 (1970).
54. Housley, R. M., E. H. Cirlin, I. B. Goldberg, and H. R. Crowe, *7th Lunar Science Conference Proceedings*, Houston, Texas, 1976, in press.
55. Hyde, J. S., "Experimental Techniques in EPR" in Proc. 6th Annual NMR-EPR Workshop, Varian Associates Instrument Division, Palo Alto, California, November 5-9, 1962.
56. Ingalls, R. B., and G. A. Pearson, *Anal. Chim. Acta*, 25, 566 (1961).
57. Ingram, D. J. E., Free Radicals, as Studied by Electron Spin Resonance, Butterworths, London, 1958.
58. Ingram, D. J. E., Spectroscopy at Radio and Microwave Frequencies, 2nd Ed., Plenum Press, New York, 1967.
59. Janzen, E. G., *Accounts Chem. Res.*, 4, 31 (1971).
60. Janzen, E. G., *Anal. Chem.*, 44, 113R (1972).
61. Janzen, E. G., *Anal. Chem.*, 46, 478R (1974).
62. Jones, M. T., *J. Chem. Phys.*, 38, 2892 (1963).
63. Judeikis, H., *J. Appl. Phys.*, 35, 2615 (1964).
64. Kaiser, E. T., and L. Kevan, eds., Radical Ions, Interscience, New York, 1968.
65. Kastening, B., "Joint Application of Electrochemical and ESR Techniques" in Electronanalytical Chemistry, Vol. 10, H. W. Nürnberg, ed., Wiley, New York, 1974.
- 65a. Klyvera, N. D., G. E. Muratova, A. I. Kashlinskii, and A. V. Sokolov, *J. Anal. Chem. USSR*, 22, 235 (1967).
66. Kohnlein, W., and A. Müller, "A Double Cavity for Precision Measurements of Radical Concentrations" in *Free Radicals in Biological Systems*, M. Blois, ed., Academic Press, New York, 1961, Chapter 7.
67. Kohnlein, W., and A. Müller, *Phys. Med. Biol.*, 6, 599 (1961).
68. Kokoszka, G. F., and G. Gordon, *Tech. Inorg. Chem.*, 7, 151 (1968).

69. Kuska, H. A., and M. T. Rogers, "Electron Spin Resonance of First Row Transition Metal Complex Ions" in Radical Ions, E. T. Kaiser and L. Kevan, eds., John Wiley, New York, 1968, Chapter 13.
70. Landolt-Bornstein Numerical Data, Group II. Atomic and Molecular Physics: Vol. I. Magnetic Properties of Free Radicals; Vol. II. Magnetic Properties of Transition Metal Ions.
71. Leute, R. K., E. F. Ullman, A. Goldstein, and A. Herzenberg, Nature New Biol., 236, 93 (1972).
72. Loveland, D. B., and T. N. Tozer, J. Phys., E 5, 535 (1972).
73. Lukiewicz, S., and T. Sarna, Folia Histochem. and Cytochem., 9, 127, 203 (1971).
74. McConnell, H. M., Magnetic Resonance in Biological Systems, Pergamon Press, New York, 1967.
75. McKinney, T., "Electron Spin Resonance and Electrochemistry" Vol. 10, A. J. Bard, ed., Dekker, New York, 1976.
76. Meisel, T., and G. G. Guilbault, Anal. Chim. Acta, 50, 143 (1970).
77. Miller, T. A., J. Chem. Phys., 54, 330 (1971).
78. Möbius, K., Z. Naturforschg., 20A, 1102 (1965).
79. Moyer, E. S., and G. G. Guilbault, Anal. Chim. Acta, 52, 281 (1970).
80. Moyer, E. S., and W. J. McCarthy, Anal. Chim. Acta, 48, 79 (1969).
81. Murib, J. H., and D. M. Ritter, J. Am. Chem. Soc., 74, 3394 (1952).
82. Myers, R. J., Molecular Magnetism and Magnetic Resonance Spectroscopy, Prentice-Hall, New Jersey, 1973.
83. Narni, G., H. S. Mason, and I. Yamazaki, Anal. Chem., 38, 367 (1966).
84. Oei, A. T. T., and J. L. Garnett, J. Catal., 19, 176 (1970).
85. Orton, J. W., Electron Paramagnetic Resonance, Iliffe, Ltd., London, 1968.
86. Pake, G. E., Paramagnetic Resonance, W. A. Benjamin, New York, 1962, Chapter 2.

87. Poole, C. P., Electron Spin Resonance, Interscience, New York, 1967.
88. Posener, D. W., J. Magn. Resonance, 14, 129 (1974).
89. Povich, M. J., Anal. Chem., 47, 346 (1975).
90. Randolph, M. L., "Quantitative Considerations in Electron Spin Resonance Studies of Biological Materials" in Biological Applications of Electron Spin Resonance, H. M. Swartz, J. R. Bolton, and D. C. Borg, eds., John Wiley, New York, 1972.
91. Randolph, M. L., Rev. Sci. Instrum., 31, 949 (1960).
92. Roberts, E. M., R. L. Rutledge, and A. P. Wehner, Anal. Chem., 33, 1879 (1961).
93. Rokushika, S., H. Taniguchi, and H. Hatano, Anal. Letters, 8, 205 (1975).
94. Rosenthal, J., and L. Yarmus, Rev. Sci. Instrum., 37, 381 (1966).
95. Sales, K. D., Adv. Free Radical Chem., 3, 139 (1969).
96. Saraceno, A. J., D. T. Fanale, and N. D. Coggeshall, Anal. Chem., 33, 590 (1961).
97. Segal, B. G., M. Kaplan, and G. K. Fraenkel, J. Chem. Phys., 43, 4191 (1965) with correction in R. Allendoerfer, J. Chem. Phys., 55, 3615 (1971).
98. Singer, L. S., J. Appl. Phys., 30, 1463 (1959).
99. Smith, G. W., J. Appl. Phys., 35, 1217 (1964).
100. Sorin, L. A., and M. V. Vlasova, Electron Spin Resonance of Paramagnetic Crystals, Plenum Press, New York, 1973.
101. Swartz, H. M., J. R. Bolton, and D. C. Borg, eds., Biological Applications of Electron Spin Resonance, John Wiley, New York, 1972.
102. Szwarc, M., Carbanions, Living Polymers and Electron Transfer Processes, Wiley-Interscience, New York, 1968.
103. Tinkham, M., and M. W. P. Strandberg, Phys. Rev., 97, 937, 951 (1955).
104. Ueda, H., Anal. Chem., 35, 2213 (1963).

105. Uehara, H., and S. Arimitsu, *Anal. Chem.*, 45, 1897 (1973).
106. Ulbert, K., *Coll. Czech. Chem. Communi.*, 27, 1438 (1962).
107. Vigouroux, B., J. C. Gourdon, P. Lopez, and J. Pescia, *J. Phys.*, E 6, 557 (1973).
108. Wahlquist, J., *J. Chem. Phys.*, 35, 1708 (1961).
109. Wertz, J. E., *Chem. Rev.*, 55, 829 (1955).
110. Wertz, J. E., and J. R. Bolton, Electron Spin Resonance: Elementary Theory and Practical Applications, McGraw-Hill, New York, 1972.
111. Wertz, J. E., and J. R. Bolton, pp. 463-467.
112. Westenberg, A. A., *Prog. Reaction Kinetics*, 7, part 1, 23 (1973).
113. Westenberg, A. A., *J. Chem. Phys.*, 43, 1544 (1965).
114. Westenberg, A. A., and N. deHaas, *J. Chem. Phys.*, 40, 3087 (1964).
115. Wilmshurst, T. H., Electron Spin Resonance Spectrometers, Adam Hilger, Ltd., London, 1967.
116. Yamamoto, D., and N. Ikawa, *Bull. Chem. Soc. Jpn.*, 45, 1405 (1972).
117. Yamamoto, D., T. Fukumoto, and N. Ikawa, *Bull. Chem. Soc. Jpn.*, 45, 1403 (1972).
118. Yamamoto, D., and F. Ozeki, *Bull. Chem. Soc. Jpn.*, 45, 1408 (1972).
119. Yao, H. C., and H. C. Heller, *Anal. Chem.*, 41, 1540 (1969).
120. Yen, T. F., ed., Electron Spin Resonance of Metal Complexes, Plenum Press, New York, 1969.
121. Zavoisky, E., *J. Phys.*, U.S.S.R., 9, 211 (1945).

Figure Captions

Fig. 1 Comparison between an optical spectrometer and a simple ESR spectrometer.

Fig. 2 Examples of derivative ESR spectra of solids.

- (a) Typical isotropic line
- (b), (c) Spectrum of species with axial symmetry $g_{\perp} > g_{\parallel}$ and narrow linewidth (b); broad linewidth (c).
- (d) spectrum of species with low symmetry $g_x \neq g_y \neq g_z$.

Fig. 3 Energy level diagram of the hydrogen atom and typical spectrum.

Fig. 4 Interaction of the unpaired electron with two equivalent protons.

Fig. 5 A spectra due to interaction of unpaired electrons with:

- (a) Two nonequivalent protons
- (b) Two nonequivalent sets of two equivalent protons
- (c) Variation of spectra for interaction of two sets of equivalent pairs of protons for different values of the coupling constants a_1 and a_2

Fig. 6 Spectrum of V^{4+} showing unequal line spacings due to second-order shifts, and broadening effects.

Fig. 7 Effect of second-order splittings on the spectrum from three equivalent $I = 1/2$ particles, with an unpaired electron.

Fig. 8 Mechanism of spin polarization mechanism.

Fig. 9 Block diagram of typical ESR spectrometer employing 100 KHz field modulation. (Courtesy of J. E. Wertz and J. R. Bolton)

Fig. 10 Resonant cavities and the electric and magnetic fields of the standing waves.

Fig. 11 Typical rectangular cavity assembly and waveguide. (Courtesy of Varian Associates)

Fig. 12 Hybrid T (or Magic T) bridge element.

Fig. 13 A modern ESR spectrometer. The electromagnet and microwave bridge are at the right, the power supplies, amplifiers and recorder are contained on the console on the left. (Courtesy of Varian Associates)

Fig. 14 Errors due to truncated integration of ESR lines.

Fig. 15 Peak-to-peak width and relative signal amplitude of a Lorentzian line as a function of modulation amplitude.

Fig. 16 ESR spectra of a large magnetic sample for a critically coupled (a) and undercoupled (b) cavity. Overcoupling results in a similar curve as (a) but with slightly lower intensity.^{44a}

Fig. 17 First derivative curve, integral and double integral of a line of the F-atom signal or a concentration of 3×10^{-13} moles/cm².⁴⁷

Fig. 18 ESR spectrum of Mn(II) sulfate solution, 10^{-4} M (Varian Model E-3 spectrometer; time constant, 0.3 sec; r.f. power, 10 mW; modulation amplitude, 10 G).⁵⁰ (Courtesy of Analytical Letters)

Fig. 19 Variation of signal (S) with r.f. power for a 3.5×10^{-3} M MnCl₂ solution.²¹ (Courtesy of Analytica Chimica Acta)

Fig. 20 ESR spectra of (a) anthracene, (b) perylene, (c) 9,10-dimethyl-anthracene (adsorbed from CS₂), and (2) naphthacene (adsorbed from benzene) obtained by treatment with activated silica-alumina.⁴² (Courtesy of Talanta)

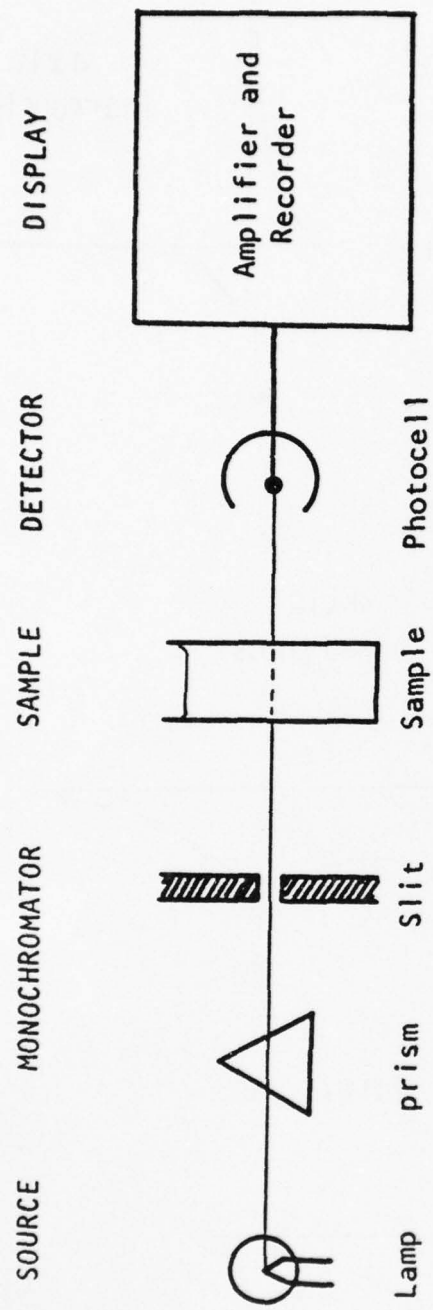
Fig. 21 Spectra of a mixture of perylene and pyrene successively reduced with alkali metals. (a) Perylene anion; (b)-(d) Further reduction of the perylene anion to the dianion and appearance of the pyrene anion; (e) Pyrene anion showing no perylene anion.^{44a}

Fig. 22 Stable nitroxides.

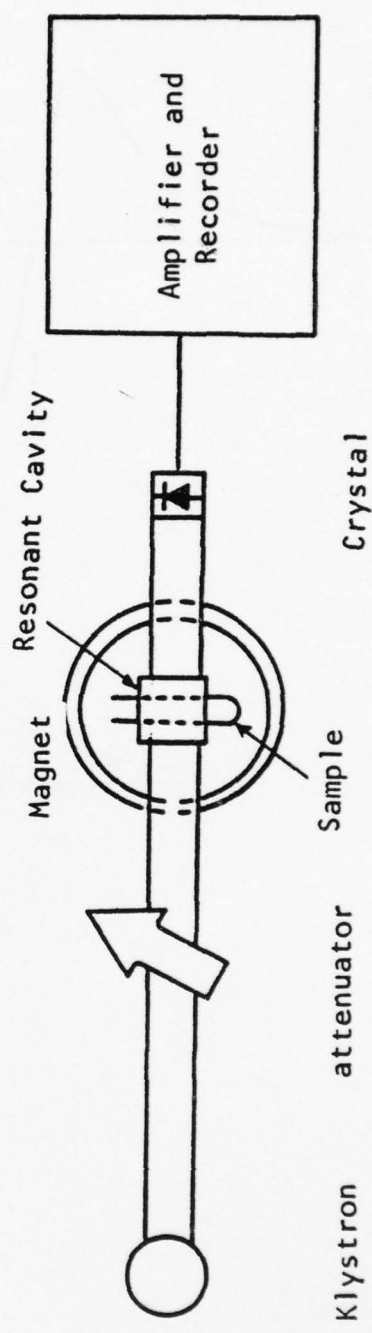
Fig. 23 (a) Typical ESR spectrum of "free" nitroxide radical in aqueous solution; (b) typical ESR spectrum of immobilized nitroxide; the extent of broadening and spectrum in any given case depends upon environment, orientation and motion of the spin label. (Courtesy of Aldrich Chemical Co.)

Fig. 24 (a) Morphine; (b) morphine antigen formed by coupling to bovine serum albumin; (c) spin labeled morphine antigen.

Fig. 25 Optical emission rate for O_2 in the ${}^1\Delta_g$ state vs. square of the $O_2({}^1\Delta_g)$ pressure determined by EPR spectroscopy.^{44b}



OPTICAL SPECTROMETER



ESR SPECTROMETER

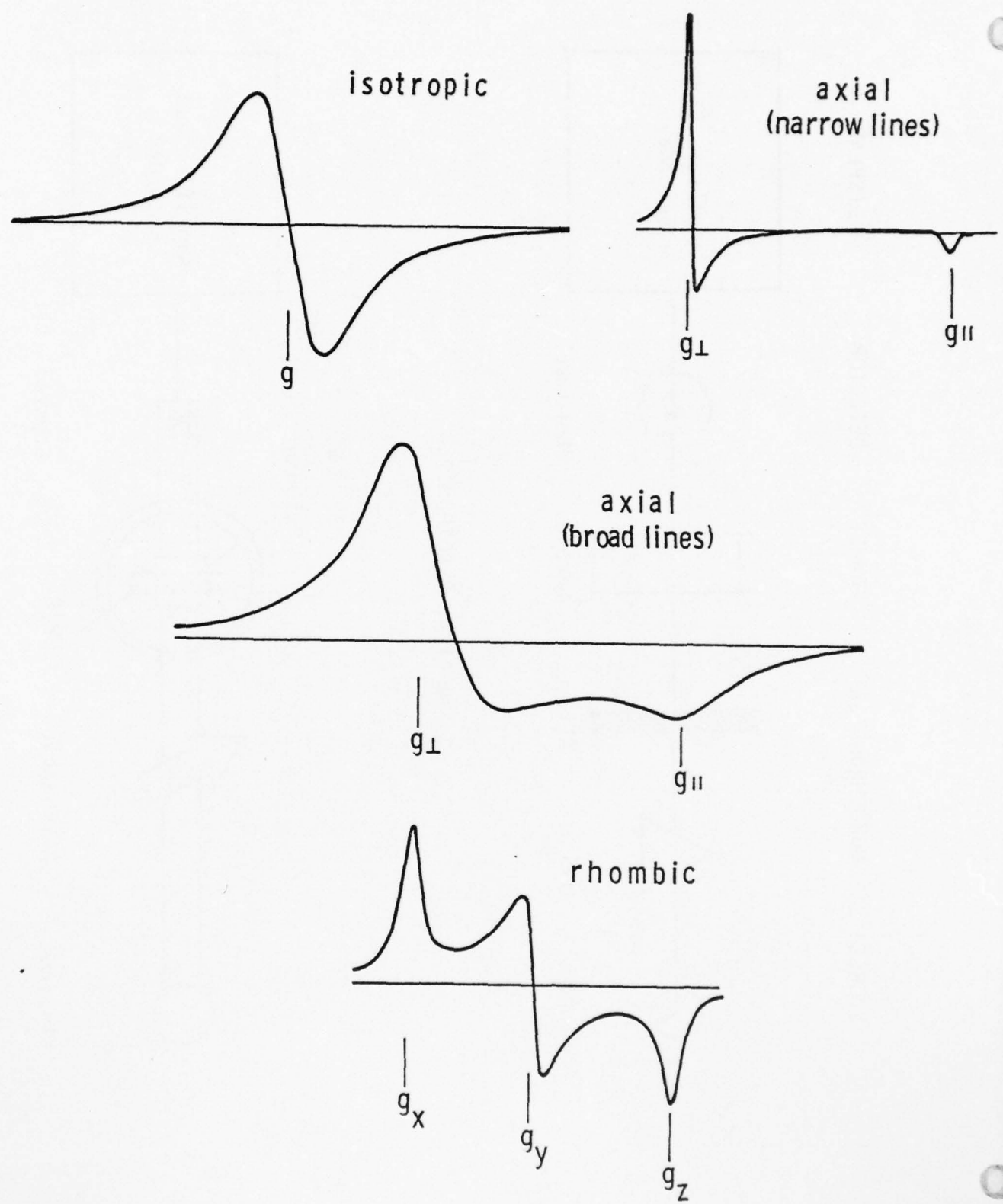


Fig. 2

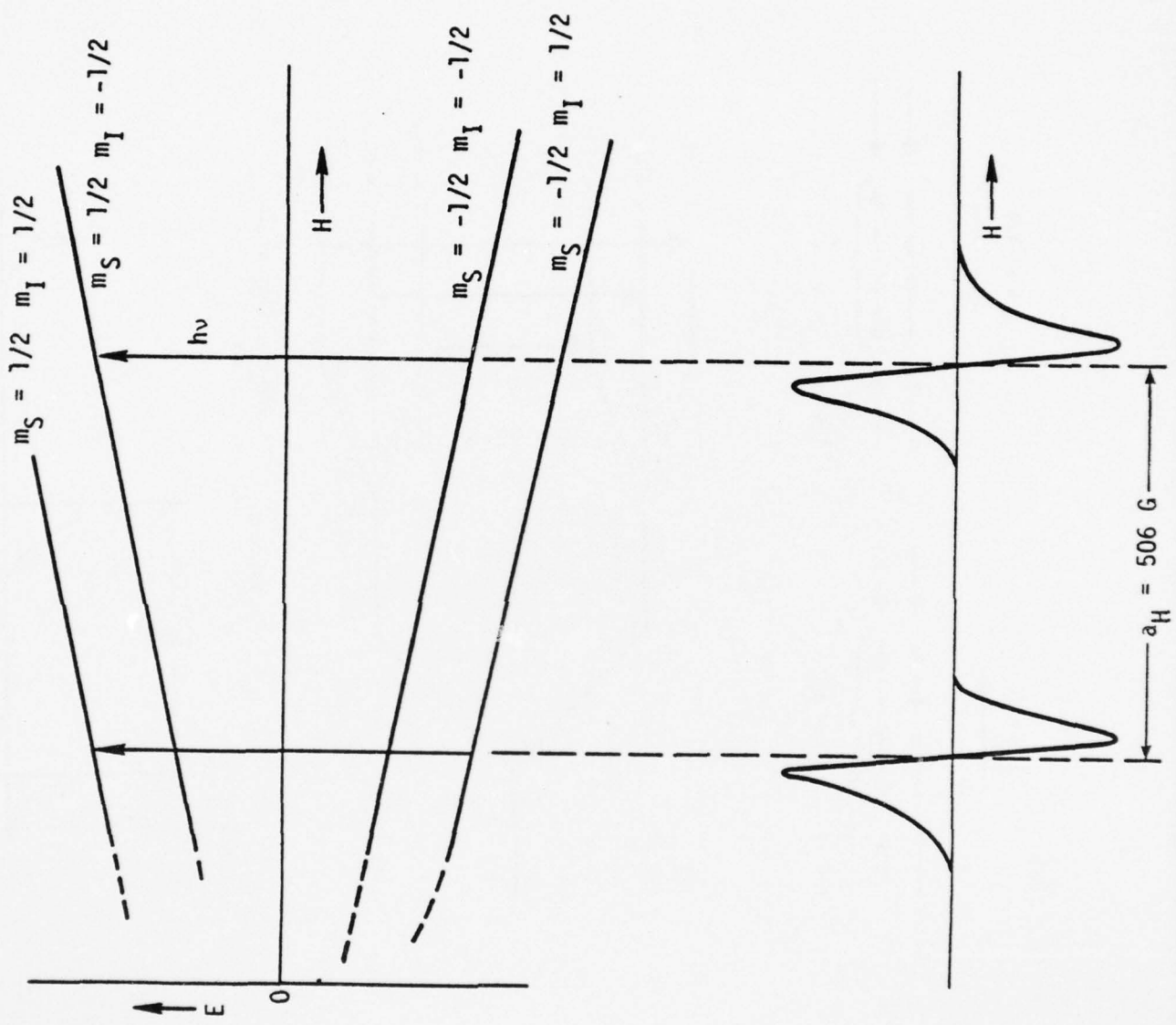


Fig. 3

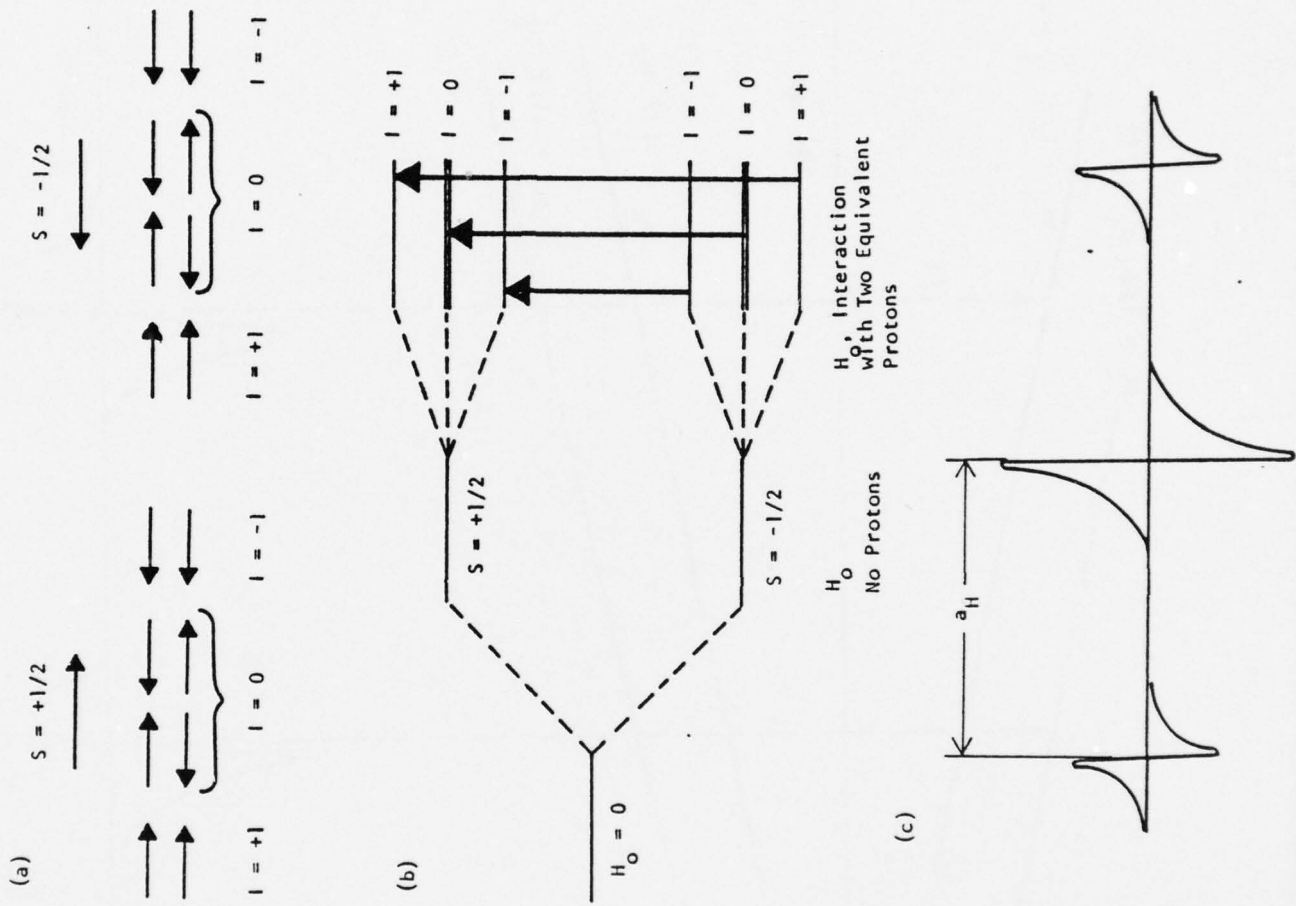


FIG. 4

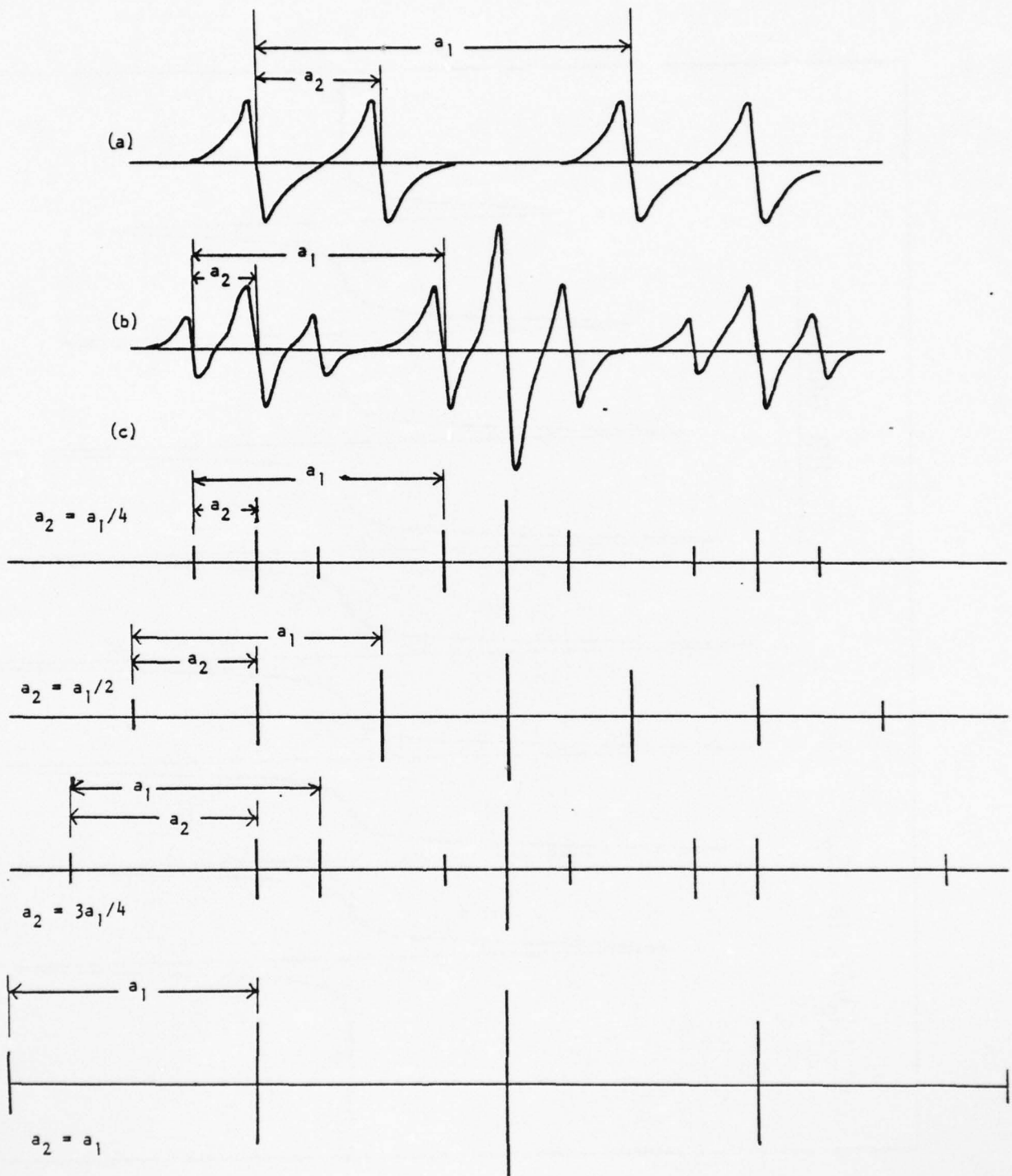


Fig. 5

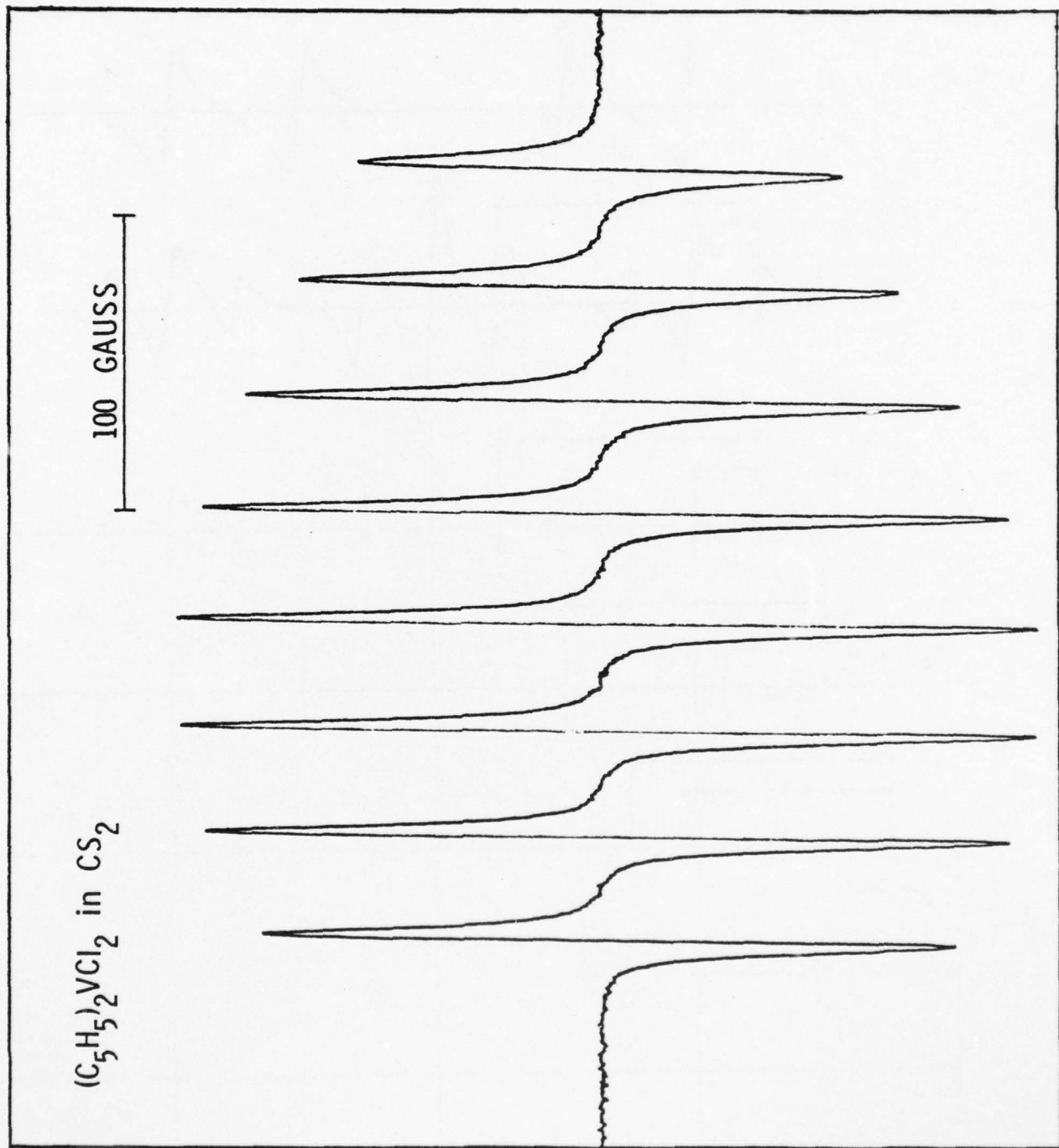


FIG. 6

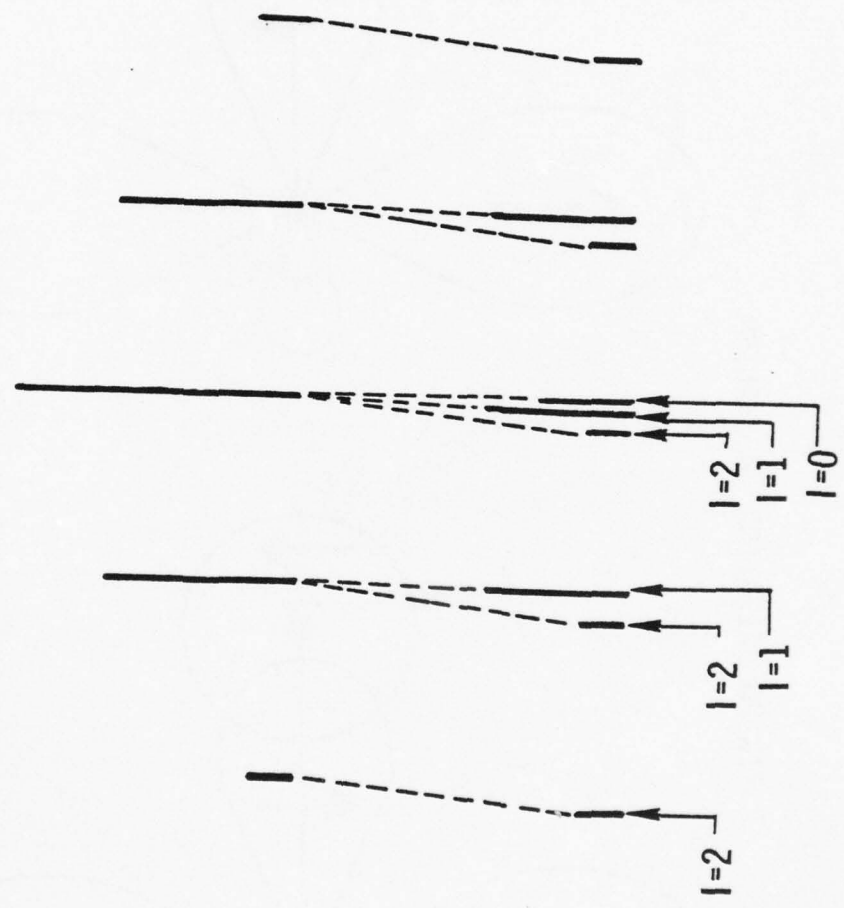


Fig. 7

"SPIN POLARIZATION" MECHANISM

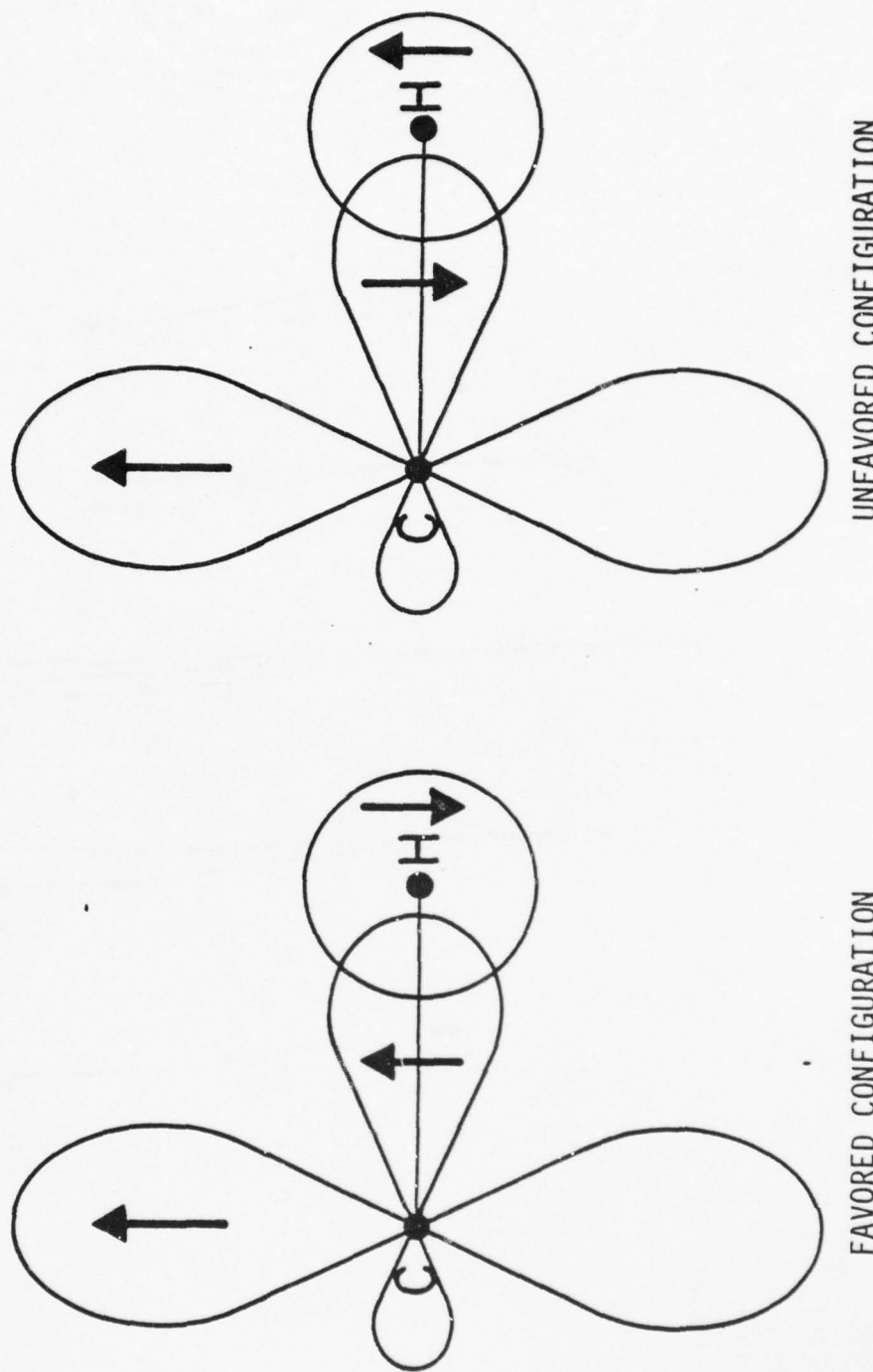


FIG. 8

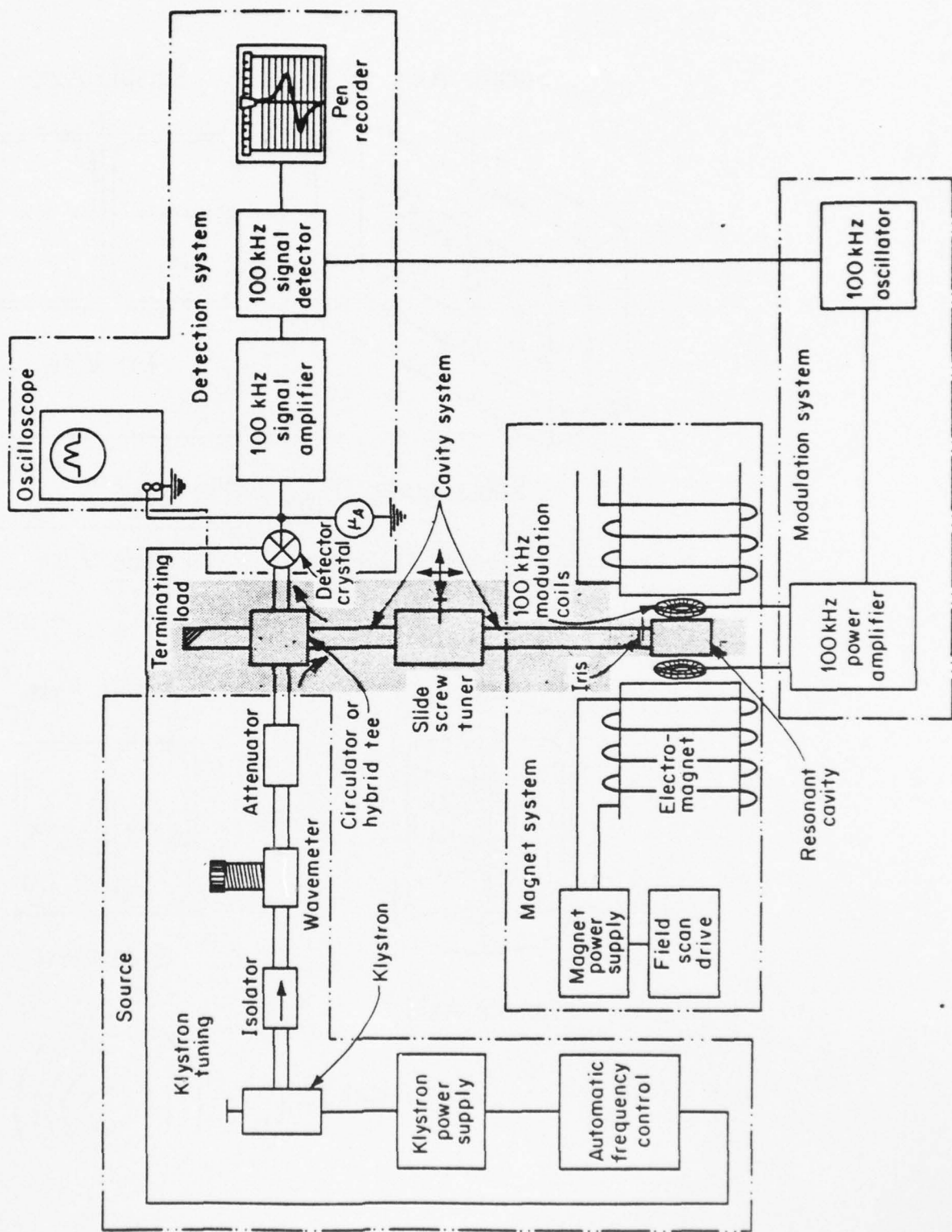


Fig. 9

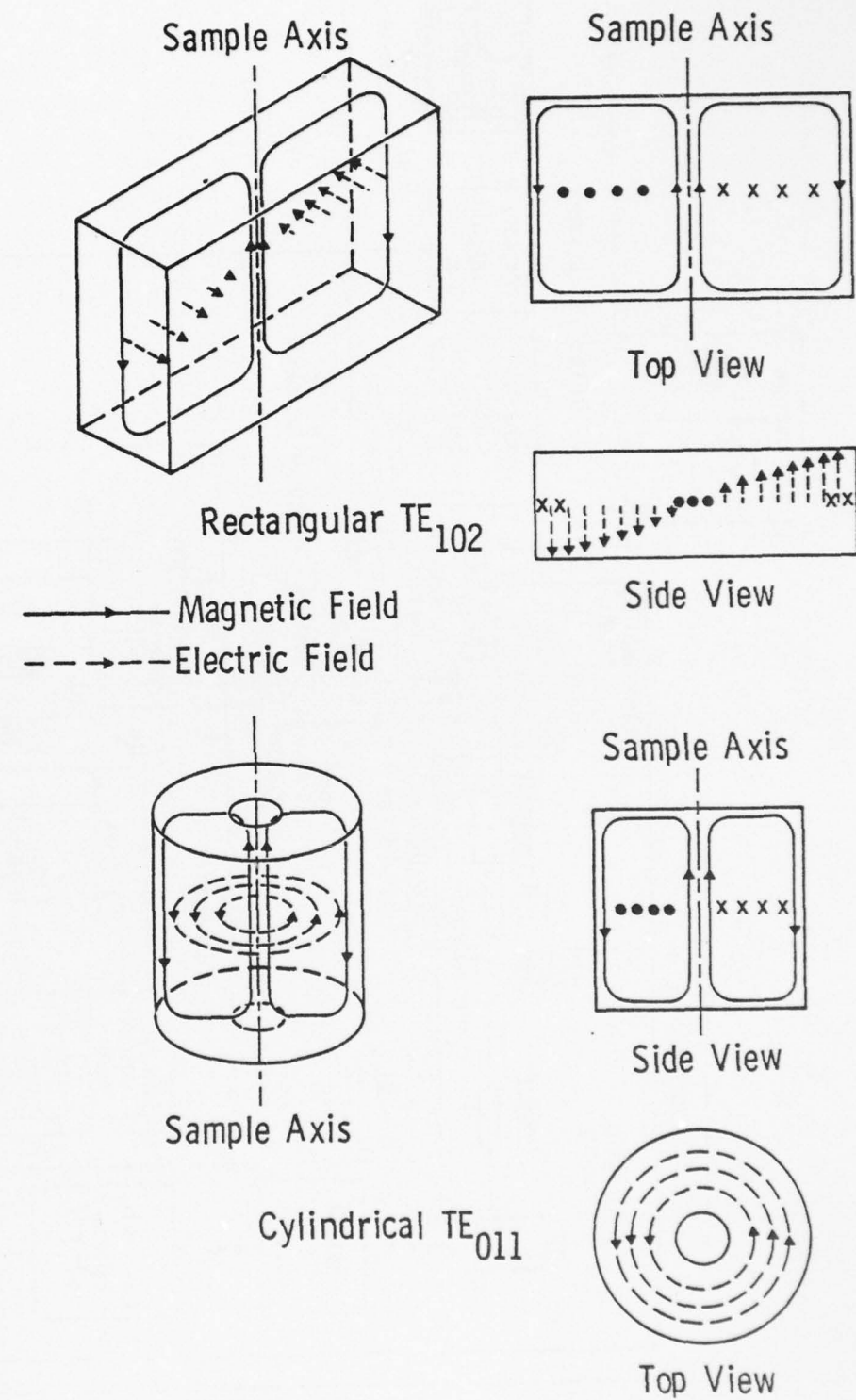


Fig. 10

AD-A031 078

ROCKWELL INTERNATIONAL THOUSAND OAKS CALIF SCIENCE --ETC F/G 7/4
ANALYTICAL APPLICATIONS OF ELECTRON SPIN RESONANCE. (U)
SEP 76 I B GOLDBERG

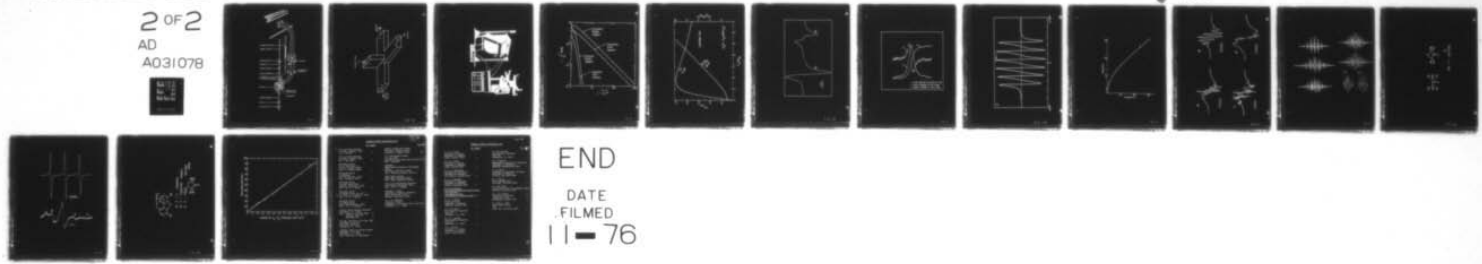
N00014-73-C-0325

NL

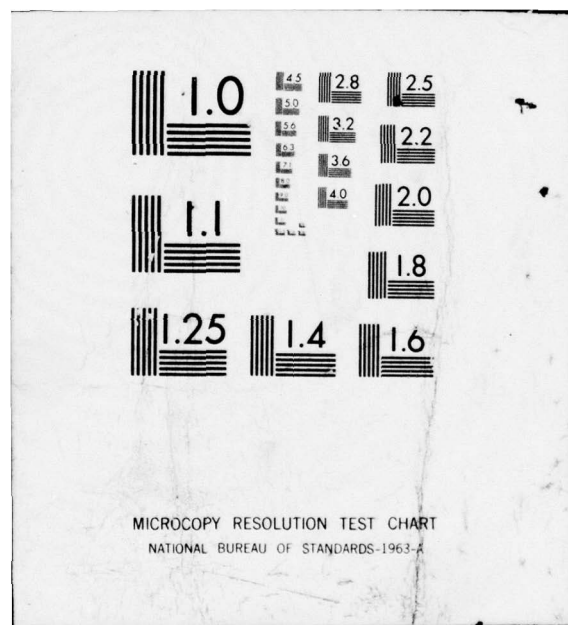
UNCLASSIFIED

2 OF 2
AD
A031078

SC549.19TR



END
DATE
FILMED
11-76



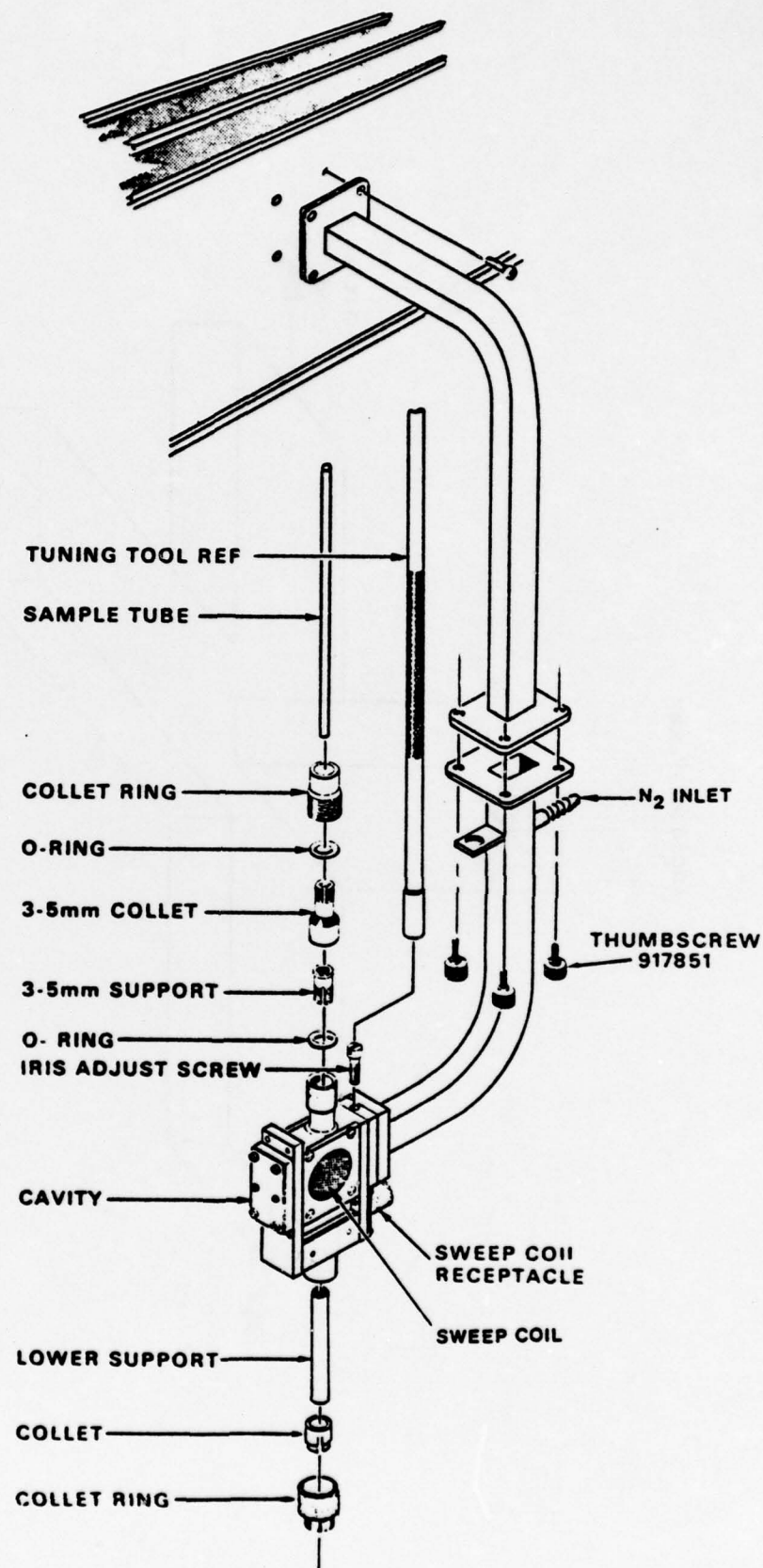


Fig. 11

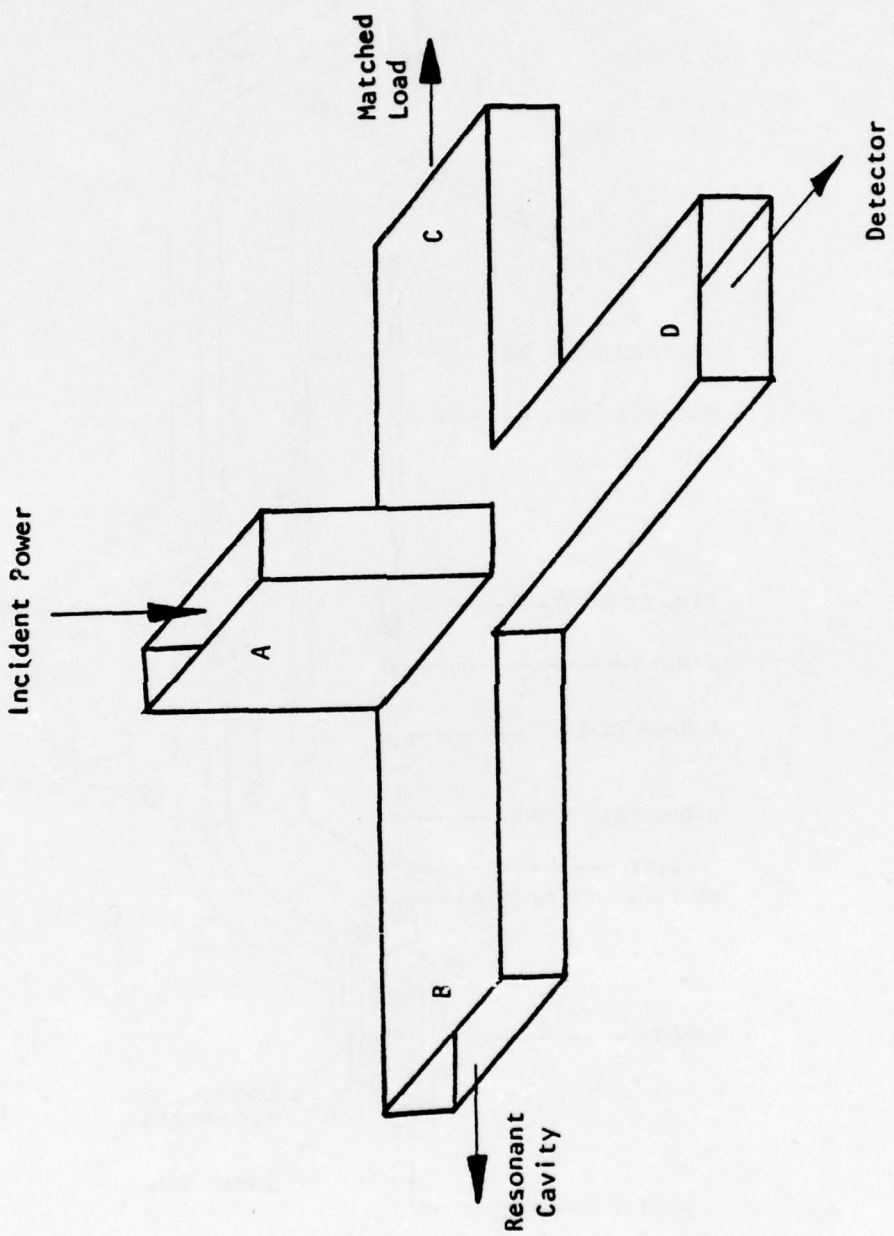
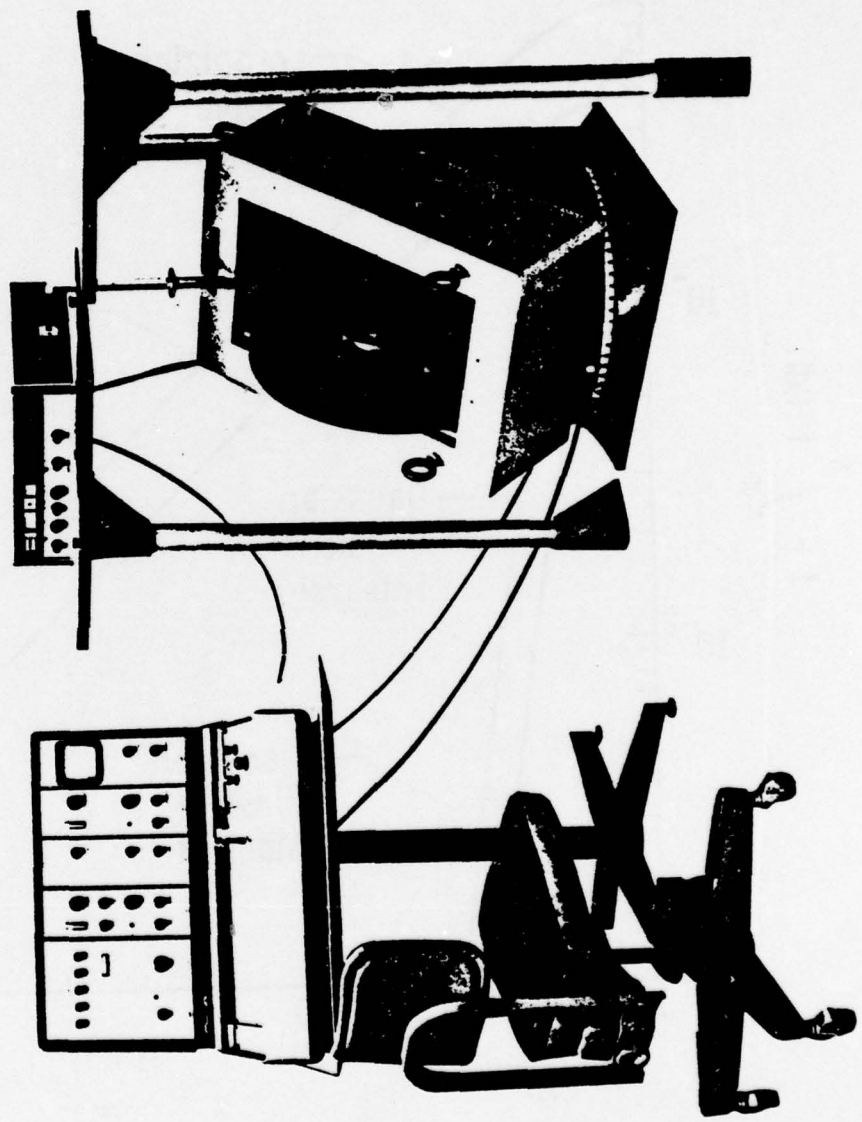


Fig 12



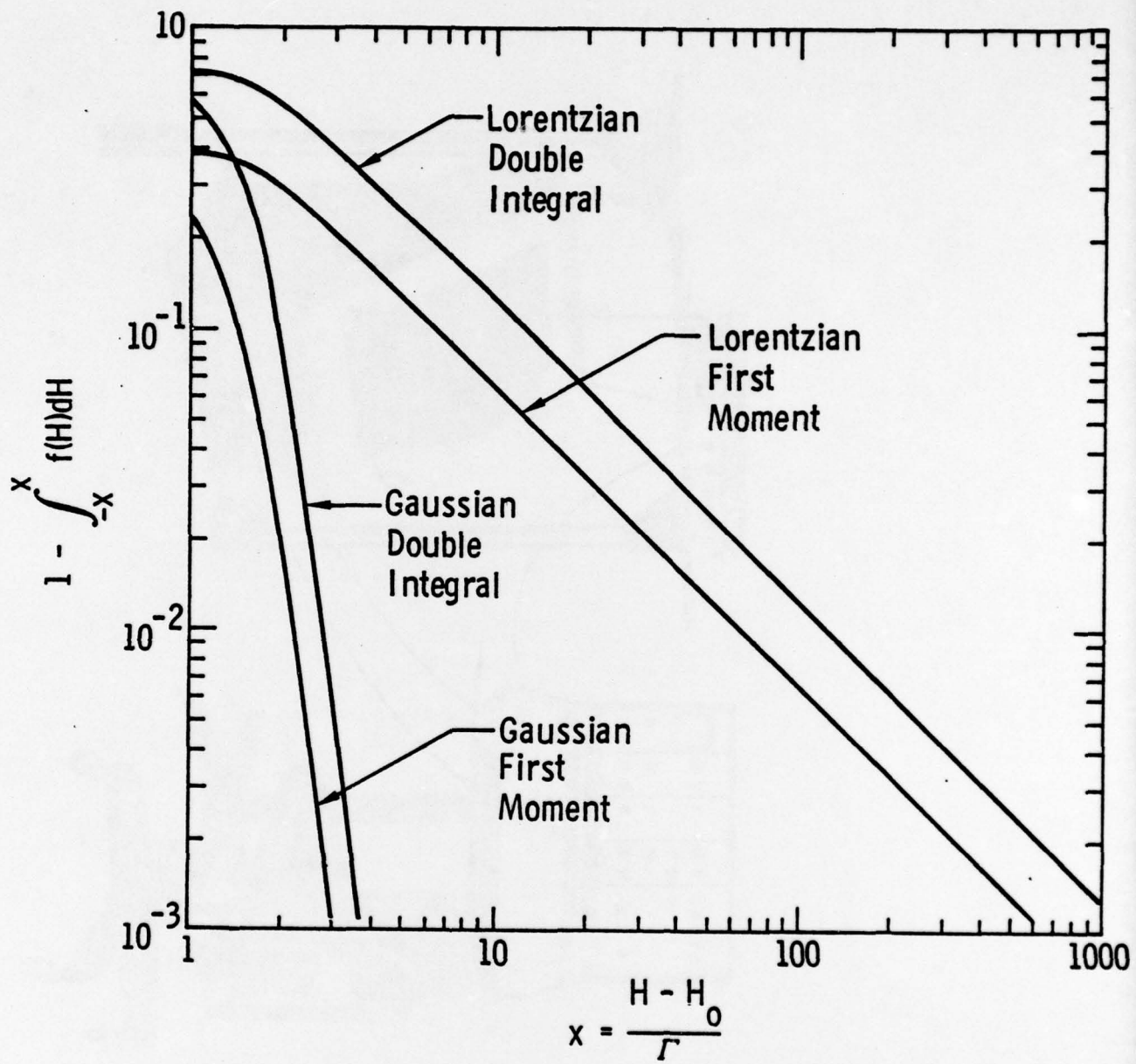


Fig. 14

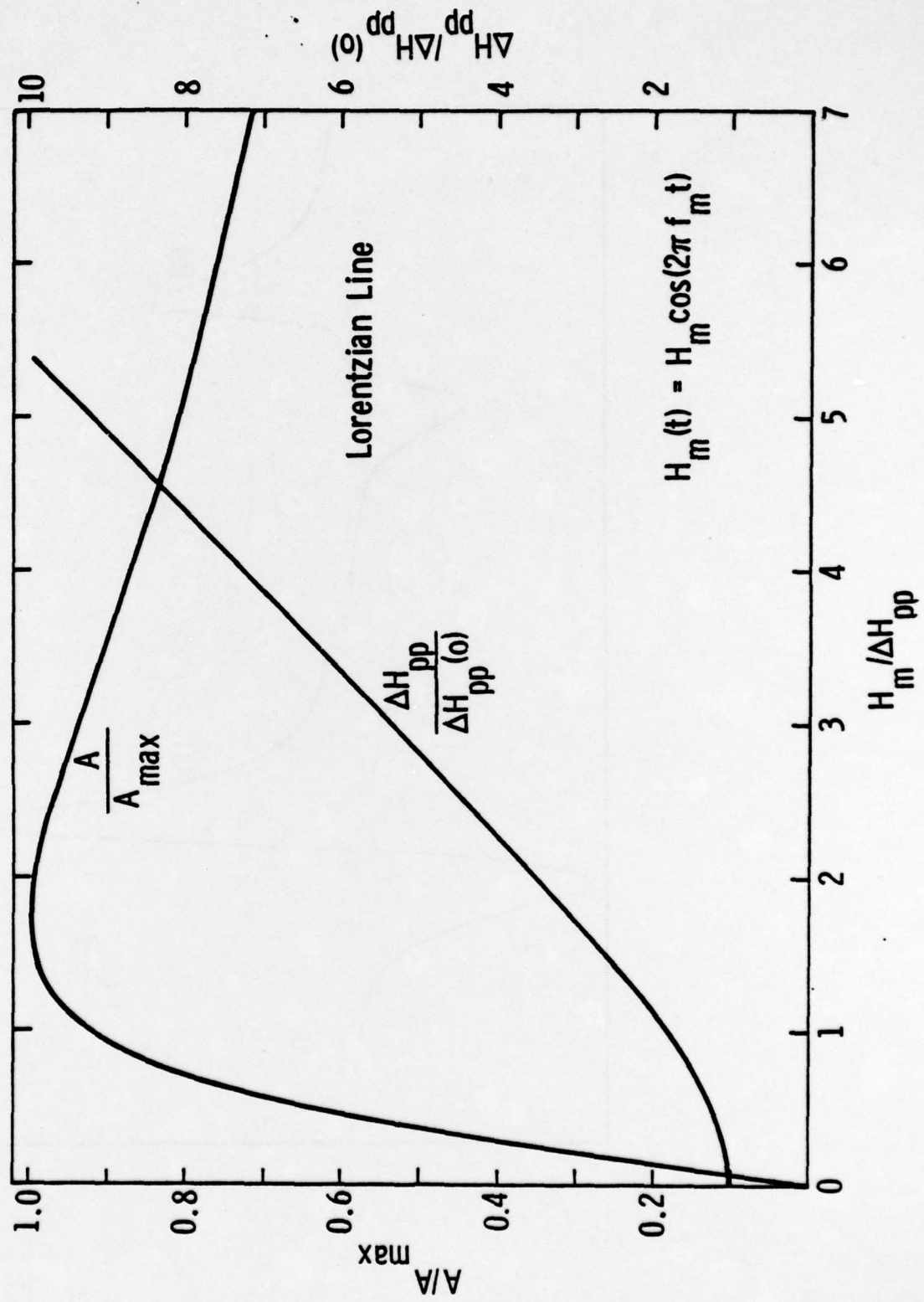


Fig. 15

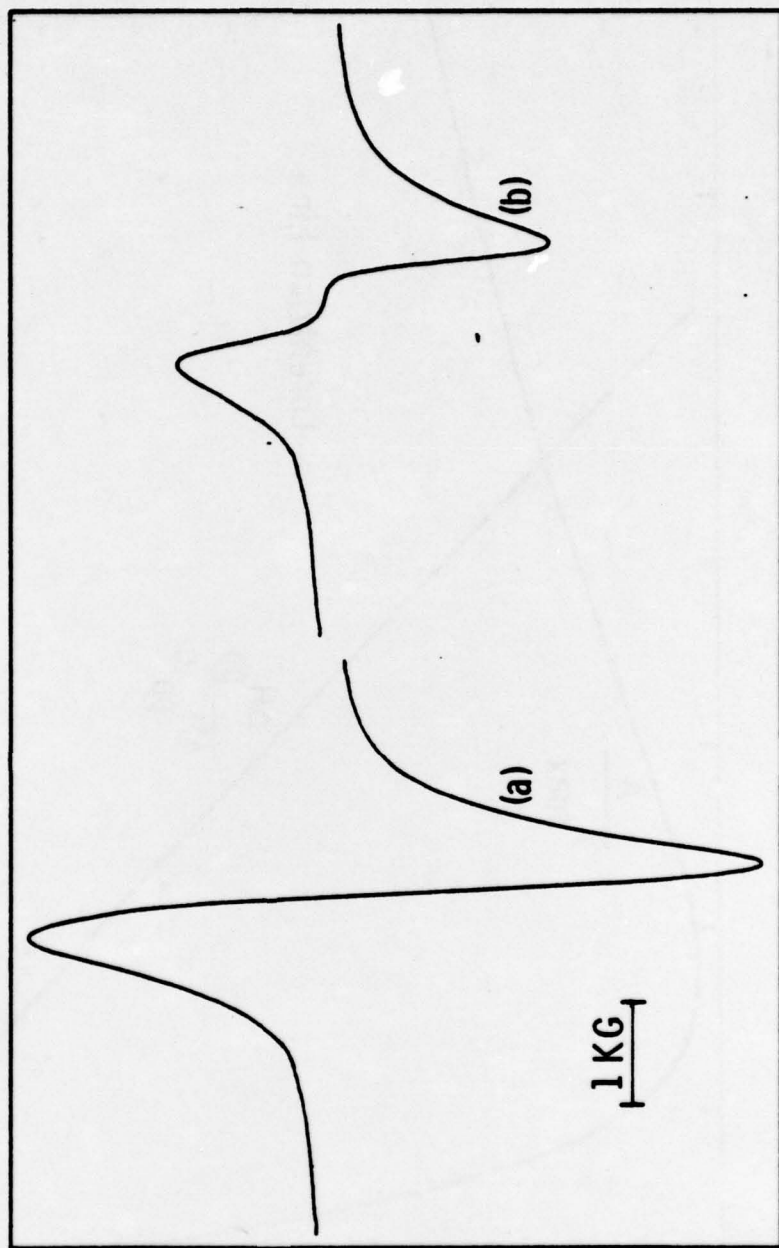


FIG. 16

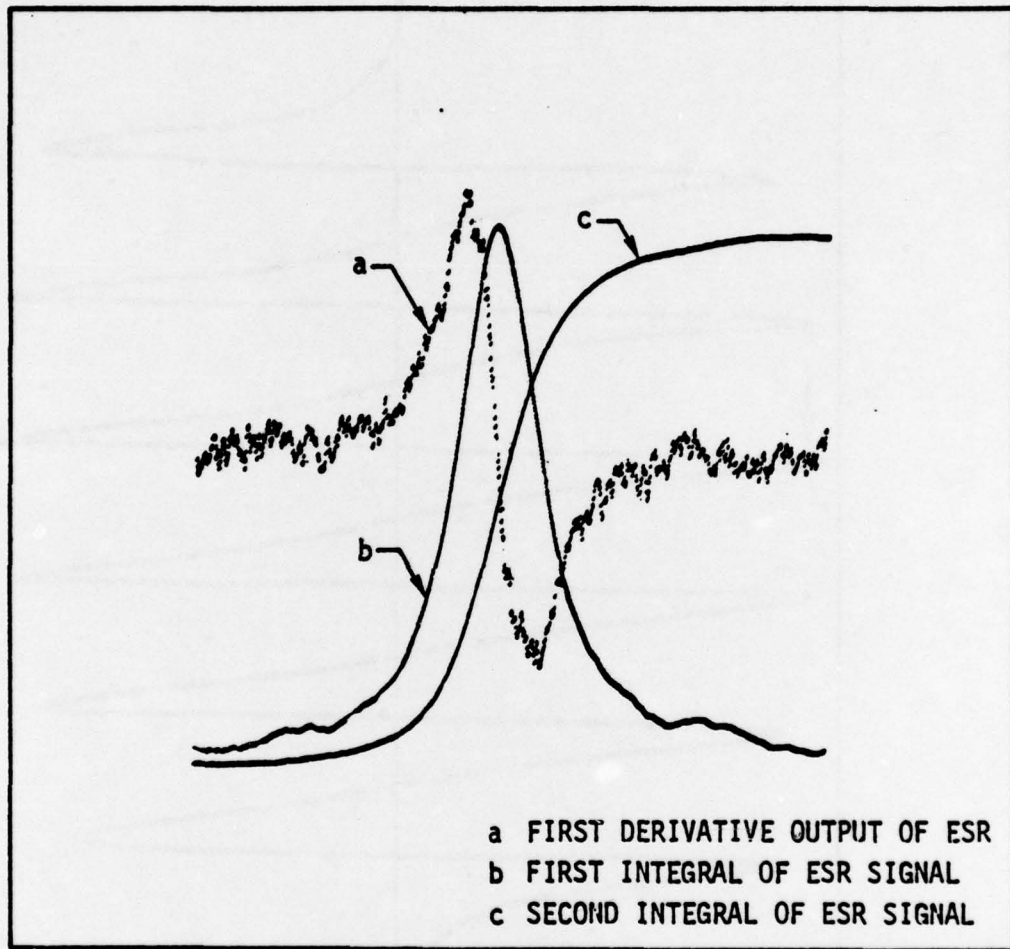


Fig. 17

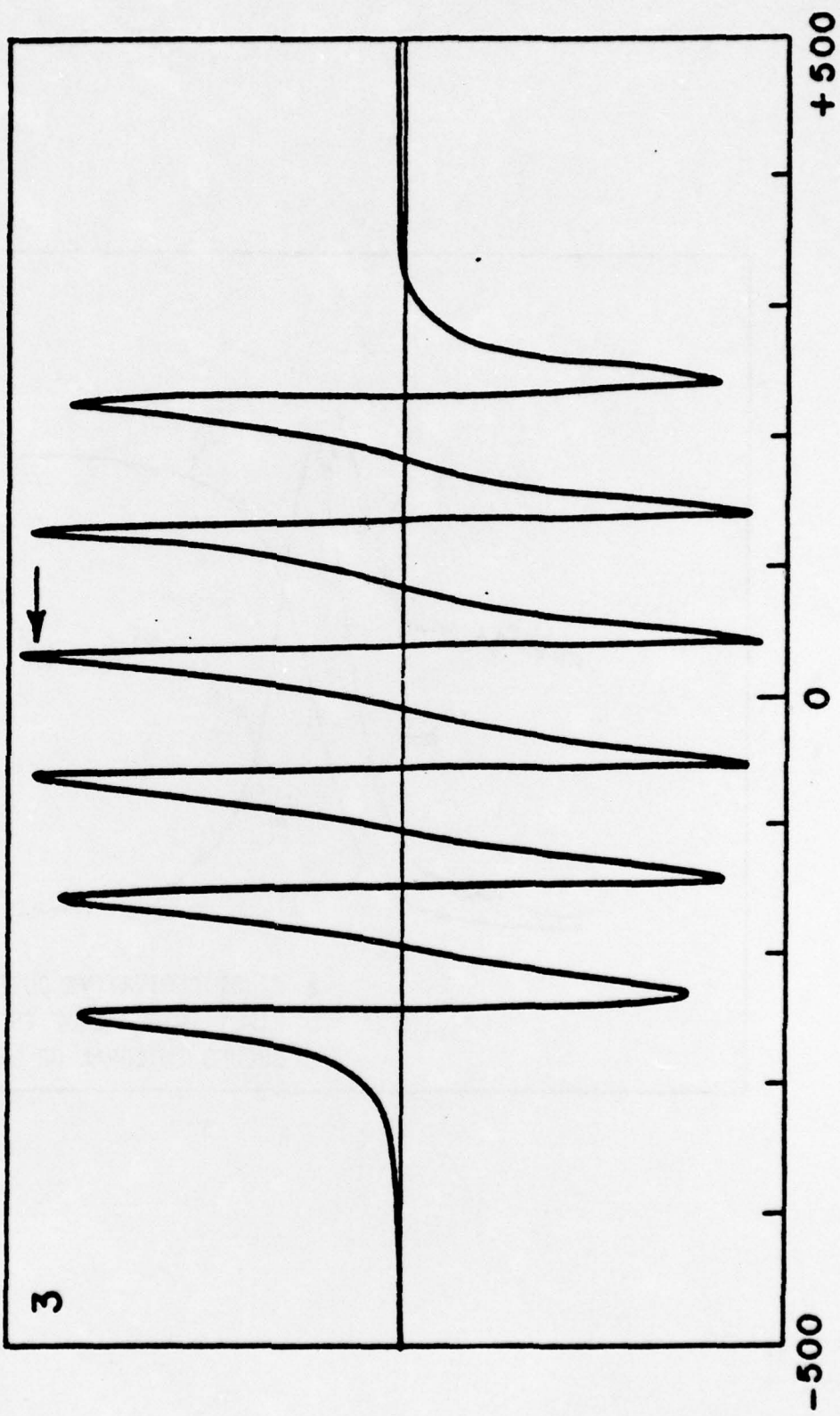


FIG. 18

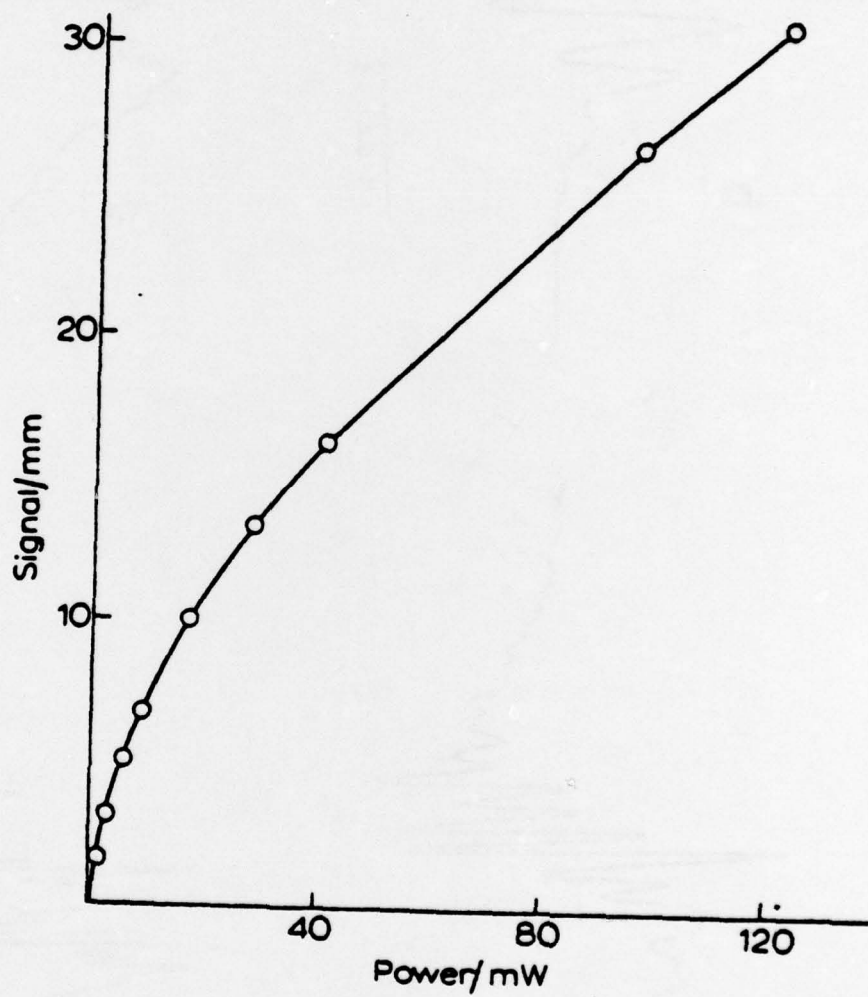


Fig. 19

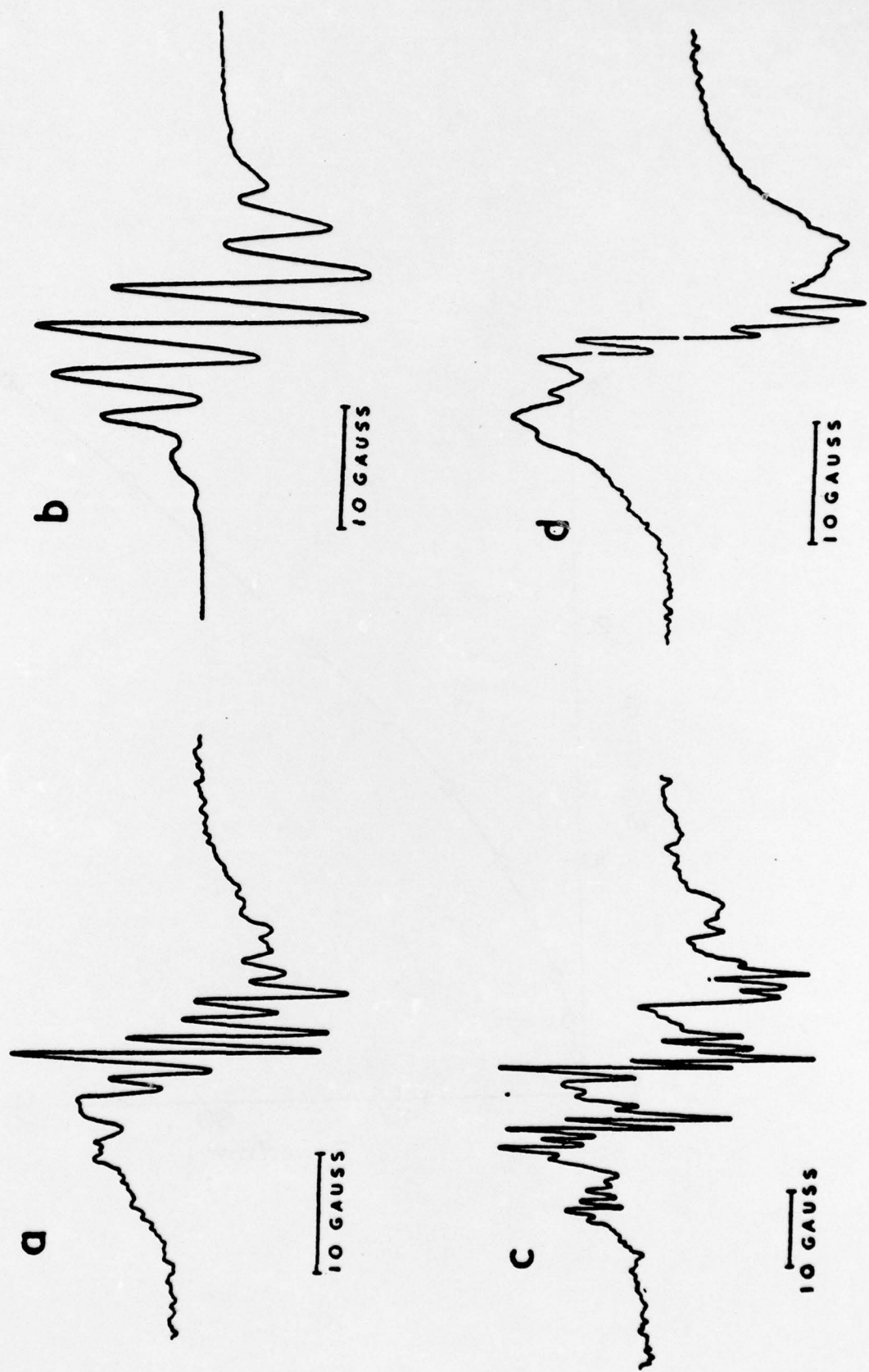


FIG 20

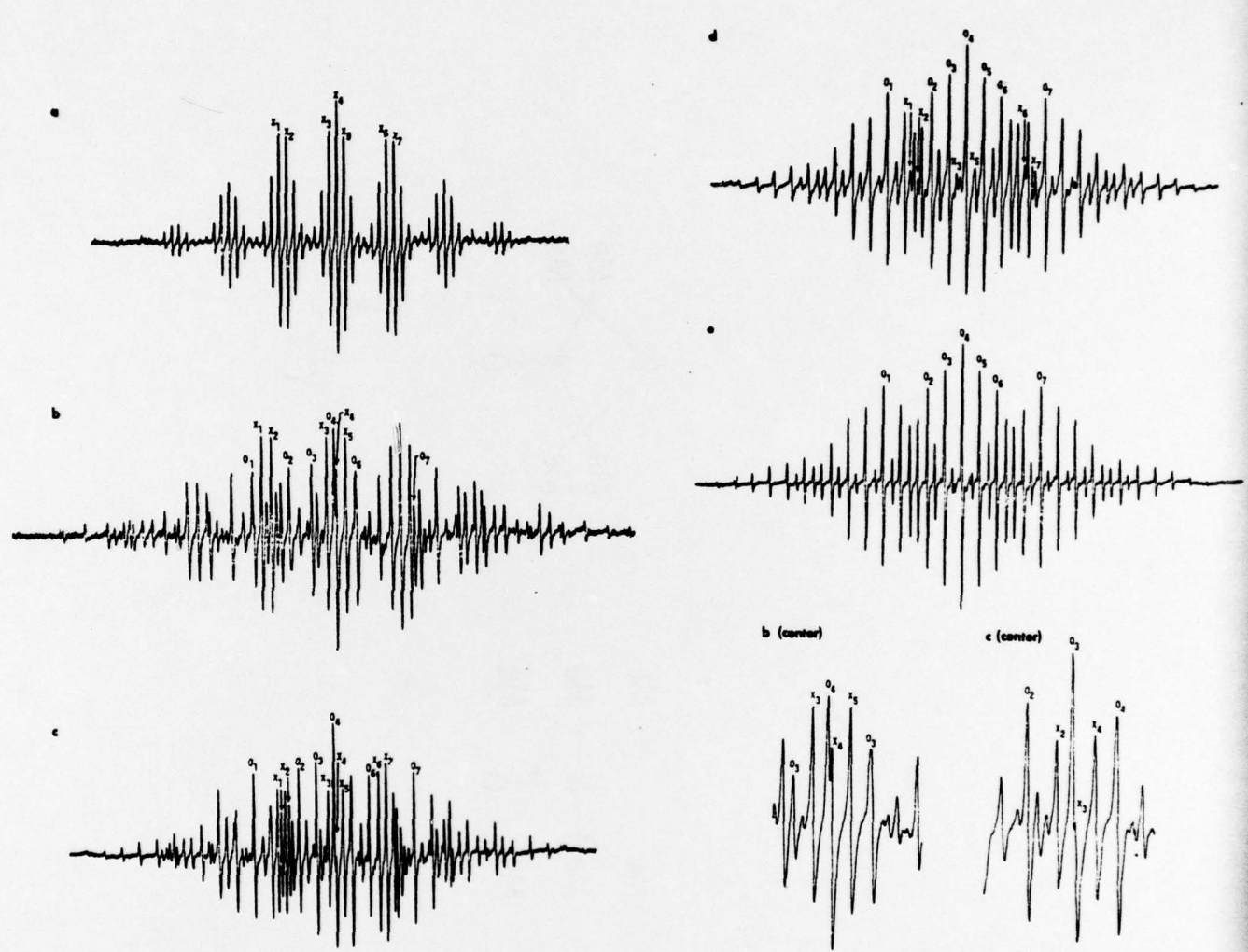


Fig. 21

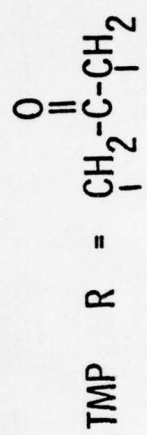
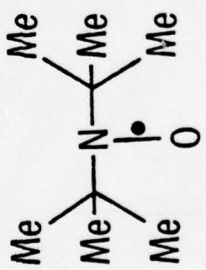
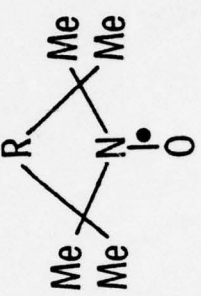


FIG. 22

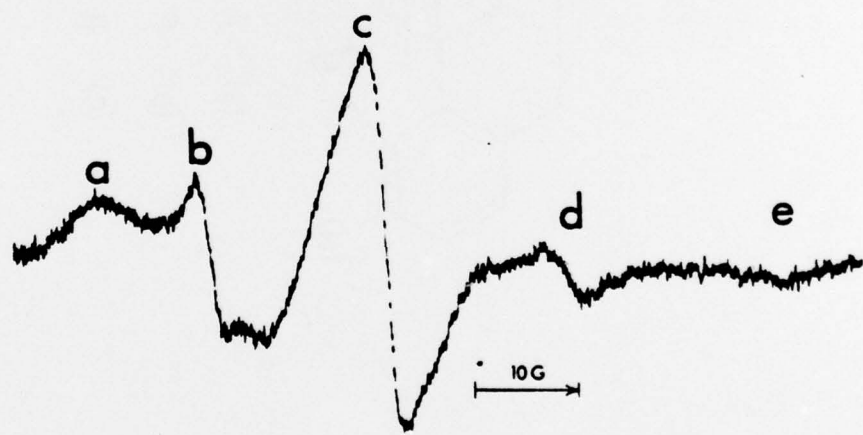
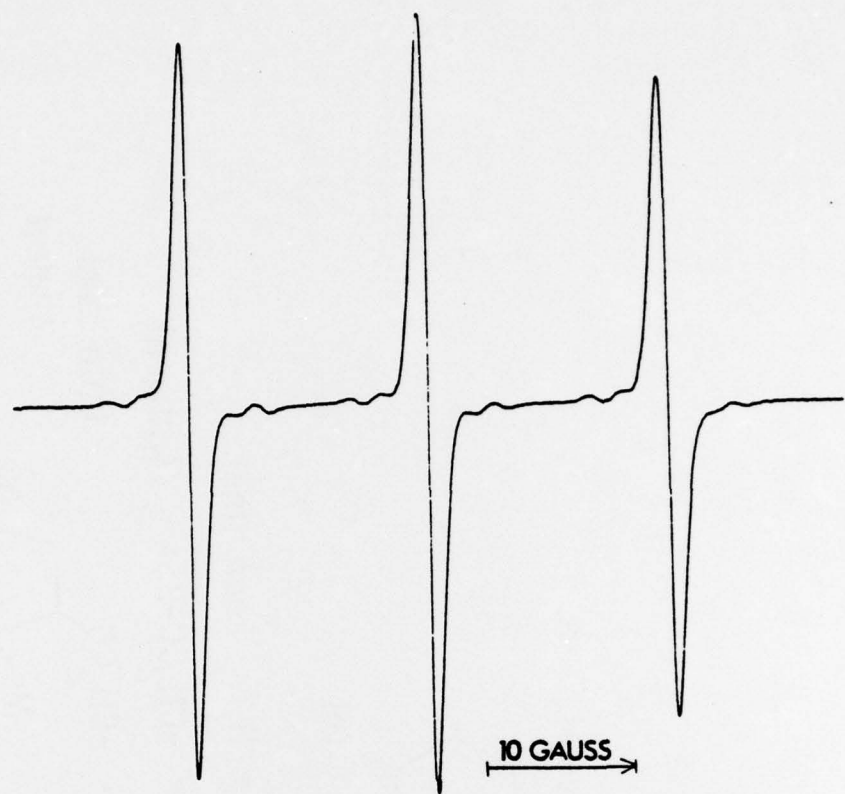


Fig. 23

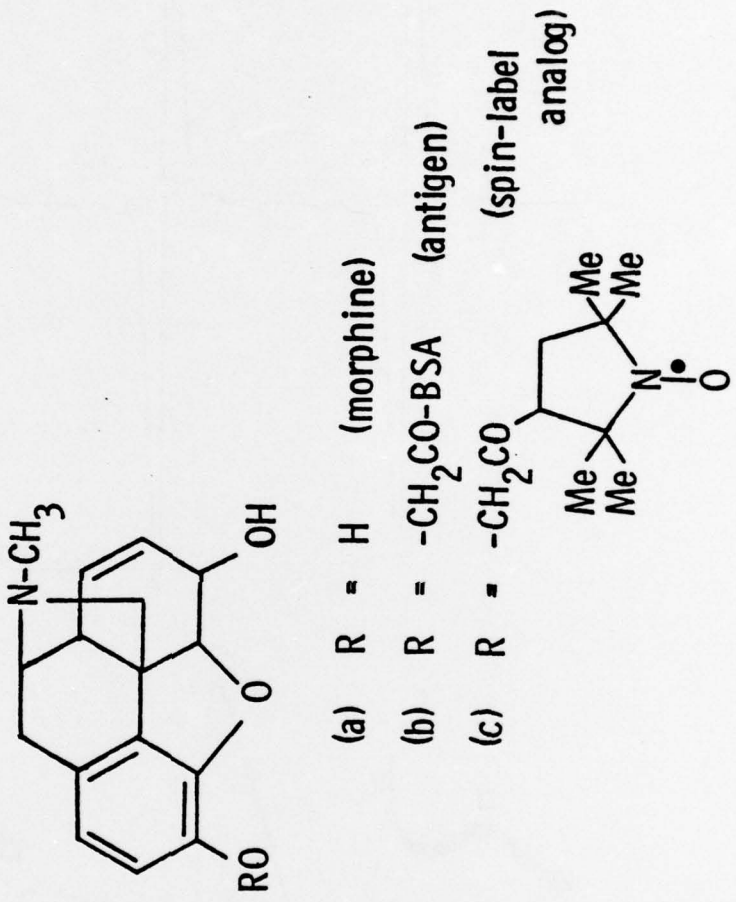


FIG. 24

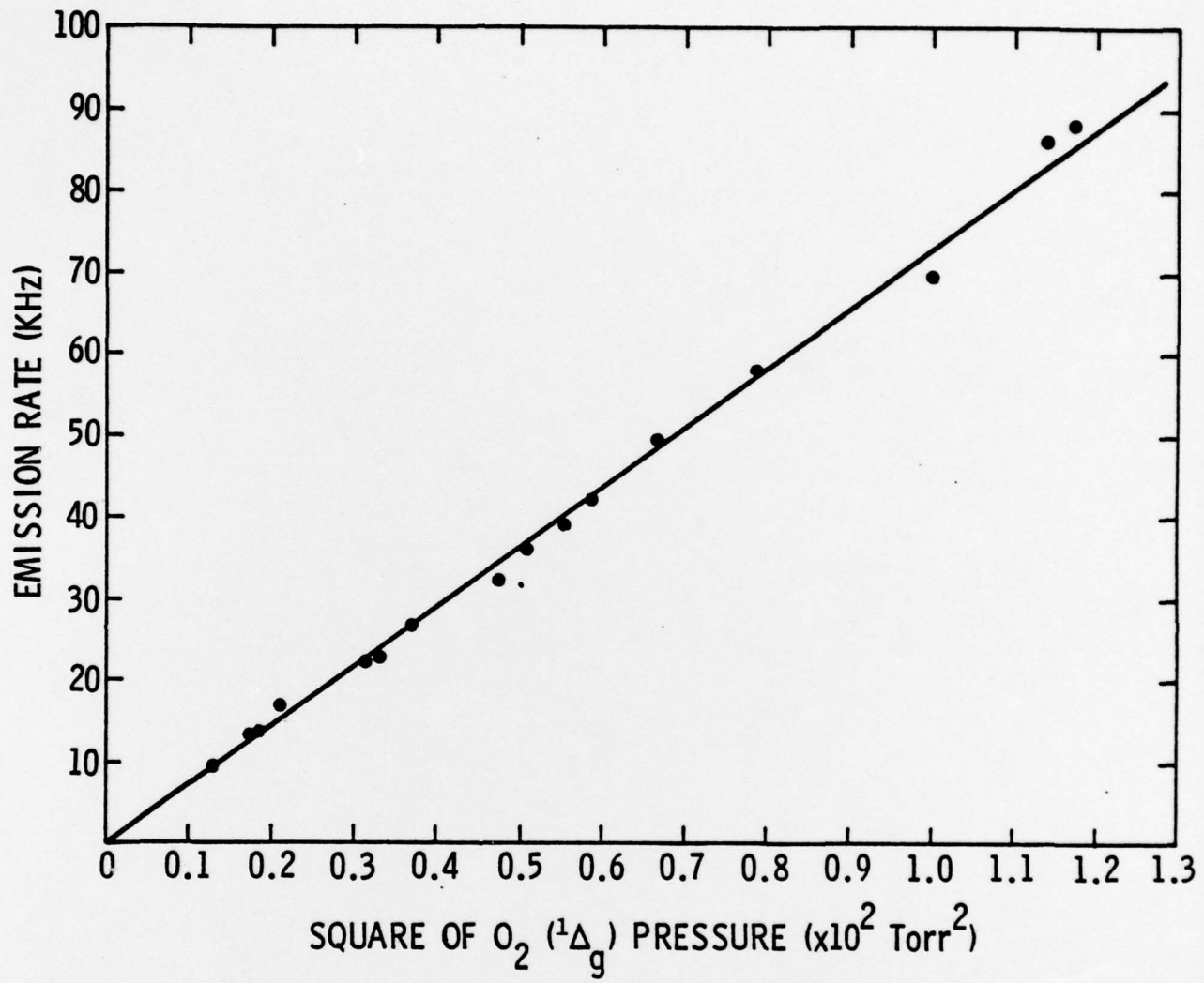


Fig. 25

Revised
July 1976

TECHNICAL REPORT DISTRIBUTION LIST

<u>No. Copies</u>	<u>No. Copies</u>		
Office of Naval Research Arlington, Virginia 22217 Attn: Code 472	2	Defense Documentation Center Building 5, Cameron Station Alexandria, Virginia 22314	12
Office of Naval Research Arlington, Virginia 22217 Attn: Code 102IP	6	U.S. Army Research Office P.O. Box 12211 Research Triangle Park, North Carolina 27709 Attn: CRD-AA-IP	1
ONR Branch Office 536 S. Clark Street Chicago, Illinois 60605 Attn: Dr. George Sandoz	1	Commander Naval Undersea Research & Development Center San Diego, California 92132 Attn: Technical Library, Code 133	1
ONR Branch Office 715 Broadway New York, New York 10003 Attn: Scientific Dept.	1	Naval Weapons Center China Lake, California 93555 Attn: Head, Chemistry Division	1
ONR Branch Office 1030 East Green Street Pasadena, California 91106 Attn: Dr. R. J. Marcus	1	Naval Civil Engineering Laboratory Port Hueneme, California 93041 Attn: Mr. W. S. Haynes	1
ONR Branch Office 760 Market Street, Rm. 447 San Francisco, California 94102 Attn: Dr. P. A. Miller	1	Professor O. Heinz Department of Physics & Chemistry Naval Postgraduate School Monterey, California 93940	1
ONR Branch Office 495 Summer Street Boston, Massachusetts 02210 Attn: Dr. L. H. Peebles	1	Dr. A. L. Slafkosky Scientific Advisor Commandant of the Marine Corps (Code RD-1) Washington, D.C. 20380	1
Director, Naval Research Laboratory Washington, D.C. 20390 Attn: Library, Code 2029 (ONRL) Technical Info. Div. Code 6100, 6170	6 1 1		
The Asst. Secretary of the Navy (R&D) Department of the Navy Room 4E736, Pentagon Washington, D.C. 20350	1		
Commander, Naval Air Systems Command Department of the Navy Washington, D.C. 20360 Attn: Code 310C (H. Rosenwasser)	1		

July 1976

TECHNICAL REPORT DISTRIBUTION LIST

<u>No. Copies</u>	<u>No. Copies</u>		
Dr. M. B. Denton University of Arizona Department of Chemistry Tucson, Arizona 85721	1	Dr. Fred Saalfeld Naval Research Laboratory Code 6110 Washington, D.C. 20375	1
Dr. G. S. Wilson University of Arizona Department of Chemistry Tucson, Arizona 85721	1	Dr. H. Chernoff Massachusetts Institute of Technology Department of Mathematics Cambridge, Massachusetts 02139	1
Dr. R. A. Osteryoung Colorado State University Department of Chemistry Fort Collins, Colorado 80521	1	Dr. K. Wilson University of California, San Diego Department of Chemistry La Jolla, California 92037	1
Dr. B. R. Kowalski University of Washington Department of Chemistry Seattle, Washington 98105	1	Dr. A. Zirino Naval Undersea Center San Diego, California 92132	1
Dr. I. B. Goldberg North American Rockwell Science Center P.O. Box 1085 1049 Camino Des Rios Thousand Oaks, California 91360	1	Dr. John Duffin United States Naval Post Graduate School Monterey, California 93940	1
Dr. S. P. Perone Purdue University Department of Chemistry Lafayette, Indiana 47907	1	Dr. G. M. Hieftje Department of Chemistry Indiana University Bloomington, Indiana 47401	1
Dr. E. E. Wells Naval Research Laboratory Code 6160 Washington, D.C. 20375	1	Dr. Victor L. Rehn Naval Weapons Center Code China Lake, California 93555	1
Dr. D. L. Venezky Naval Research Laboratory Code 6130 Washington, D.C. 20375	1		
Dr. H. Freiser University of Arizona Department of Chemistry Tucson, Arizona 85721	1		